THE UNIVERSITY OF MICHIGAN

COLLEGE OF ENGINEERING
Cast Metals Laboratory

Final Report

CASTING TECHNIQUES FOR CUNISIBE METAL

D. R. Askeland
P. K. Trojan
J. L. Herron
R. A. Flinn

ORA Project 01086

under contract with:

OFFICE OF NAVAL RESEARCH
CONTRACT NO. N00140-67-C-0503
CHICAGO, ILLINOIS

administered through:

OFFICE OF RESEARCH ADMINISTRATION ANN ARBOR

August 1968

TABLE OF CONTENTS

TABLE OF CONTENTS (Concluded)

LIST OF TABLES

LIST OF FIGURES

LIST OF FIGURES (Continued)

LIST OF FIGURES (Concluded)

SUMMARY

Many cast shapes are produced by an expensive time-consuming cut and try method. With the development of the new Cunisibe alloy, a complete analysis of the castability was desirable in order to give the foundryman the information necessary to produce high integrity castings.

The present research has provided the necessary castability data which ranged from melting practice to riser size determinations. Since Cunisibe is found to be an alloyed version of cupro-nickel, a comparison has been made wherever possible. In almost every instance the general castability of Cunisibe has been found to be somewhat superior.

Finally the data have been applied to a cast pressure fitting to indicate the production utility of the information under various foundry practices. The data can therefore be immediately used to produce radiographically sound cast components of Cunisibe metal.

INTRODUCTION

In the quest for a higher strength copper base alloy, the Navy developed a modified cupro-nickel alloy with the following composition:

	Cu	Ni	Si	Be	Fe	Mn
Weight %	Rem.	29-30	0.55/0.65	0.40/0.60	0.80/1.00	1.25/1.15

	C	P	S	P
Weight %	0.15	0.005	0.01 max.	0.02 max.

Since the initial intent for the alloy was as a cast material, it was necessary to develop casting design information and compare it to the better known 70Cu-30Ni alloys.

The object of the research was therefore to provide castability information on Cunisibe metal in order to allow the foundry to produce high integrity castings. The report evaluates melting and pouring practice, solidification characteristics, fluidity, hot tear susceptability, riser size, riser placement, and use of various exothermic componds. Finally the results have been applied to a small ell casting to evaluate the data utility in a production situation.

EXPERIMENTAL PROCEDURE

The general procedure is detailed under the following major headings:

(1) Raw Materials
(2) Melting and Pouring
(3) Molding
(4) Inspection
(5) Special Castings

RAW MATERIALS

The initial experimentation was conducted from Cunisibe metal ingot supplied by the Naval Applied Science Laboratory. Three separate ingot casts were forwarded as indicated in Table I. After several heats the virgin material had been exhausted which required a charge made up of remelted stock.

A complete list of input materials, castings poured, and the ultimate chemical analyses has been included in Table II. Since over 4000 lb of castings were produced from the original 500 lb of ingot, a large number of remelt cycles were required. The chemical analyses of several cupro-nickel heats have also been included in Table II.

MELTING AND POURING

A 3000-cycle, induction heated, lift coil was used with a number 60 graphite crucible. Melting and pouring was therefore conducted in the same crucible. Throughout the melting cycle, dry nitrogen was introduced through a hole in the graphite crucible cover in order to minimize the oxidation and vaporization loss of beryllium. The nitrogen flow rate was maintained at approximately 0.3 standard cubic feet per minute. No deoxidant was used in the melting practice.

A standard pouring temperature of from 2300-2350°F was used for all heats. The temperature was recorded on a strip chart with an immersion Pt-Pt 10% Rh thermocouple. Expendable fused silica protected thermocouples were found to offer the most economical means for temperature measurement within the designated temperature range.

Since different castings were poured from each heat, the pouring times necessarily varied. However, 100-lb melts were generally poured off into 3 or

4 molds in approximately 30 secs. The short pouring times were required in order to minimize temperature loss from the beginning to the end of the pour.

HOLDING

Dry sand molds have been used throughout the investigation and had the following composition for each batch:

140 mesh N.J. washed silica sand	152 lb
Western bentonite	8 lb (4.5%)
Dextrine	2 lb (1.2%)
Water	8 lb (4.5%)

New sand was mixed each time to be used for facing; old sand was tempered with water only and was used for backing sand. Several of the specialty castings had aluminum patterns and were hand molded. All bars and plates poured for the riser size and placement used wood patterns and were also hand molded.

After ramming the molds were baked for 12 hours at 300°F. When insulating and exothermic riser sleeves were employed, there were rammed into place during the molding sequence and were also exposed to the baking cycle. This was considered to be advantageous since these materials have a tendency to pick up moisture upon prolonged storage. In the event chills were used, they were machined from graphite and were also rammed into place. Further explanation of the procedure is included under "Special Castings".

INSPECTION

In numerous instances, the casting soundness could be ascertained from a simple visual inspection of a slice through the casting. However borderline riser sizes and feed distances required examination by radiographic techniques. A 1/2" vertical slice was first cut from the centerline of these castings with a large hydraulically-operated cut off wheel (see Figure 1). The pieces were then radiographed at 180 KV and 10 ma. for 15 sec.

Although Cunisibe alloy has not been found to be a mushy alloy (very large liquidus to solidus temperature difference), there is often difficulty encountered in radiography interpretation due to microshrinkage. In order to evaluate the radiography sensitivity, samples were also pressure tested. Several 1/2" thick pieces were machined to approximately 0.060" thicknesses first. (Although 0.030" thickness is more desirable, machinability difficulty with a shaper prevented thinner sections.) Dry nitrogen gas at 100 psig was then introduced to one side of the sample through an "O" ring seal. Any gas leakage was detected by passage through a gas burette. In this way a leak rate could be determined for various portions of the castings and correlated with shrinkage detected in the radiograph. The area pressure tested was 3/8" or 3/4" in diameter, depending upon the casting tested. A complete discussion of the technique and its sensitivities is contained in the literature (1) (2).

In some of the preliminary heats, difficulty was encountered with dross. A molybdenum mesh screen was inserted between the riser and the casting which resulted in shrinkage (Figure 2). The screen would undoubtedly work better in the gating system although dross was found to cause no difficulty if the metal was skimmed before pouring

SPECIAL CASTINGS

A number of special techniques were applied to various castings in order to study the several indices of castability such as fluidity, hot tears, thermal gradients, riser size, riser placement, and production shapes. These casting procedures have been included separately due to their unique applications.

1. Fluidity

A standard fluidity spiral as shown in Figure 3 has been cast for both Cunisibe and 70-30 cupro-nickel. The spiral casting has been designed to maintain a constant head upon pouring. Metal is poured into one side of the dual pouring basin where metal in excess of that required to fill the spiral "flows off" into the other pouring basin. Thus a constant metal head has been maintained with the length of the spiral determined only by the metal "flowability." The spiral length is measured in inches from the 2" bosses cast into the spiral. The length can then be correlated with degrees super heat above the liquidus. In all cases the pouring temperatures and liquidus temperatures have been measured with a Pt-Pt 10% Rh immersion thermocouple protected within a fused silica tube. Again a permanent temperature record was made on a strip chart potentiometer.

Although a drawing of the fluidity spiral has not been included in the report, the particular spiral used has been completely described in conjunction with other copper base founding principles (3).

2. Hot Tear Susceptability

A standard technique for aluminum alloys has been employed for both Cunisibe and 70-30 cupro-nickel to evaluate the susceptability to hot cracking (4). A sample set of castings is shown in Figure 4. The "U" shaped series of bars are identical except for a change in the radius at the reentrant angle closest to the sprue. The radii have been varied from 1/16" to 3/4". The mold material between the legs of the "U" inhibit contraction of the metal during solidification of the last liquid. Since the strength of the composite liquid-coherent solid has been found to be low, a small constraint could cause hot tears. For a given casting material, the degree of cracking will be dependent upon the stress concentration provided by the reentrant angle and the constraint provided by the mold material. A hot crack index is then the smallest radius of the fillet at which the metal will indicate a crack. All radii smaller than this value would show a crack whereas larger radii should inhibit the hot crack formation.

Since mold materials offer various degrees of constraint, CO_2 sand was used for one series in order to compare the results with the normal dry sand molds previously described. The 140 mesh sand was bonded with 5% sodium silicate and rammed in the normal was. The mold was not gassed with CO_2 however, but rather was dried for 2 hours at 250°F just before pouring. The resultant mold was very hard with high room temperature strength.

3. Thermal Gradients

It has long been appreciated that directional solidification toward a riser results in a thermal gradient which reaches a minimum somewhere within the casting geometry. In an attempt to correlate cast material, thermal gradient and shrinkage occurrence, a castability bar 2" x 2" x 12" chilled on one end has been developed (2) (5) (6). A large riser (4" diax 6" high) has been provided with bottom gating through a tapered sprue. The casting configuration and gating system were very much similar to those shown for the smaller bar in Figure 5. Six fine chromel-alumel (28 gauge) thermocouples protected from the liquid metal by 1 mm bore fused silica tubes are placed at various distances from the chilled end. The 6 cooling curves are then continuously recorded at the centerline but at different distances from the chilled end (as an example 1", 3", 5", 7", 9", and 11" from the chilled end. Since the bar is 12" long, 11" from the chilled end is 1" from the riser). From these cooling curves, the thermal gradient can be obtained at either the solidus temperature or the midpoint between the liquidus and solidus (both temperatures have found favor in the literature as being the point where restriction to liquid metal flow results in shrinkage). Two techniques have been used in the past to determine the thermal gradient.

(a) Tangent. By definition the thermal gradient has units of °F/in. or is the slope dT/dx. Therefore the cooling curves must be replotted as temperature versus thermocouple position where time is a constant parameter. The thermal gradient is then the slope of the iso-time curves at the temperature of interest (solidus or solidus-liquidus midpoint) (5). The technique, though exact, is extremely time consuming and incorporates further error due to the need for the replots of the data.

(b) Secant. A much more simple method requires direct use of the cooling curves with no replot of data. As an example, the thermal gradient at the solidus for a given position is obtained by determination of the temperature at the nearest hotter position and dividing by the distance between the two positions. Assume a solidus of 1940°F (Cunisibe) (see Figure 6), the thermocouple at 3" from the chill reached 1940°F at approximately 400 sec. At the same time (400 sec.) the next hottest couple was at 1970°F (5" from the chill). The thermal gradient at the 3" position can then be approximated as:

$$\frac{1970°F - 1940°F}{5'' - 3''} = 15°F/in.$$

This technique gives a secant rather than a true tangent, however due to its simplicity the method has been employed for the present investigation, to represent the thermal gradient.

4. Riser Size and Riser Placement

Development of feed distance for plates and bars has been conducted with and without chills. Graphite chills were used with a thickness equal to the thickness of the cross-section of the casting. As an example, a 2" x 2" cross-section bar had a chill 2" x 2" x 2" whereas a 6" x 1" cross-section plate used a chill 1" x 1" x 6". A bar has been defined as a section where the width is less than 3 time the thickness ($W < 3T$), whereas in a plate, $W > 3T$. Open risers were used throughout the study and were covered with an insulating compound after pouring (Cuprit; Foseco EP 2534 B). The risers were larger than necessary in order to insure that shrinkage occurred due to "choking off" of feed metal rather than an "inadequate supply" of feed metal.

The minimum riser size was determined for bars and plates for several different sets of conditions as outlined below:

(a) Side riser - insulating topping (Cuprit)
(b) Top riser - insulating topping (Cuprit)
(c) Top riser - insulating topping (Cuprit) and insulating sleeves (Kalmin; Foseco precast sleeves)
(d) Top riser - exothermic topping (Feedol 9; Foseco)
(e) Top riser - exothermic topping (Feedol 9; Foseco) and exthermic sleeves (Feedol 9; Foseco)

It was then possible to evaluate the effectiveness of insulating and exothermic compounds in order to maximize the casting yield. Previous data from 70-30 cupro-nickel also allowed a comparison with Cunisibe (7) (8).

5. Production Casting

As a check on the applicability of the riser size and placement data, a small 1-1/4" - 90° elbow was selected as an example of a production shape.

The casting was initially specified to be cast in Navy "M" and withstand 1200 psi gas or water pressure. Riser calculation was based upon visualization of a lengthwise cut along the centerline and flattening out as would be done if a tin can was cut along the seam and unrolled to provide a single sheet. The resultant section was approximately 5-1/2" x 5-5/8" x 5/8" (a plate section).

Three castings were made as outlined below. (In each case the riser had the height equal to the diameter (2-1/8") and was selected to be 1/4" larger in both the height and diameter than given by the minimum riser size curves for exothermic topping).

(a) Top riser; both ends chilled; bottom gated to the reentrant corner; exothermic topping (Feedol 9); see Figures 7, 8, and 9
(b) End riser; one end chilled; gated into riser; exothermic topping (Feedol 9)
(c) Top riser; both ends chilled; bottom gated to the reentrant corner; insulating topping (Cuprit)

RESULTS AND DISCUSSION

For ease of presentation, the data have been divided into the following categories:

1. Melting, Pouring, and Safety Precautions
2. General Castability—Fluidity, Hot Tears, Thermal Gradients
3. Riser Size and Placement—Feed Distance for Bar Sand Plates, Evaluation of Insulating and Exothermic Riser Compounds
4. Production Casting

MELTING, POURING, AND SAFETY PRECAUTIONS

The normal procedure has been described previously; however since beryllium is known to constitute a health hazard the initial experiments were monitored by Professor W. A. Cook; Industrial Health; School of Public Health at The University of Michigan. The beryllium content in the various experimental stages is given below:

Operation	(Concentration micrograms/meter^3)
Melting (covered crucible with N_2)	3
Pouring (through air)	70
Cutting (wet abrasive wheel)	300

It was interesting that melting constituted the least hazard whereas cutting was most hazardous. An attempt was therefore made to use other cutting techniques such as power hacksaws; however the operation was too slow. Therefore wet abrasive cut off wheels were used for all sectioning operations even though the beryllium toxicity level was high. Since the normal tolerance of 5 micrograms per miter^3 was well exceeded in most instances, any person in the area has been required to wear a filter type respirator approved by the U. S. Bureau of Mines for protection against fume. As an added precaution exhaust ventilation was used if the operation was sufficiently close to the intake system.

GENERAL CASTABILITY OF CUNISIBE

1. Fluidity

Fluidity curves for both Cunisibe and 70-30 cupro-nickel are shown in

Figure 10 (Heats 320-323; Table II). It can be seen that Cunisibe has slightly higher fluidity than cupro-nickel. The equations of the curves are:

$$\text{Cunisibe - Spiral length} = 0.120x\ (^\circ\text{F Superheat})$$

$$\text{Cu-Ni - Spiral length} = 0.102x\ (^\circ\text{F Superheat})$$

where

$$^\circ\text{F Superheat} = \text{pouring temperature} - 2110^\circ\text{F (Cunisibe)}$$

$$= \text{pouring temperature} - 2240^\circ\text{F (Cu-Ni)}$$

The slight difference in fluidity may possibly be attributed to the occurrence of an eutectic in Cunisibe. It is a well-known phenomenon that an eutectic and a pure material will generally show higher fluidity than alloys which exhibit a broad liquidus to solidus distance. However the difference between the two alloys as tested is so slight as to be insignificant from the point of view of castability.

2. Hot Tears

The hot tear castings as shown in Figure 4 did not indicate cracks for either of the alloys for even the smallest radius of 1/16". Such was the case for both dry sand and the more rigid CO_2 sand molds. This does not mean the alloys will not hot tear, since the use of still more rigid mold materials may cause the experimental castings to crack. However a separate investigation of various investment mold materials would be required to completely evaluate the hot tearing tendency under the most severe casting conditions. In conclusion it is of importance to realize that semi-rigid mold materials will not cause hot tears in a "U" shaped casting with a 7" span with a poor foundry practice of less than generous fillets. Therefore, with normal practice, hot tearing should not be a problem as generous fillets, streamlined gates and runners, and streamlined casting geometry are most often used.

As a matter of record an x-ray of the 1/16" radius Cunisibe casting in a CO_2 mold is included in Figure 11 (Heat 361, Table II). It can be noted that shrinkage has occurred along the centerline due to inadequate feeding and at the 3/4" radius hot spot. It should also be pointed out that shrinkage would promote the occurrence of hot tearing; however a crack is not evident in this case.

3. Thermal Gradients

The cooling curve for the 2" x 2" x 12" bar cast of Cunisibe alloy was previously shown in Figure 6. Figure 12 shows the corresponding set of cooling curves for 70-30 cupro-nickel (Heat 320). The liquidus and solidus temperatures for Cunisibe were approximately 2110°F and 1940°F, respectively (Figure 6). There was of course, a variation in these "arrest" temperatures from one thermocouple to the other due to the interdependence of constitutional supercooling and thermal gradient. The "arrest" at 1940°F was probably due to an eutectic as seen in a brief metallographic examination of the casting.

When compared to the cupro-nickel with a liquidus of 2240°F and a 102°F liquidus to solidus range, the broader (170°F) range for the Cunisibe suggested greater difficulty with soundness. This was not borne out by the feed distance relations as will be pointed out later in the report.

Two temperatures of interest have been used in the literature; the thermal gradients at the solidus and half way between the liquidus and solidus. The practical temperature at which the thermal gradient would be most important would be the point where the liquid can no longer feed through the dendrites and shrinkage results. Since the degree of liquid-solid coherence as related to shrinkage is unknown and is undoubtedly dependent upon the alloy system, the solidus and liquidus-solidus midpoints have been assumed to be of greatest interest. It would seem logical that somewhere between these two temperatures is the point of most significance which as yet has not been defined. In any event the thermal gradients at the two temperatures as determined by the secant method have been summarized in Figure 13.

Therefore, the table below provides interesting comparison between the two alloys as obtained from the thermal gradient curves and X-rays.

2" x 2" x 12" Bar-End Chilled

	Cunisibe	70-30 Cupro-Nickel
Liquidus Temperature	2110°F	2240°F
Solidus Temperature	1940°F	2138°F
Freezing Range	170°F	102°F
Liquidus-Solidus Midpoint	2025°F	2189°F
Gross Shrinkage (Measured from chill)	4-3/4"	6"
Minor Shrinkage (Measured from chill)	None	4"
Thermal Gradients		
Gross Shrinkage - Solidus	7.25°F/in.	8.4°F/in.
Gross Shrinkage - Liq.-Sol. Midpt.	2.5°F/in.	1.8°F/in.
Minor Shrinkage - Solidus	None	18.5°F/in.
Minor Shrinkage - Liq.-Sol. Midpt.	None	5.5°F/in.

As pointed out previously, it appeared that Cunisibe should be more difficult to cast since it had a longer freezing range (170°F). However the X-rays indicate that the length of sound bar (2" x 2" cross section) is slightly greater for Cunisibe than 70-30 (Figure 14). On the other hand the thermal gradient developed for Cunisibe is also greater which should result in greater soundness.

Figure 13 and the previous table suggested that a shorter bar would be sound due to higher thermal gradient. Therefore a 2" x 2" x 10", end chilled castability bar was poured in Cunisiby alloy. The cooling curves and thermal gradients are given in Figures 15 and 16.

Radiographs of the casting have indicated it to be sound which of course would be due to the higher thermal gradients. It can be seen that the minimum thermal gradient in Figure 16 is well above that where shrinkage occurred in the 2" x 2" x 12" casting discussed in the previous table (2.5°F/in. for shrinkage in the longer bar versus 7°F/in. in the shorter, sound bar at the solidus-liquidus midpoint).

Although the reasons for casting soundness or lack of it is dependent upon the thermal gradient, a more rapid utilization of the data is generally found through feeding distance relationships as presented in the following section.

RISER SIZE AND PLACEMENT

In a normal risering problem, two questions must be answered. First how large must the riser be in order that it freeze after the casting? Secondly, where should the riser be placed in order that dendritic solidification of the casting does not choke off the feeding of liquid metal from the reservoir or riser? Since the preceding section dealt with the directional solidification or feeding distance, the latter question will be discussed first.

1. Feeding Distance

(a) Bar Sections. A complete list of castings poured for the bar feeding distance has been included in Table III. In all cases the riser was larger than necessary in order to be assured that it froze last. Again insulating compound (Cuprit) was applied to the open risers, when small bars were poured, several where radiated from the same riser as shown in Figure 17.

Graphical representation of the results are included in Figures 18a (unchilled bars) and 18b (chilled bars). The maximum feed distance can best be summarized below in equation form:

	Feed distance in bars (FD) (T = bar thickness in inches)
Cunisibe - Unchilled	FD = 2T + 5" for $T \geq 1"$
Cunisibe - Unchilled	FD = 7T for $T \leq 1"$
Cunisibe - End Chilled	FD = 2T + 6" for $T \geq 1"$
Cunisibe - End Chilled	FD = 8T for $T \leq 1"$
70-30 CuNi - Unchilled (7)	FD = 2T + 4" for $T \geq 1"$
70-30 CuNi - End Chilled (7)	FD = 2T + 5" for $T \geq 1"$

The maximum length bar which can be made sound in Cunisibe is therefore 1" longer than in the same cross section cast in 70-30 CuNi. Since the increased feed distance for the addition of an end chill is 1", and end chilled 70-30 CuNi bar will give the same feed distance as an unchilled Cunisibe casting.

It is also note worthy that feed distance data for bars has seldom been carried below a thickness of 1" for any of the more common cast metals. However it is most logical that the upper linear portion of the curve must break and proceed to the origin when the thickness has become sufficiently small. The reasoning is based upon the extensive feeding resistance imposed by the dendrites rapidly growing from four sides. The best curve for the small thicknesses again appeared to be linear as shown in Figures 18a and 18b with the break point at approximately 1" thicknesses. Since cupro-nickel data have not been carried below the 1" thicknesses, the Cunisibe advantage over cupro-nickel cannot be evaluated at the smaller sizes (7).

Finally an attempt has been made to divide the feed distance relationships into an "end" and "riser" contribution as shown in the figures. The total feed distance is then the sum of the two individual contributions. The use of radiographs to determine these cutoff points does not allow for maximum accuracy, therefore the end and riser contributions are shown as crosshatched influences. That is to say the accuracy associated with the individual contributions were a degree of unsoundness must be determined, is not as well defined as the more simple choice; is it or is it not sound? As might be anticipated however, the addition of an end chill essentially only increases the end contribution and has little or no effect on the riser contribution.

(b) Plate Sections. The summary of plate castings poured is given in Table IV. Plates smaller than 1/2" thick were not poured due to the small feed distances at these thicknesses. However when small thicknesses were poured, a gating technique similar to that for small bars was used (Figure 19). Again large risers and riser insulating compound were used.

The graphical results are shown in Figures 20a and 20b. The corresponding equations for the straight lines are given below

Feeding Distance in Plates
(T = Plate thickness in inches)

Cunisibe - Chilled	FD	$= T + 2\text{-}1/4'' \text{ for } T \geq 1/2''$
Cunisibe - Unchilled	FD	$= 1/2T + 1\text{-}1/4'' \text{ for } T \geq 1/2''$

Unfortunately published data for plate sections are unavailable for 70-30 cupro-nickel. Therefore a comparison for the two alloys cannot be made. However, there is no reason to believe that Cunisibe will be poorer than 70-30 CuNi; since most previous information on the castability of the two materials has indicated the opposite to be true.

Again an attempt was made to divide the total feed distance into and end and riser contribution with the associated difficulty. It should be noted that 1/2" thicknesses have not resulted in the break toward the origin as was the case with bars; therefore no attempt should be made to use the data below 1/2" sections. The addition of an end chill has increased the feed distance by approximately 1" as with bars, where the increased feeding is felt basically in an increased end contribution.

A comparison between plates and bars can best be made from the summary curves in Figure 21. The plates have somewhat less than one half the feed distance of that found in bars of the same thickness. This general trend is obtained in most cast materials due to the dendritic growth which chokes off feeding in the relatively thin plate sections.

(c) Pressure Testing. As pointed out previously, the radiography sensitivity was checked by pressure testing 0.060" thick pieces cut from the 1/2" thick radiographic bar samples. The results of the pressure test are included in Figure 22. Radiographs of 2" x 2" x 9" unchilled and 1" x 1" x 8" chilled bars had shown the castings to have marginal soundness. These castings were just below or on the feed distance curves shown in Figures 18a and 18b. Even though a cupro-nickel 0.0140" penetrameter with a 0.0310" hole was distinguishable in the radiograph, the possibility of shrinkage placed the castings in the marginal category. The pressure test results have verified the choice and the leak rate was small.

On the other hand the existence of easily distinguishable shrinkage as in the 1" x 1" x 8" unchilled bar resulted in much higher leak rates as compared to the chilled bar. Since some difficulty was anticipated with dross in these two bars, both a 3/8" and 3/4" diameter area was pressure tested. It should be noted that the maxima occurred at the same distance from the riser with the larger area giving a higher leak rate.

Therefore gross radiographic unsoundness has given very high leak rates. As the radiograph became more difficult to interpret the leak rate decreased. The "soundness" in the present study is that determined by radiography. It is entirely possible that pressure testing in thin sections may result in leakage even though the casting appeared radiographically sound. However, radiographs of the 0.060" sections all showed unsoundness as shown in the pressure tests.

Soundness then has become a problem in definition. It would appear that Cunisibe has a tendency to disperse shrinkage, which made radiography of the 1/2" sections difficult to interpret, when the castings approached the minimum feed distance. Therefore the feed distance curves should not be used without the addition of a margin of safety.

Finally it should be mentioned that 70-30 cupro-nickel castings are somewhat easier to treat radiographically. The more clear cut difference between shrinkage and soundness may be due to the shorter liquidus to solidus temperature range (102°F vs 170°F for Cunisibe).

2. Riser Size

All of the risers used in the feed distance study have been larger than necessary in order to guarantee a high thermal gradient at the riser end. Therefore shrinkage occurrence would be due to dendrite choking of metal flow within the casting and not due to an inadequate supply of liquid metal in the riser. The feed distance curves then provide information as to riser placement. The present information deals with optimum riser size.

Before proceeding to the risering curves, several terms are defined below:

V_r - Riser Volume

V_c - Casting Volume

H - Riser Height

D - Riser Diameter

L - Casting Length

W - Casting Width

T - Casting Thickness

V_r/V_c - Volume Ratio

(L+W)/T - Casting Shape Factor

Several variables which effect the riser size have been investigated as pointed out in the experimental procedure. These will be discussed in the following sequence:

(a) Side riser - insulating topping
(b) Top riser - insulating topping
(c) Top riser - insulating topping and insulating sleeves

(d) Top riser - exothermic topping
(e) Top riser - exothermic topping and exothermic sleeves

(a) Side riser - insulating topping. In the past, various researchers have pointed out the importance of the height to diameter ratio of the riser (H/D). Unfortunately there has been very little consistency as to how it should be measured. Since the volume ratio (V_r/V_c) should be minimum for maximum efficiency and economy, the H/D ratio should be determined as a function of the volume ratio. The dependence of height to diameter ratio upon the volume ratio is shown in Figure 23. The corresponding castings poured are given in Table V. Shrinkage occurred in these side risered bars (2" x 2" x 8") when the riser became too small to maintain a sufficiently high thermal gradient. The pipe seldom ended up in the casting, but rather centerline shrinkage appeared in the casting in very much the same way as with inadequate feeding distance. It should be pointed out that a 2" x 2" x 8" long bar is within the feed distance relationship if the riser is sufficiently large to maintain the necessary thermal gradient (greater than 5°F/in. at the solidus-liquidus midpoint). Here again a higher H/D ratio for the riser would provide the necessary gradient.

The shape factor versus the volume ratio for side risered castings was not determined since it became evident that the shape factor could not be varied over a significant range due to the feeding distance limitations. Therefore top risered castings were used for the remainder of the riser size determination.

(b) Top riser - insulating topping. The interrelationship between the volume ratio and (H/D) is shown in Figure 24. The limiting value for soundness would be when the shrinkage pipe is pulled down into the casting. Therefore, higher H/D ratios would inhibit this occurrence as shown.

In general the most economical and practical H/D ratios fall between 0.5 and 1.0 as seen in Figure 24. Lower values decrease casting yield whereas higher ratios begin to lose their effectiveness as seen by the decreasing slope at H/D values greater than 1.0 Therefore the actual riser size can be determined from the curves in Figure 25 for H/D values of either 0.5 or 1.0. The data can be used for either plates or bars where insulating topping is used on open risers. The complete summary of castings poured in this series has been given in Table VI.

It should be pointed out that H/D ratios were maintained by the use of "flow-offs." The casting rigging is shown in Figures 26 and 27.

(c) Top riser - insulating topping and insulating sleeves. The volume ratio versus H/D and the volume ratio versus the shape factor curves are given in Figures 28 and 29 with the castings poured enumerated in Table VII. It will be noted that the conjunctive use of insulating topping plus sleeves has shown a lesser interdependence between the volume ratio and the H/D ratio than when insulating topping was used alone (Figures 24 and 28). Therefore an H/D value of 0.50 was used to establish the risering curve shown in Figure 29.

(d) Top riser - exothermic topping. The working graphs and tabular data are included in Figures 30 and 31 and Table VIII. Again (H/D) values of 0.50 were chosen to establish the risering curve. As a point of interest, a casting with a shape factor of 5.0, $V_r/V_c = 0.6$, and H/D = 0.50 was made in the normal manner; however Feedol 1 (less active) was used for the exothermic topping rather than the normal Feedol 9 (more active). Whereas the risering curve (Figure 31) would show the Feedol 9 casting to be marginal, the Feedol 1 casting was definitely unsound with rather gross shrinkage. Therefore all exothermic compounds are found not to be the same, and difficulty may be anticipated when risers are selected which fall close to the minimum sizes advised by the curves. Furthermore, past experience has shown active exothermic compounds to become more inactive with long storage, possibly due to moisture pick up.

(e) Top riser - exothermic topping and exothermic sleeves. Graphical representation of the results are presented in Figures 32 and 33. Tabulation of the castings poured is given in Table IX. The general trends are seen to be quite similar to those previously discussed.

Perhaps the best comparison of the experimental variables can be appreciated from Figures 34 and 35 which summarize all of the riser size data. The experimental points have not been plotted but rather only the average curves derived from the data presented in Figures 23-33. Data have also been plotted for 70-30 cupro-nickel (8), which provided an interesting comparison with Cunisibe alloy.

Many conclusions could be drawn from the summary curves, however the following are considered to be of greatest significance:

1. Side risers are not considered very economical since the feed distances can easily be exceeded and large volume ratios are required.

2. For Cunisibe, exothermic topping gives better yield than if only insulating topping is used. Insulating topping plus insulating sleeves is as good if not better than exothermic topping and exothermic sleeves. (The possible production of toxic beryllium fume is also decreased when insulating compounds are used.)

3. Little is gained by the addition of exothermic sleeves to exothermic topping for Cunisibe whereas a large increase in yield is to be appreciated for 70-30 cupro-nickel. Therefore a higher yield is evident for Cu-Ni when exothermic are used except when only an exothermic topping is used which provided Cunisibe with a higher casting yield (a lower volume ratio for a given casing geometry.

These results are difficult to rationalize since the cast materials possess different thermal blocks due to different phase equilibria upon solidification. It is also possible that the exothermic compounds used in the cupronickel study (8) were of a different activity level than those in the present work. Finally, the solidification and occurrence of a riser pipe suggested a source of error as shown in Figures 36 and 37. The use of only insulating topping gave a pipe in the riser from which shrinkage could be easily found radiographically if not by visual examination (Figure 36). On the other hand, piping was not evident for the other combinations of riser compounds as exemplified by the insulating topping and insulating sleeves in Figure 37. The casting was radiographically unsound, however a casting which had been radiographically sound may still not be pressure tight in very thin machined sections as discussed previously.

Therefore some variation in the risering curves (Figures 34 and 35) should be anticipated. It would be possible to have particular combinations of riser compounds disperse the shrinkage to the point where radiography would not reveal a defective casting. These interpretations could only be evaluated through an extensive evaluation of pressure testing, thermal measurements and radiography. However if the next riser size higher is used as determined from the risering curves, the castings would indicate X-ray quality sound castings.

PRODUCTION OR EXAMPLE CASTING

The incorporation of this section has been to illustrate the utility and flexability of the data; in particular the riser size and placement information. Therefore a rather complete analysis of the problem has been included.

First, consider the casting geometry as shown in Figure 38. Through straightening of the 90° ell and then unrolling of the cylinder, a plate has been approximated with dimensions of 5-1/2" x 5-5/8" x 5/8".

$$\text{Equivalent length} = 4\text{-}1/8'' + 1\text{-}1/2'' = 5\text{-}5/8''$$

$$\text{Equivalent width} = \text{median circumference} = 5\text{-}1/2''$$

The volume of the casting (V_c) and the shape factor ($(L+W)/T$) can then be calculated.

Secondly, it was decided to use H/D values for the riser which would be equal to one. Although the curves have been given for insulating topping (Figures 24 and 25), they had not been provided for exothermic topping which was to be used for two of the castings. However a replot of points from Figure 30 for H/D = 1.0 on Figure 31 would give a new risering curve for exothermic topping. It should be noted that this is only possible because the risering curves are parallel when the H/D value is changed, as seen in Figure 25. The summary of data used for the minimum riser determination is therefore given below when $(L+W)/T$ is extrapolated to 17.8.

Type	H/D	V_r/V_c	H and D	Feeding Distance*
Insulating Topping	1.0	0.73	2.6"	1.5"
Exothermic Topping	1.0	0.265	1.9"	1.9"

Three castings were poured from the same heat to illustrate the following:

1. Correct riser size with inadequate feeding due to riser placement at one end of the ell with the other end chilled.

2. Adequate feeding with a top riser at the reentrant corner, however with an inadequate size riser.

3. Correct riser size and placement.

The three finished castings with the gates removed and the risers still in place are shown in Figure 39. In each case the riser attachment area was decreased to facilitate riser removal.

1. Consider first the correct riser size with poor riser position. The riser was to be covered with exothermic topping; therefore with $(L+W)/T = 17.8$ (Figure 38) and $H/D = 1.0$ (interpolation from Figures 30 and 31) the volume ratio V_r/V_c is equal to 0.265. Since the $V_c = 19.4$ in.^{3}, $V_r = 5.14$ in.^{3} or $H = D = 1.9$ which is the minimum riser size. If a safety factor of 1/4" is added to this riser, the size would be H = D = 2-1/8".

The feeding distance of a riser placed at one end of a 5/8" thick plate chilled on one end would be: FD = T + 2-1/4" = 2-7/8". The total feeding from the edge of the riser would then be: D + 2-7/8" = 2-1/8" + 2-7/8" = 5" whereas the casting is 5-5/8" long. Therefore the feeding would be inadequate.

A section of the casting is shown in Figure 40. As might be expected, the shrinkage has broken through to the cope surface of the cored section and is most prevalent at the hot spot or reentrant corner.

2. Since the riser placement above was incorrect, assume the same riser size (H = D = 2-1/8"); however centrally located the riser at the corner. The potential feeding distance is 2-7/8" if both ends are chilled. The riser would feed 2-7/8" + 2-1/8"/2 or approximately 4" in either direction which of course is much longer than required.

*Feeding Distance = 5-5/8" - D/2 for the top riser centrally placed (see Figure 38).

However assume insulating topping to be substituted for the exothermic. From Figure 25 at $H/D = 1.0$ $V_r/V_c = 0.73$ with $V_c = 19.4$ in.^{3}; $H = D = 2.6"$ whereas only a 2-1/8" riser has been used. The result is clearly shown in Figure 41. The shrinkage pipe has been drawn down into the casting. A 2-3/4" riser ($H = D$) with insulating topping would probably have given a sound casting.

3. Finally, the use of a 2-1/8" diameter riser top placed at the corner with both ends chilled would give a sound casting if exothermic riser topping was used. The resultant casting is shown in Figure 42. A radiograph of the sectioned component also indicated it to be sound. Some surface imperfection was evident at the cored surface, however a core wash would undoubtedly alleviate the situation.

It is therefore evident that the castability data obtained for Conisibe alloy can be applied to a production shape. It is then possible to consistently produce high integrity castings from this material.

CONCLUSIONS

The comparison between Cunisibe alloy and 70-30 cupro-nickel has indicated a similarity between the two materials. In almost every instance the castability for Cunisibe has been shown to be somewhat superior. These indices have included:

1. Slightly higher fluidity.
2. Low susceptability to hot tears.
3. Lower thermal gradients to produce radiographically sound section.
4. Longer feeding distance in bars.
5. Smaller size risers to produce a radiographically sound section (dependent upon riser compounds).

Supplementary data have also been generated for melting and pouring practices, feeding distances in plate sections, riser sizes for various combinations of insulating and exothermic compounds, and pressure testing of selected thin sections. Finally all of these data have been applied to a small illustrative casting.

Therefore a complete set of castability data for Cunisibe alloy has resulted which would direct the foundry man to the production of high integrety castings.

The authors wish to acknowledge the excellent laison with Mr. M. L. Foster and Mr. J. R. Crisci of the U. S. Naval Applied Science Laboratory.

BIBLIOGRAPHY

1. Trojan, P. K. and Flinn, R. A., "Pressure Tightness in 85-5-5-5 Bronze Castings," Trans. AFS, 64, 339-343 (1956).

2. Trojan, P. K. and Flinn, R. A., "Pressure Tightness in 85-5-5-5 Bronze Castings," Trans. AFS, 65, 238-246 (1957).

3. Flinn, R. A., "Copper, Brass, and Bronze Castings; Their Structures, Properties, and Applications," Non-Ferrous Founders Society, 121 (1963).

4. Gamber, E. J., "Hot Cracking Test for Light Metal Alloys," Trans. AFS, 67, 237-241 (1959).

5. Flinn, R. A. and Mielke, C. R., "Pressure Tightness of 85-5-5-5 Bronze," Trans. AFS, 67, 385-392 (1959).

6. Flinn, R. A. and Kunsmann, H., "Copper Base Casting Alloys—Physical Properties and Void Volume Correlation with Solidification," Trans. AFS, 69, 208-220 (1961).

7. Weins, M. J., de Botton, J.L.S., and Flinn, R. A., "Data for Calculation of Riser Placement in Copper Alloy Castings," Trans. AFS, 72, 832-839 (1964).

8. Rotė, F. E., Guichelaar, P. J., and Flinn, R. A., "Riser Design for Copper Alloys of Narrow and Extended Freezing Ranges," Trans. AFS, 74, 380-388 (1966).

TABLE I

CHEMICAL ANALYSIS OF CUNISIBE METAL INGOT

	Ingot Identification					
	BRO - 101		BRO - 102		BRO - 103	
Element	Avg.	Range	Avg.	Range	Avg.	Range
Cu	65.42	65.36-65.47	65.47	65.26-65.64	65.92	65.88-65.99
Ni	30.60	30.48-30.82	30.32	30.04-30.70	30.11	30.00-30.22
Mn	1.32	1.30- 1.34	1.35	1.33- 1.37	1.29	1.28- 1.31
Fe	1.07	.99- 1.11	1.01	1.00- 1.02	.99	.94- 1.04
Pb	<.01	<.01	<.01	<.01	<.01	<.01
P	<.01	<.01	<.01	<.01	<.01	<.01
S	.006	.003- .009	.005	.003- .007	.006	.003- .009
Si	1.02	.98- 1.14	1.08	1.05- 1.11	1.09	1.05- 1.13
Be	.54	.53- .56	.57	.51- .62	.52	.48- .54
C	.02	.02- .03	.02	.02- .03	.02	.02- .03
Cb	<.01	<.01	<.01	<.01	<.01	<.01
Amount Shipped (lb)	167		165		170	

TABLE II

SUMMARY OF HEATS

Heat Number	Charge Material	Castings Poured	Analysis Cu	Ni	Be	Si	Mn	Fe	S	C
319	Cunisibe	2 x 2 x 12 Castability bar	66	30	0.34 0.40	0.55 0.53	1.31 1.32	0.082 0.082	.005 .004	0.06 0.05
320	Cu-Ni	2 x 2 x 12 Castability bar Fluidity Spirals								
321	Cu-Ni	Hot Tear Casting and Fluidity Spirals	66.37 66.36	31.90 31.90	0 09 0.09	0.43 0.46	0.39 0.38	0.81 0 81	0.008 0.009	<0.01
322	95# 103	Fluidity Spirals and "Y" Blocks			0.52 0.54	1.17 1.15				
323	72# 103	Hot Tear Casting and Fluidity Spirals			0.52 0.50	1.16 1.20				
324	80# 322 25# 323	Feeding Distance, Bars			0.45 0.46	1.17 1.16				
325	108# 102	Feeding Distance, Bars			0.53 0.53	1.08 1.07				
326	110# 101	Feeding Distance, Bars			0.50 0.49	1.04 1.03				
327	58# 102 72# 325	Feeding Distance, Bars			0.53 0.54	1.08 1.07				
328	70# 101 60# 326	Feeding Distance, Bars								
329	18# 325 98# 327	Feeding Distance, Bars								
330	25# 323 55# 324	Feeding Distance, Bars								
331	22# 326 60# 328	Feeding Distance, Bars								
332	80# 329	2 x 2 x 10 Castability Bar Feeding Distance, Plate	65.81 65.81	30.30 30.30	0.35 0.32	1.01 1.04	1.34 1.35	1.14 1.14	0.002 0.003	0.02 0.02
333	70# 331	Feeding Distance, Plates	65.47 65.45	30.70 30.70	0.31 0 31	0.98 0.99	1.33 1.32	1.15 1.15	0.002 0.002	0.02 0.02

Table II (Continued)

Heat Number	Charge Material	Castings Poured	Analysis							
			Cu	Ni	Be	Si	Mn	Fe	S	C
334	25# 323 65# 330 5# 333	Feeding Distance, Plates	65.97 65.90	30.20 30.20	0 30 0.37	1.15 1.14	1.29 1.30	1.09 1.10	0.003 0.003	0.01 0.01
335	15# 333 82# 334	Feeding Distance, Plates	65.99 66.07	30.30 30.20	0.35 0.36	1.00 1.03	1.28 1.28	1.02 1.02	.002 .003	.05 .05
336	10# 327 70# 332 15# 333	Feeding Distance, Plates	65.77 65.66	30.50 30.60	0.40 0.39	0.94 0.91	1.31 1.30	1.06 1.05	.002 .002	.04 .04
337	19# 333 82# 335	Feeding Distance, Plates	65.77 65.84	30.60 30.60	0.34 0.35	0.94 0.90	1.29 1.29	1.03 1.02	.004 .003	.04 .04
338	42# 328 7-1/2# 332 3-1/2# 335 82# 336	Riser Size, Bars	65.51 65.58	31.00 30.90	0.40 0.39	0.63 0.67	1.34 1.33	1.09 1.09	.003 .003	.04 .04
339	80# 327 7-1/2# 332 14-1/2# 333 3-1/2# 335 2# 336	Riser Size, Bars	65.83 65.74	30.50 30.50	0.32 0.34	1.00 1.02	1.30 1.30	1.02 1.01	.004 .003	.05 .05
340	110# 338	Riser Size, Bars and Plates	65.62 65.58	30.60 30.50	0.34 0.34	1.02 1.04	1.36 1.36	1.02 1.02	.003 .004	.04 .05
341	4# 328 4# 329 4# 330 4# 331 4# 336 80# 339	Riser Size, Bars and Plates	65.80 65.76	30.50 30.50	0.39 0.40	0.97 0.99	1.35 1.36	0.99 0.99	.003 .003	.03 .02
342	13-1/2# 325 10# 338 95-1/2# 340	Riser Size, Bars and Plates	65.65 65.65	30.50 30.50	0.43 0.45	1.01 1.02	1.36 1.36	0.98 0.99	.003 .004	.03 .04
343	12# 339 90# 341	Riser Size, Bars	65.80 65.76	30.40 30.40	0.40 0 40	1.01 1.01	1.35 1.35	0.99 0.99	.003 .003	.04 .04
344	4-1/2# 324 6# 325 85# 343 8# cuBe	Riser Size, Bars								

Heat Number	Charge Material	Castings Poured	Analysis Cu	Ni	Be	Si	Mn	Fe	S	C
345	7-1/2# 340 1# 341 101-1/2# 342 10# CuBe	Riser Size, Bars and Plates								
346	4# 394 4# 337 92# 344	Riser Size, Bars Feeding Distance, Bars								
347	110# 345	Riser Size, Bars and Plates								
348	90# 346	Feeding Distance, Plate Riser Size, Bars								
349	84-1/2# 348	Riser Size, Bars								
350	4# 326 2-1/2# 328 2-1/2# 329 99# 347	Riser Size, Bars and Plates								
351	77# 349 17# 350	Riser Size, Bars and Plates								
352	80# 350 8# 351	Riser Size, Bars								
353	74# 351 20# 352	Riser Size, Plates								
354	60# 352 40# 353	Riser Size, Bars and Plates								
355	48# 353 42# 354	Riser Size, Bars and Plates								
356	44# 354 80# 355	Riser Size, Bars and Plates								
357	90# 356	Riser Size, Bars, Plates and Cubes								
358	5# 355 20# 356 80# 357	Riser Size, Plates and Cubes								
359	96# 358	Riser Size, Bar and Cube Feeding Distance, Plates								

Table II (Concluded)

Heat Number	Charge Material	Castings Poured	Analysis							
			Cu	Ni	Be	Si	Mn	Fe	S	C
360	5# 358 85# 359	Riser Size, Plate Feeding Distance, Plates								
361	2# 326 4# 327 4# 337 82# 360	Hot Tear Casting Problem Casting Feeding Distance, Plates								
362	1-1/2# 336 1-1/2# 337 84# 361 8# chem samples	Problem Casting Feeding Distance, Plates								

Note: As the report was being published, several chemical analyses had still not been completed. Upon availability of this information, it would be forwarded to the Contractor to complete the tabular data.

TABLE III

FEEDING DISTANCE DATA FOR BAR CASTINGS OF CUNISIBE

Casting Number	Casting Size (in.)	Condition	Distance Sound (in.) From End	Distance Sound (in.) From Riser	Soundness
346-3	1/4 x 1/4 x 4		3/4	5/8	No
346-3	1/4 x 1/4 x 2-7/8	Chilled	5/8	3/8	No
346-3	1/4 x 1/4 x 2		-	-	Yes
346-3	1/4 x 1/4 x 3		5/8	3/8	No
346-3	1/4 x 1/4 x 2-1/2	Unchilled	1/2	1/4	No
346-3	1/4 x 1/4 x 1-7/8		-	-	Yes
336-5	1/2 x 1/2 x 7		1-1/4	2	No
336-5	1/2 x 1/2 x 6	Chilled	1-3/8	1-3/4	No
346-3	1/2 x 1/2 x 5		1-3/4	1	No
346-3	1/2 x 1/2 x 4		-	-	Yes
336-5	1/2 x 1/2 x 6		1	3/4	No
336-5	1/2 x 1/2 x 5	Unchilled	1	3/4	No
346-3	1/2 x 1/2 x 4		1	1/2	No
346-3	1/2 x 1/2 x 3		-	-	Yes
324-3	1 x 1 x 10		*	*	No
325-5	1 x 1 x 9		5-1/2	0	No
326-1	1 x 1 x 8	Chilled	-	-	Marginal
324-1	1 x 1 x 7		-	-	Yes
325-3	1 x 1 x 6		-	-	Yes
325-1	1 x 1 x 5		-	-	Yes
324-4	1 x 1 x 10		6	*	No
325-6	1 x 1 x 9		*	0	No
326-2	1 x 1 x 8	Unchilled	3	1	No
324-2	1 x 1 x 7		-	-	Yes
325-4	1 x 1 x 6		-	-	Yes
325-2	1 x 1 x 5		-	-	Yes
327-2	1-1/2 x 1-1/2 x 10		*	*	No
326-5	1-1/2 x 1-1/2 x 9	Chilled	-	-	Yes
326-3	1-1/2 x 1-1/2 x 8		-	-	Yes

*Clearcut contribution from the riser or end effect was difficult to interpret from the radiographs.

Table III (Concluded)

Casting Number	Casting Size (in.)	Condition	Distance Sound (in.) From End	Distance Sound (in.) From Riser	Soundness
326-6	1-1/2 x 1-1/2 x 9	Unchilled	3-1/4	2	No
326-4	1-1/2 x 1-1/2 x 8		4	1	No
327-1	1-1/2 x 1-1/2 - 7		-	-	Yes
327-3	2 x 2 x 10	Chilled	-	-	Yes
328-1	2 x 2 x 9		-	-	Yes
327-4	2 x 2 x 9	Unchilled	*	*	No
329-1	2 x 2 x 8		-	-	Yes
328-2	3 x 3 x 12	Chilled	-	-	Yes
330-1	3 x 3 x 11		-	-	Yes
329-2	3 x 3 x 11	Unchilled	-	-	Marginal
330-2	3 x 3 x 10		-	-	Yes

*Clearcut contribution from the riser or end effect was difficult to interpret from the radiographs.

TABLE IV

FEEDING DISTANCE DATA FOR PLATE CASTINGS OF CUNISIBE

Casting Number	Casting Size (in.)	Condition	Distance Sound (in.) From End	Distance Sound (in.) From Riser	Soundness
332-2	1/2 x 7 x 7	Chilled	*	1/4	No
333-1	1/2 x 6 x 6		2-1/4	1/2	No
333-2	1/2 x 5 x 5		1-3/4	1/2	No
335-4	1/2 x 4 x 4		2-1/8	1/8	No
336-3	1/2 x 3 x 3		2-1/2	1/16	No
362-4	1/2 x 2 x 2		-	-	Yes
362-4	1/2 x 1-1/2 x 1-1/2		-	-	Yes
333-3	1/2 x 5 x 5	Unchilled	1-1/2	1/4	No
333-4	1/2 x 4 x 4		1-1/2	1/8	No
335-3	1/2 x 3 x 3		1-1/2	0	No
362-4	1/2 x 2-1/2 x 2-1/2		*	*	No
336-4	1/2 x 2 x 2		1-5/8	1/8	No
362-4	1/2 x 1 x 1		-	-	Yes
335-2	1 x 6 x 6	Chilled	3	1/2	No
336-2	1 x 5 x 5		3-1/2	1/8	No
360-1	1 x 4 x 4		2-5/8	1/16	No
361-4	1 x 3 x 3		-	-	Yes
335-1	1 x 5 x 5	Unchilled	2-3/8	3/8	No
337-3	1 x 4 x 4		1-9/16	0	No
348-1	1 x 3 x 3		1-15/16	3/16	No
361-4	1 x 2 x 2		1-1/4	1/8	No
334-2	1-1/2 x 7 x 7	Chilled	4	5/8	No
336-1	1-1/2 x 6 x 6		3-3/4	0	No
337-1	1-1/2 x 6 x 6		3-3/4	0	No
359-4	1-1/2 x 5 x 5		3-1/4	0	No
360-2	1-1/2 x 4 x 4		3-3/8	1/8	No
361-3	1-1/2 x 3 x 3		-	-	Yes
334-1	1-1/2 x 6 x 6	Unchilled	3	1/2	No
337-2	1-1/2 x 5 x 5		2-1/2	0	No
359-3	1-1/2 x 4 x 4		1-7/8	3/16	No
360-3	1-1/2 x 3 x 3		1-1/4	1/4	No
361-3	1-1/2 x 2 x 2		1-1/8	3/16	No

*Clearcut contribution from the riser or end effect was difficult to interpret from the radiographs.

TABLE V

RISER SIZE DATA: SIDE RISERING, INSULATING TOPPING

Casting Number	Casting Size (in.)	H	D	H/D	V_r/V_c	(L+W)/T	Condition
338-4	2 x 2 x 8	3-1/4	6	0.54	2.87	5	Sound
343-1	2 x 2 x 8	3-1/4	5-3/8	0.605	2.60	5	Unsound
338-3	2 x 2 x 8	4-3/8	4-3/4	0.92	2.43	5	Sound
329-1	2 x 2 x 8	6	4	1.50	2.10	5	Sound
338-2	2 x 2 x 8	4-3/16	4-3/8	0.96	1.96	5	Sound
346-2	2 x 2 x 8	4	4	1.00	1.58	5	Unsound
339-4	2 x 2 x 8	3-1/2	4	0.875	1.38	5	Unsound
338-1	2 x 2 x 8	5-1/8	3-1/8	1.54	1.22	5	Sound
341-4	2 x 2 x 8	4-1/8	3	1.38	0.91	5	Unsound

TABLE VI

RISER SIZE DATA: TOP RISERING, INSULATING TOPPING

Casting Number	Casting Size (in.)	H	D	H/D	V_r/V_c	(L+W)/T	Condition
358-4	3 x 3 x 3	2-3/8	4-3/4	0.50	0.575	2	Unsound
345-4	2 x 2 x 8	1-5/8	6-5/8	0.25	1.76	5	Sound
343-3	2 x 2 x 8	2-1/2	5	0.50	1.54	5	Sound
347-1	2 x 2 x 8	1-9/16	6-1/4	0.25	1.50	5	Unsound
342-1	2 x 2 x 8	4	3-13/16	1.05	1.425	5	Sound
340-2	2 x 2 x 8	3	4-1/4	0.706	1.33	5	Sound
339-2	2 x 2 x 8	2-3/8	4-3/4	0.50	1.32	5	Unsound
343-2	2 x 2 x 8	4-3/16	3-3/8	1.24	1.17	5	Sound
340-1	2 x 2 x 8	3-5/8	3-5/8	1.00	1.165	5	Unsound
341-1	2 x 2 x 8	4-1/6	3-1/4	1.25	1.065	5	Unsound
339-3	2 x 2 x 8	3-1/4	3-1/4	1.00	0.845	5	Unsound
339-1	2 x 2 x 8	2	4	0.50	0.785	5	Unsound
342-4	1 x 5 x 5	3	4-1/2	0.67	1.90	10	Sound
345-2	1 x 5 x 5	2-1/4	4-1/2	0.50	1.43	10	Sound
341-2	1 x 5 x 5	2-1/8	4-1/4	0.50	1.205	10	Unsound
345-1	1 x 5 x 5	3-1/4	3-1/4	1.00	1.08	10	Sound
342-2	1 x 5 x 5	3-1/8	3-1/8	1.00	0.958	10	Unsound
340-3	1 x 5 x 5	2-7/8	2-7/8	1.00	0.745	10	Unsound
347-1	1 x 6 x 6	2-7/8	4-3/4	0.50	1.17	12	Sound
345-3	1 x 7 x 7	2-11/16	5-3/8	0.50	1.24	14	Sound
341-3	1 x 7 x 7	2-1/2	5	0.50	1.005	14	Unsound
342-3	1 x 7 x 7	3-13/16	3-13/16	1.00	0.886	14	Sound
340	1 x 7 x 7	3-3/8	3-3/8	1.00	0.615	14	Unsound

TABLE VII

RISER SIZE DATA: TOP RISERING, INSULATING TOPPING AND INSULATING SLEEVES

Casting Number	Casting Size (in.)	H	D	H/D	V_r/V_c	(L+W)/T	Condition
358-2	3 x 3 x 3	1-1/2	3	0.50	0.393	2	Unsound
344-2	2 x 2 x 8	2-1/8	4-1/2	0.50	1.05	5	Sound
344-3	2 x 2 x 8	3	3	1.00	0.665	5	Sound
344-1	2 x 2 x 8	1-1/16	4-1/2	0.25	0.53	5	Sound
346-4	2 x 2 x 8	2-1/2	2-1/2	1.00	0.381	5	Sound
348-4	2 x 2 x 8	1	3-7/8	0.258	0.369	5	Unsound
344-4	2 x 2 x 8	1-1/2	3	0.50	0.33	5	Marginal
349-2	2 x 2 x 8	1-7/8	2-1/2	0.75	0.286	5	Sound
349-1	2 x 2 x 8	2-1/4	2-1/4	1.00	0.28	5	Sound
350-3	2 x 2 x 8	2	2	1.00	0.196	5	Unsound
351-3	1 x 5 x 5	1-1/2	2-5/8	0.57	0.324	10	Sound
353-4	1 x 5 x 5	1-5/16	2-5/8	0.50	0.285	10	Unsound
350-5	1 x 5 x 5	1-1/4	2-1/2	0.50	0.245	10	Unsound
350-4	1 x 7 x 7	1-3/8	2-3/4	0.50	0.167	14	Unsound
351-4	1 x 7 x 7	1-9/16	3-1/8	0.50	0.246	14	Unsound
354-4	1 x 7 x 7	1-11/16	3-3/8	0.50	0.306	14	Unsound
358-1	1 x 7 x 7	1-3/4	3-1/2	0.50	0.345	14	Sound

TABLE VIII

RISER SIZE DATA: TOP RISERING, EXOTHERMIC TOPPING

Casting Number	Casting Size (in.)	H	D	H/D	V_r/V_c	(L+W)/T	Condition
357-1	3 x 3 x 3	1-13/16	3-5/8	0 50	0.695	3	Unsound
348-2	2 x 2 x 8	3-3/8	3-3/8	1.00	0.945	5	Sound
352-2	2 x 2 x 8	1-5/16	5	0.26	0 800	5	Sound
350-1	2 x 2 x 8	1-15/16	3-7/8	0.50	0.718	5	Sound
354-1	2 x 2 x 8	1-7/8	3-3/4	0.50	0.647	5	Sound
351-2	2 x 2 x 8	1-13/16	3-5/8	0.50	0.585	5	Unsound
350-2	2 x 2 x 8	2-7/8	2-7/8	1.00	0.585	5	Sound
348-3	2 x 2 x 8	2-3/4	2-3/4	1.00	0.510	5	Unsound
353-1	1 x 5 x 5	1-11/16	3-3/8	0.50	0.605	10	Sound
354-2	1 x 5 x 5	1-5/8	3-1/4	0.50	0.54	10	Sound
356-1	1 x 5 x 5	1-9/16	3-1/8	0.50	0.481	10	Unsound
353-2	1 x 7 x 7	2-1/16	4-1/8	0.50	0.561	14	Sound
354-3	1 x 7 x 7	2	4	0.50	0.515	14	Sound
356-2	1 x 7 x 7	1-15/16	3-7/8	0.50	0.469	14	Sound
358-3	1 x 7 x 7	1-7/8	3-3/4	0.50	0.424	14	Sound
360-4	1 x 7 x 7	1-13/16	3-5/8	0.50	0.382	14	Unsound

TABLE IX

RISER SIZE DATA: TOP RISERED, EXOTHERMIC TOPPING AND EXOTHERMIC SLEEVES

Casting Number	Casting Size (in.)	H	D	H/D	V_r/V_c	(L+W)/T	Condition
359-1	3 x 3 x 3	1-3/4	3-1/2	0.50	0.625	2	Unsound
356-4	2 x 2 x 8	1-5/32	4-5/8	0.25	0.608	5	Sound
359-2	2 x 2 x 8	1-3/4	3-1/2	0.50	0.527	5	Sound
357-2	2 x 2 x 8	1-11/16	3-3/8	0.50	0.472	5	Unsound
352-4	2 x 2 x 8	1-1/16	4-1/4	0.25	0.470	5	Unsound
352-1	2 x 2 x 8	1-5/8	3-1/4	0.50	0.424	5	Unsound
352-3	2 x 2 x 8	1-3/4	3	0.58	0.388	5	Unsound
355-1	2 x 2 x 8	2-1/2	2-1/2	1.00	0.385	5	Sound
351-1	2 x 2 x 8	2-3/8	2-3/8	1.00	0.329	5	Unsound
349-4	2 x 2 x 8	2-1/8	2-1/8	1.00	0.236	5	Unsound
349-3	2 x 2 x 8	1-3/4	1-3/4	1.00	0 130	5	Unsound
357-3	1 x 5 x 5	1-9/16	3-1/8	0.50	0.479	10	Sound
355-4	1 x 5 x 5	1-1/2	3	0.50	0.424	10	Unsound
355-2	1 x 5 x 5	1-7/16	2-7/8	0.50	0.373	10	Unsound
356-3	1 x 7 x 7	1-7/8	3-3/4	0.50	0 424	14	Sound
357-4	1 x 7 x 7	1-13/16	3-5/8	0.50	0 382	14	Unsound
355-3	1 x 7 x 7	1-3/4	3-1/2	0.50	0.344	14	Unsound

Figure 1. Plate casting with a large top riser which shows the slice used for radiographic examination.

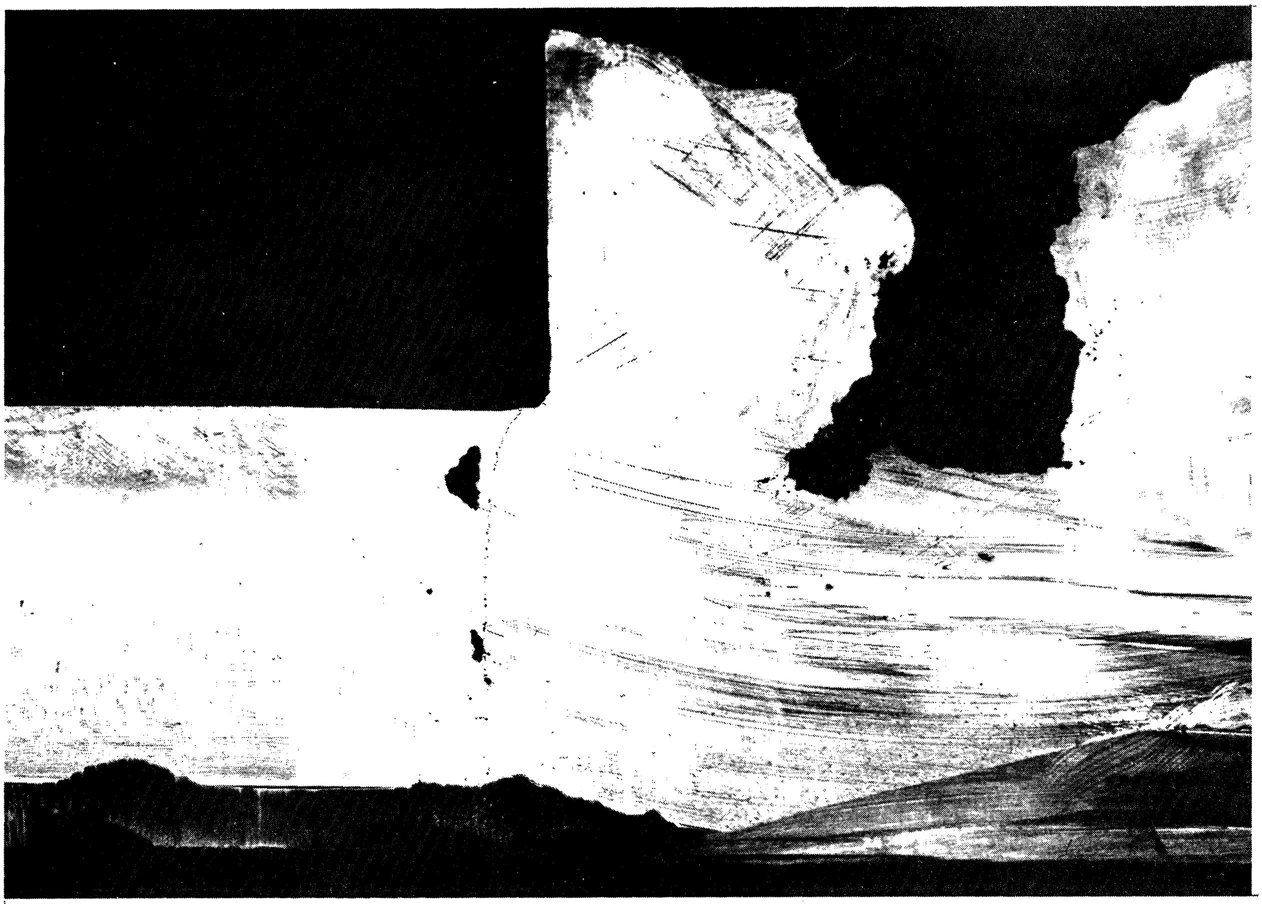

Figure 2. Section from a side risered bar with a molybdenum mesh dross trap between the casting and riser. If the mesh was inserted in the gating system the shrinkage defect would not occur.

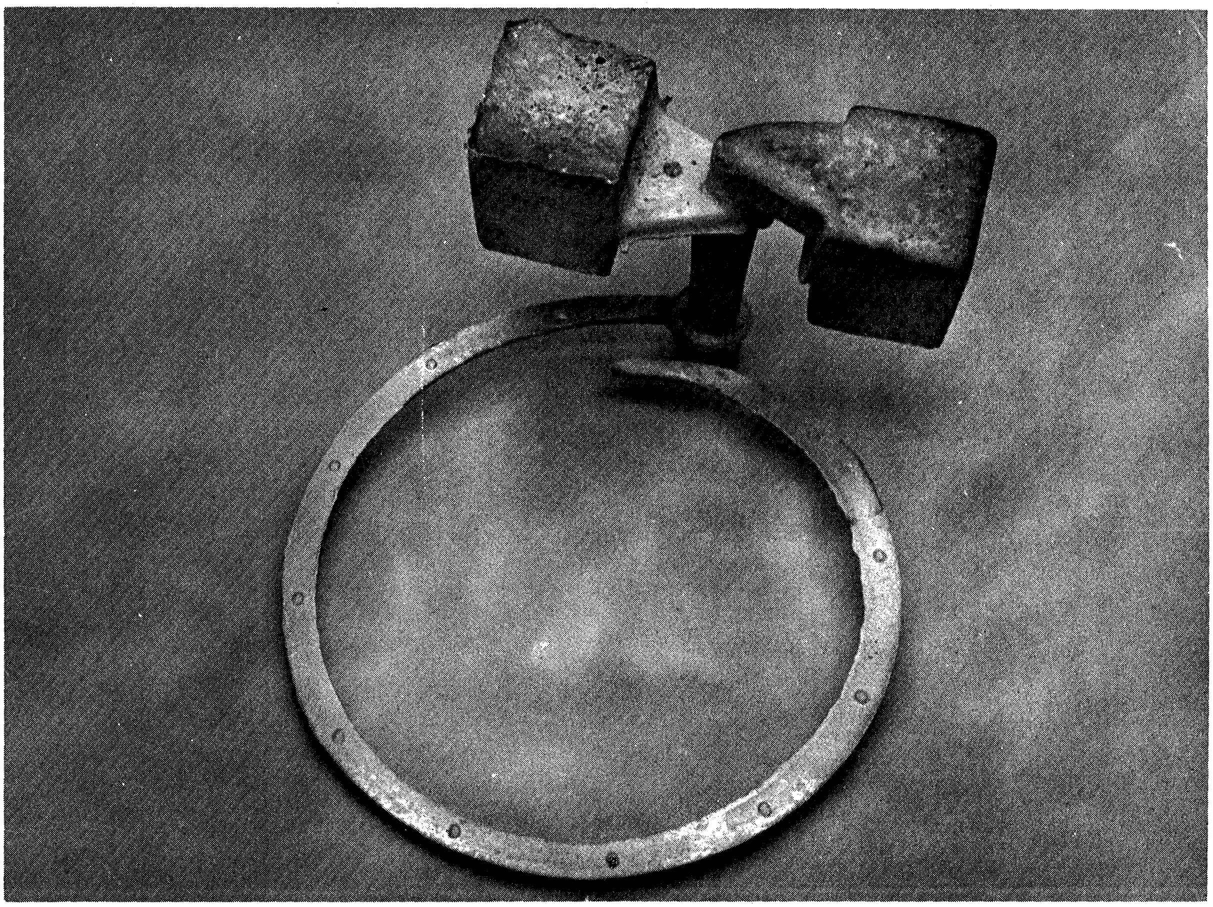

Figure 3. A typical fluidity spiral cast in 70-30 cupro-nickel. The particular spiral was cast with 250°F superheat with a resultant length of 25".

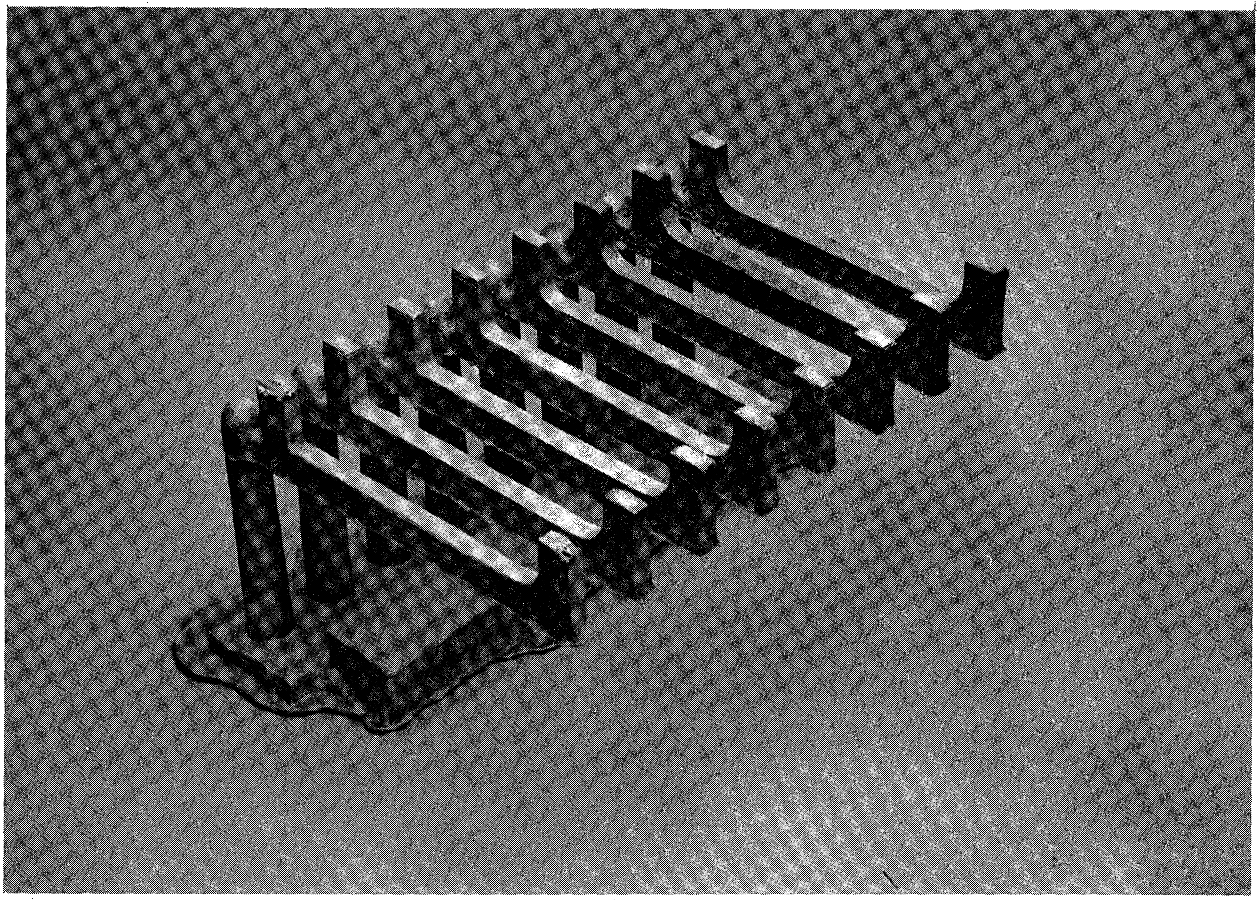

Figure 4. A typical hot tear casting assembly. One end of each leg has a 3/4" radius while the other radius progressively varies from 1/16" to 3/4" dependent upon the casting position. Each leg is 7" long.

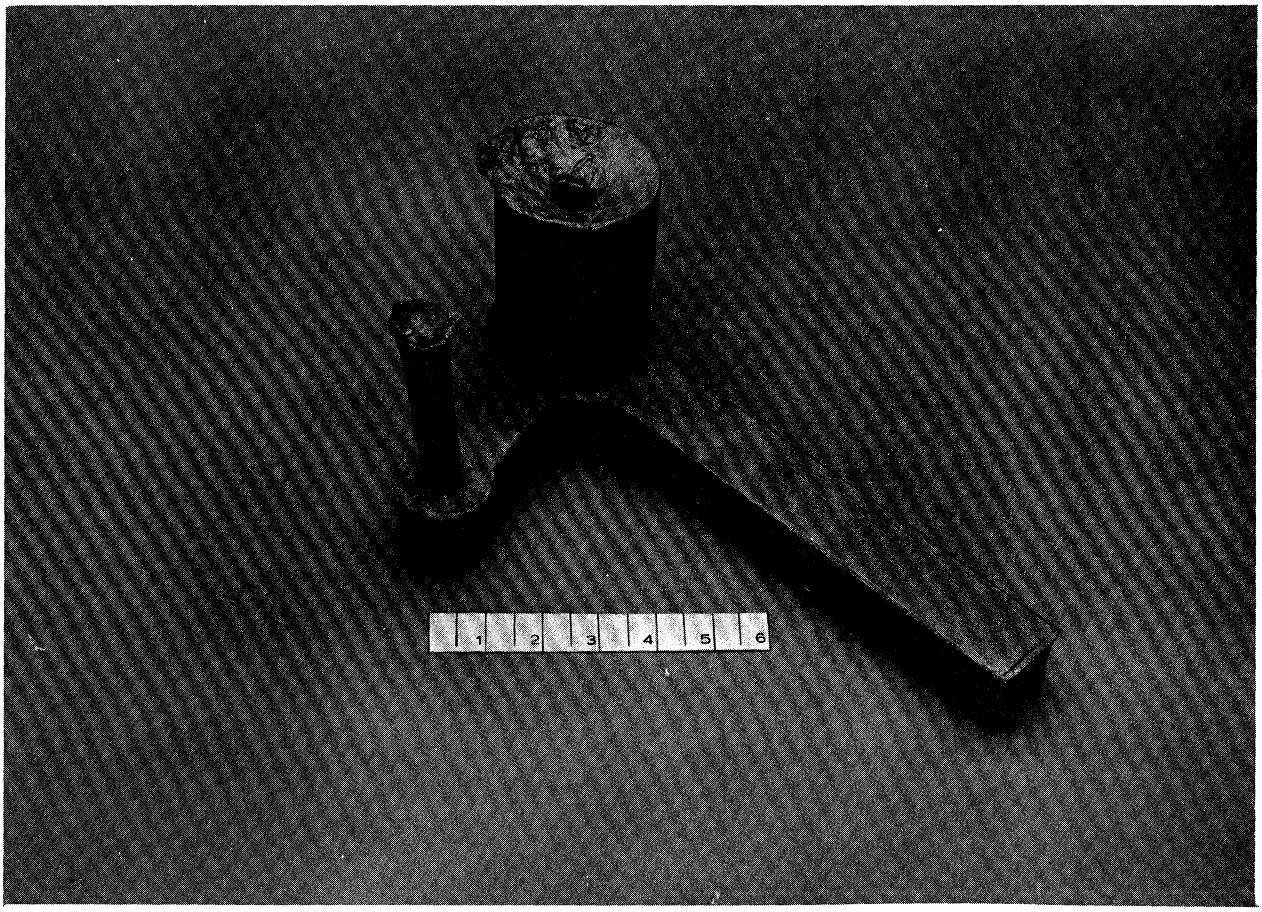

Figure 5. 1-1/2" x 1-1/2" x 10" end chilled bar. Gating and risering were similar to that used in the standard 2" x 2" x 12" castability bar (thermal gradient investigation).

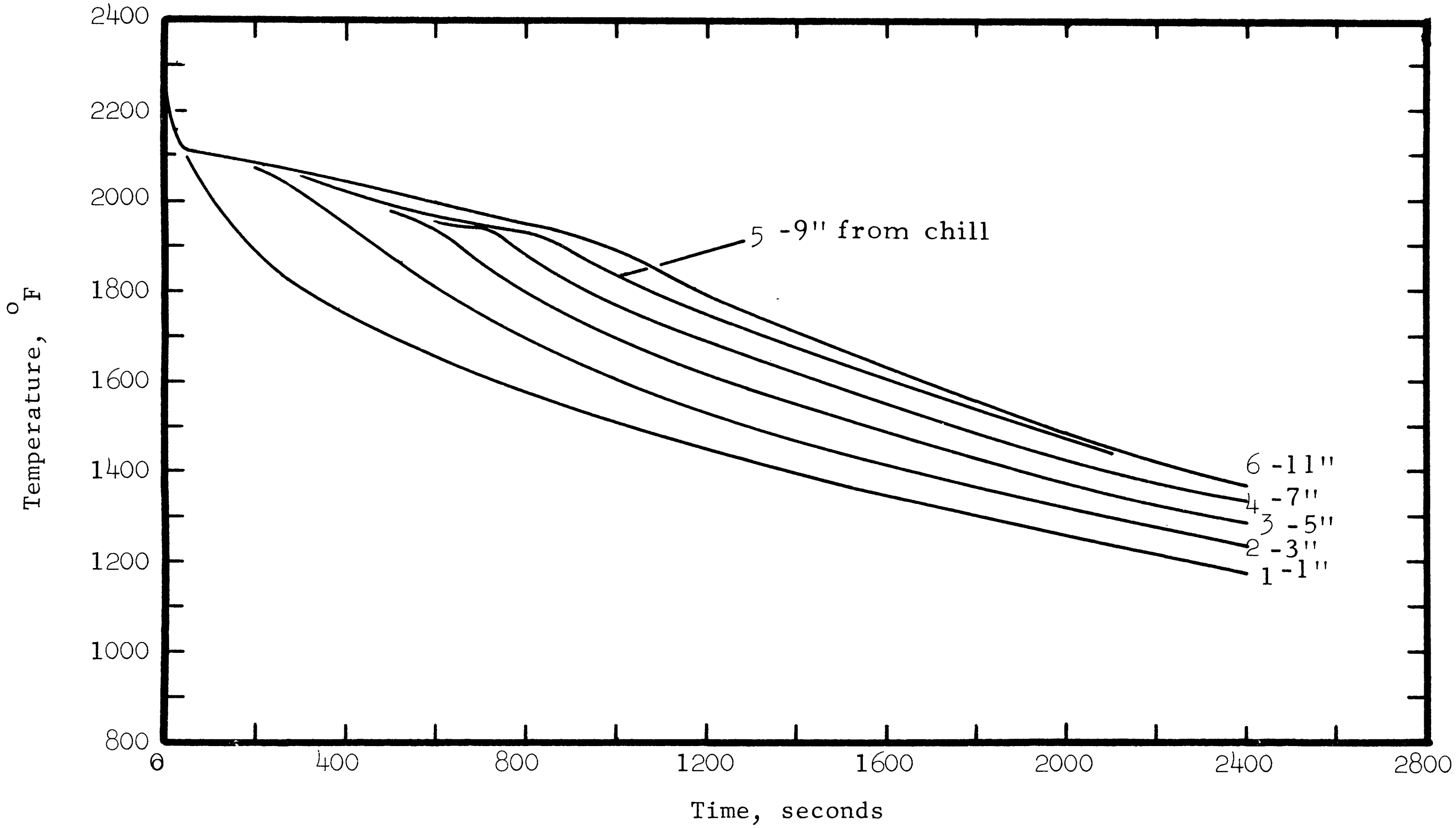

Figure 6. Cooling curves for a 2" x 2" x 12" bar; end chilled. Distances are referenced to the chilled end. No. 1 station is 1" from the chill or 11" from the riser. (Heat No. 319)

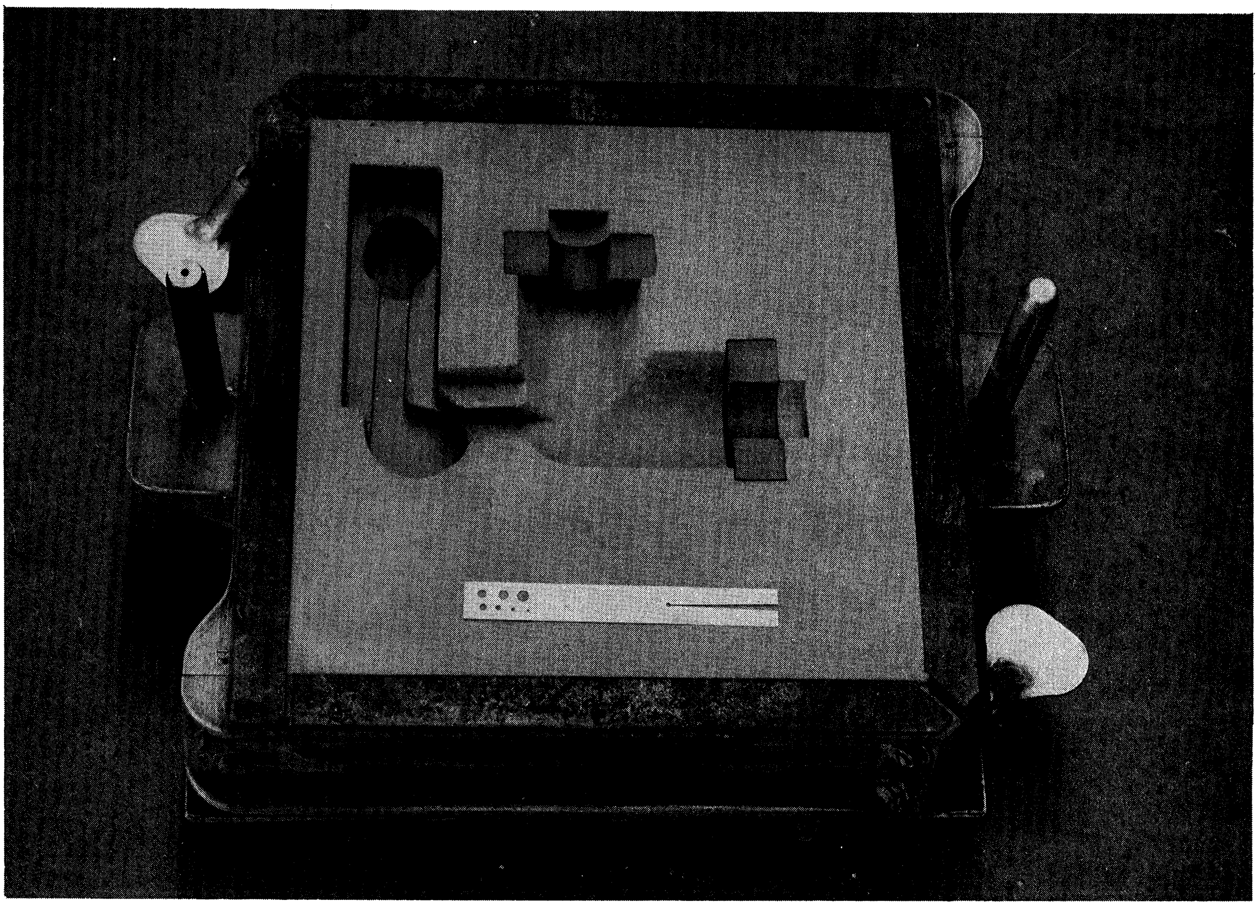

Figure 7. 1-1/4" 90° elbow drag cavity. The end chills are in place however the cores are removed to show the gating system.

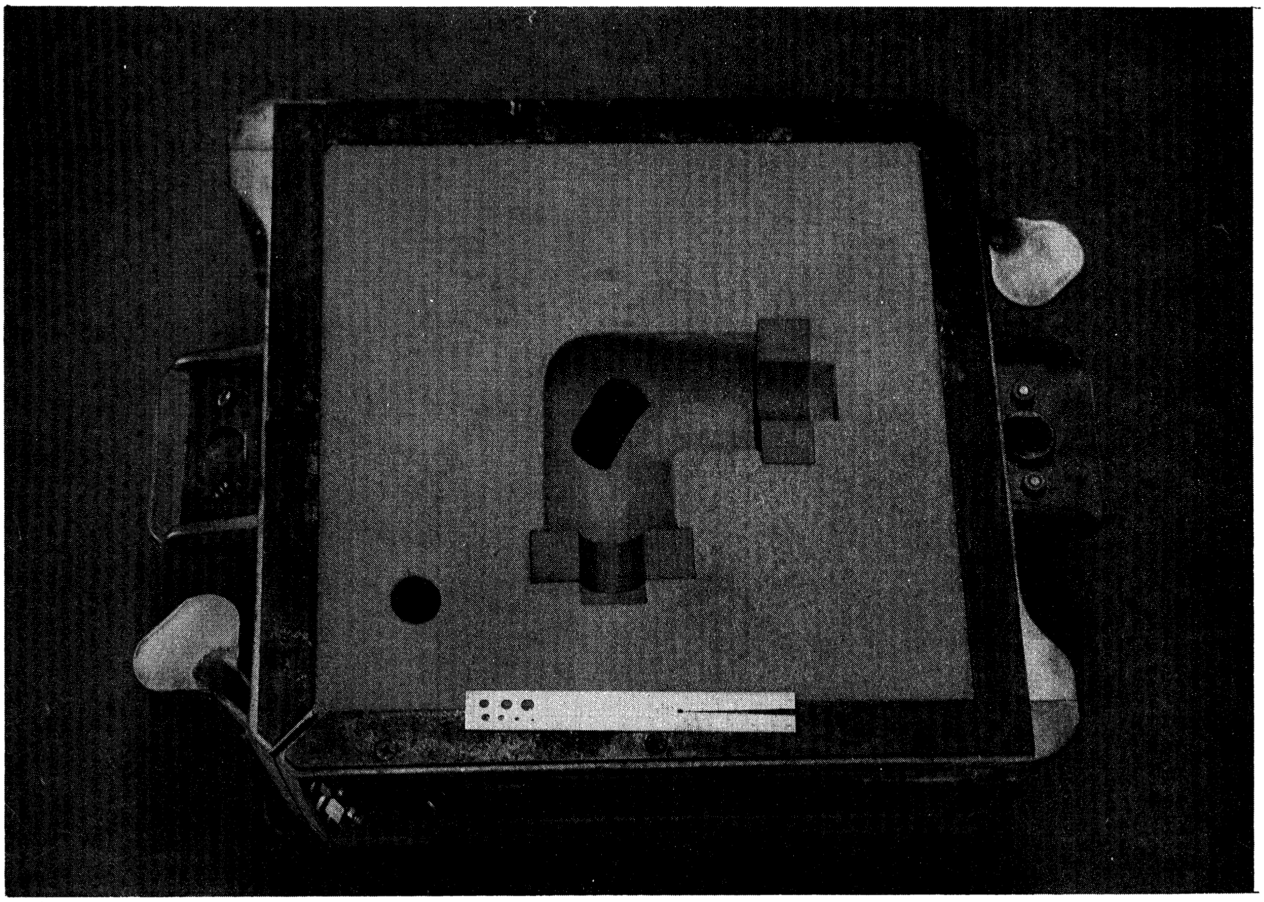

Figure 8. Open cope portion of the production casting. Anchors are attached to the cope chills to prevent their movement during mold handling. The top riser neck is attached at the reentrant corner.

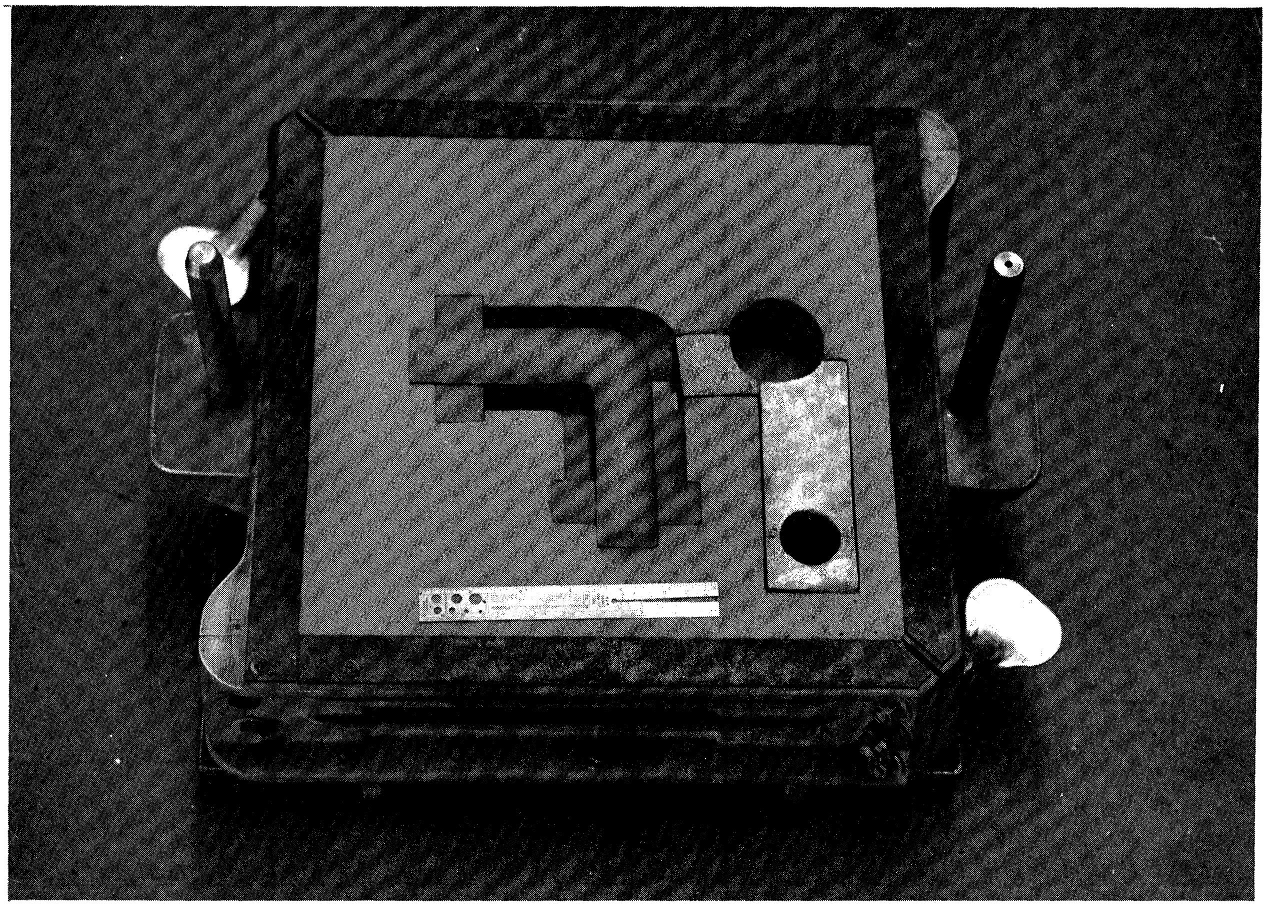

Figure 9. Drag section of the 1-1/4"-90° ell casting with all cores in place. Cores were made of CO_2 sand while the mold itself was dry sand.

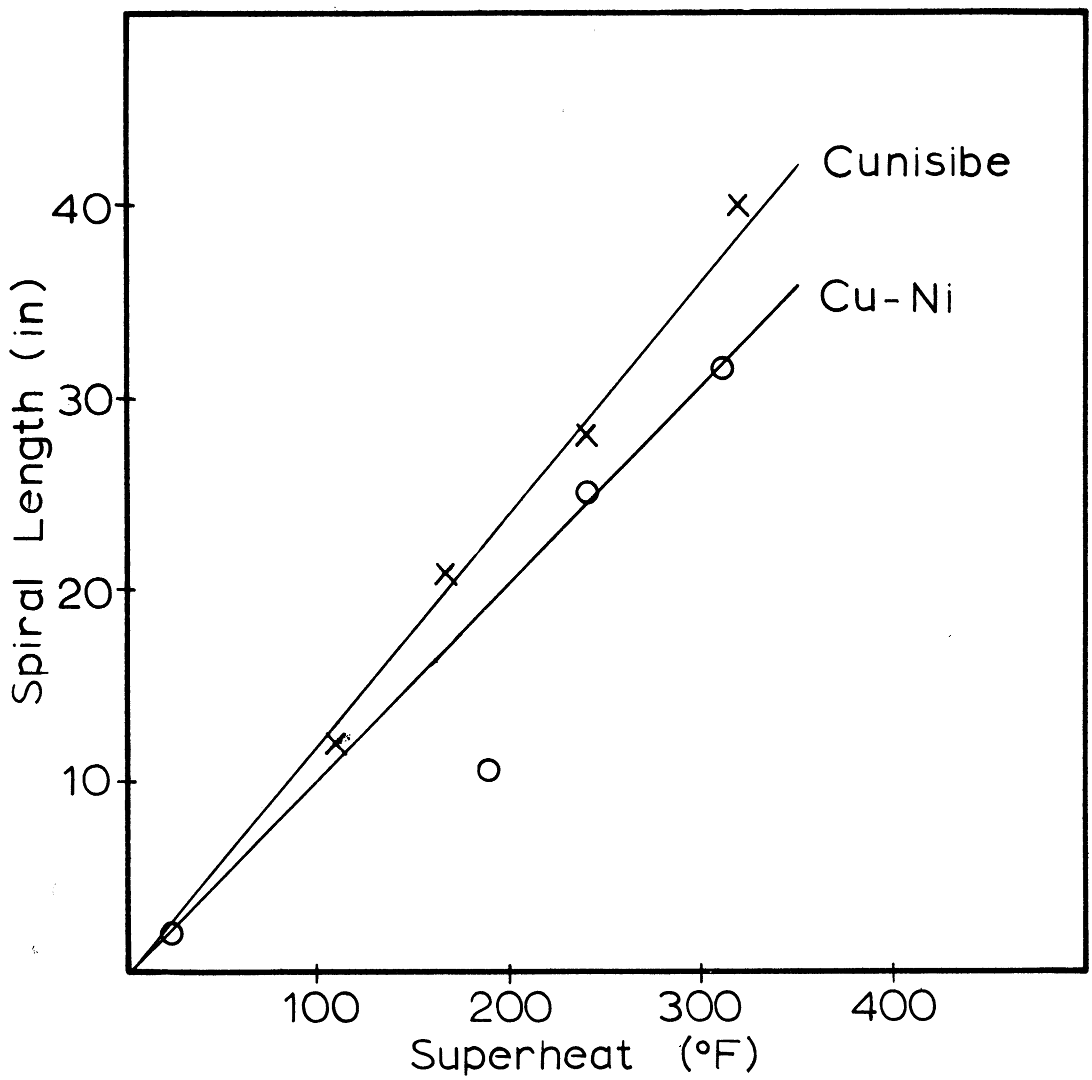

Figure 10. Fluidity Curves for Cunisibe and 70-30 cupro-nickel. Cunisibe liquidus - 2110°F; Cu-Ni liquidus - 2240°F.

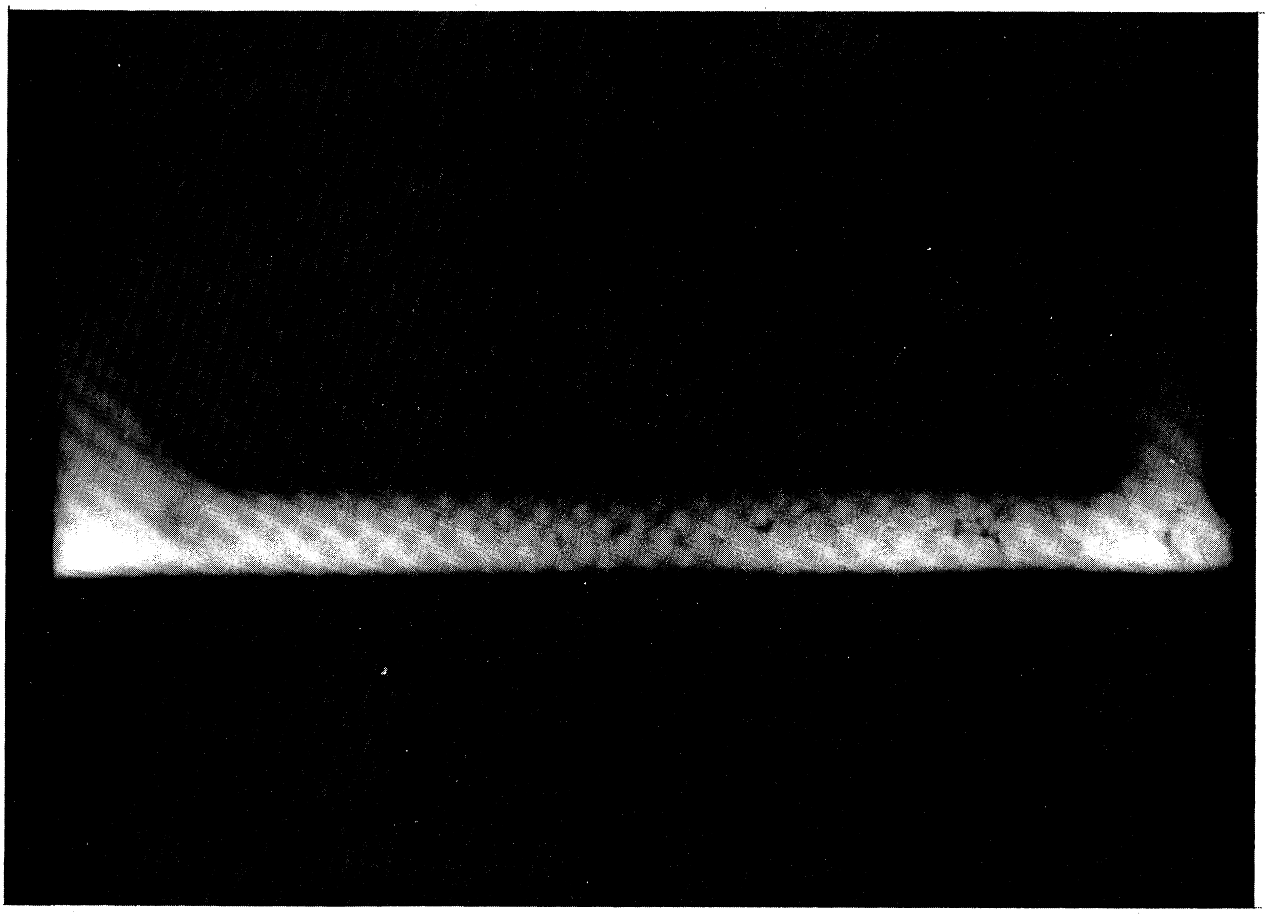

Figure 11. X-ray of a Cunisibe hot tear casting with a 1/16" radius cast in a CO_2 mold. The casting did not tear even though the fillet was smaller than would be considered good foundry practice.

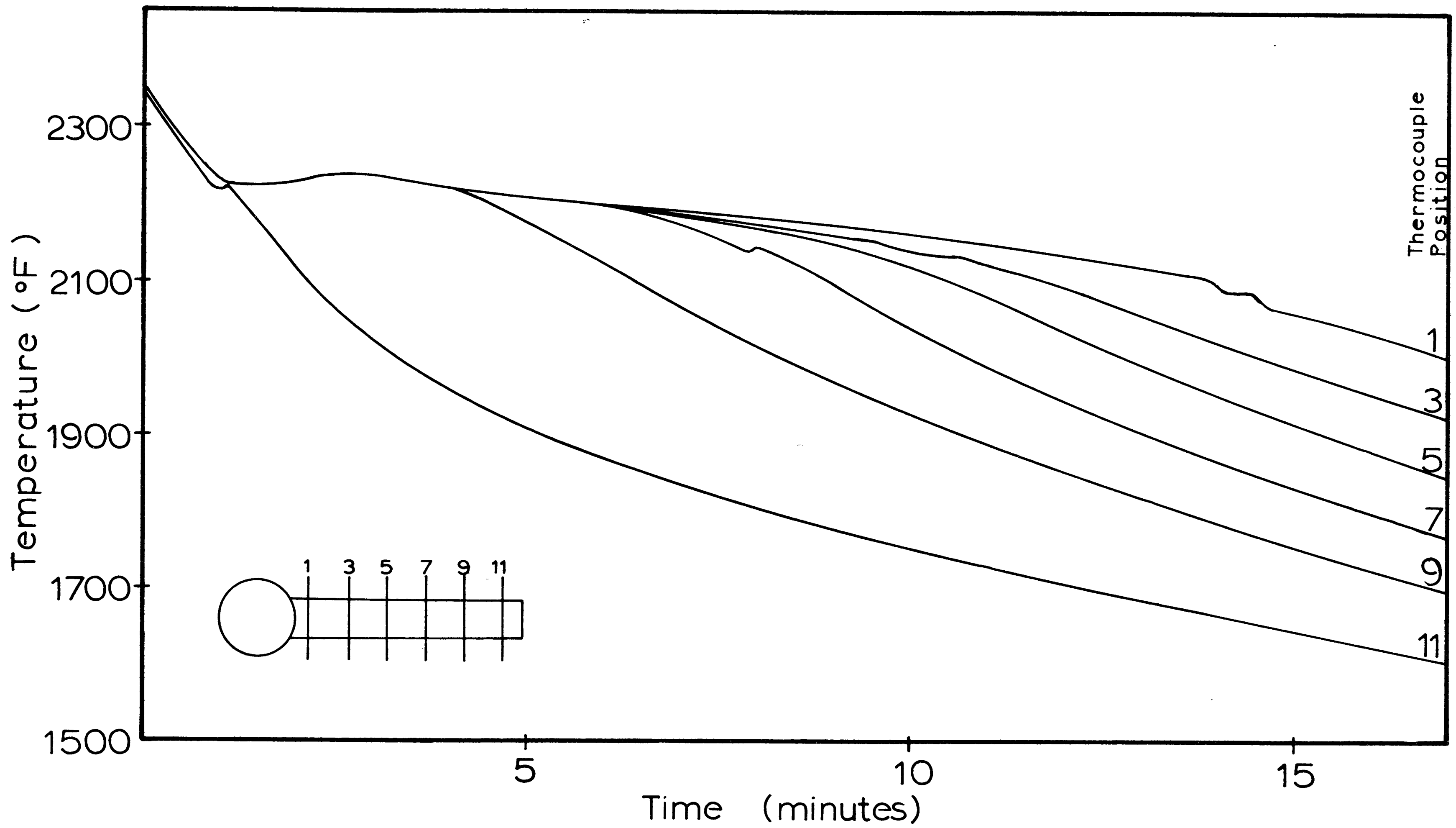

Figure 12. Cooling curves for 70-30 cupro-nickel cast in a 2" x 2" x 12" bar with an end chill. (Heat 320)

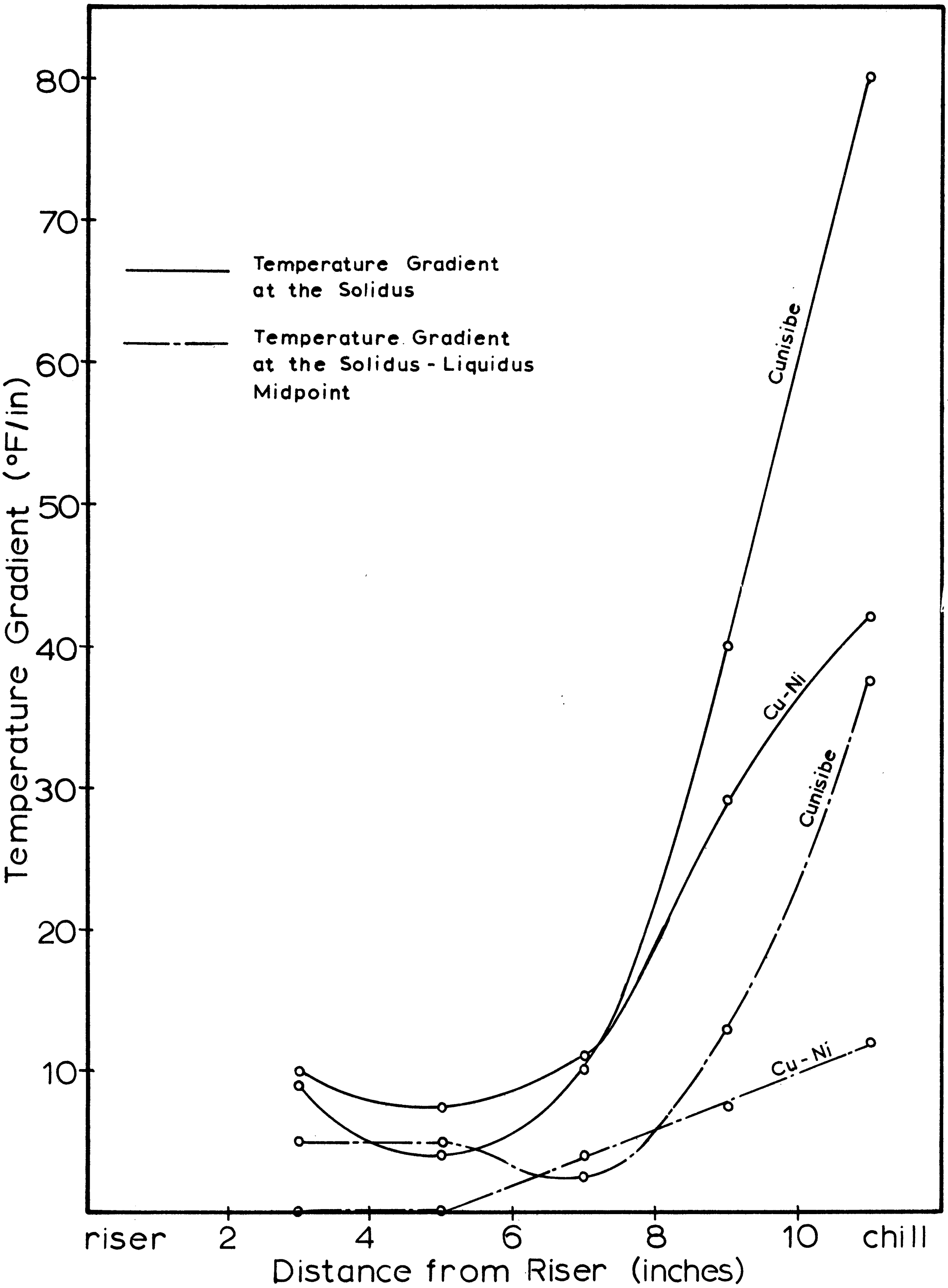

Figure 13. Thermal gradient curves for a 2" x 2" x 12" bar chilled at one end. The gradient has been determined by the secant method at two temperatures.

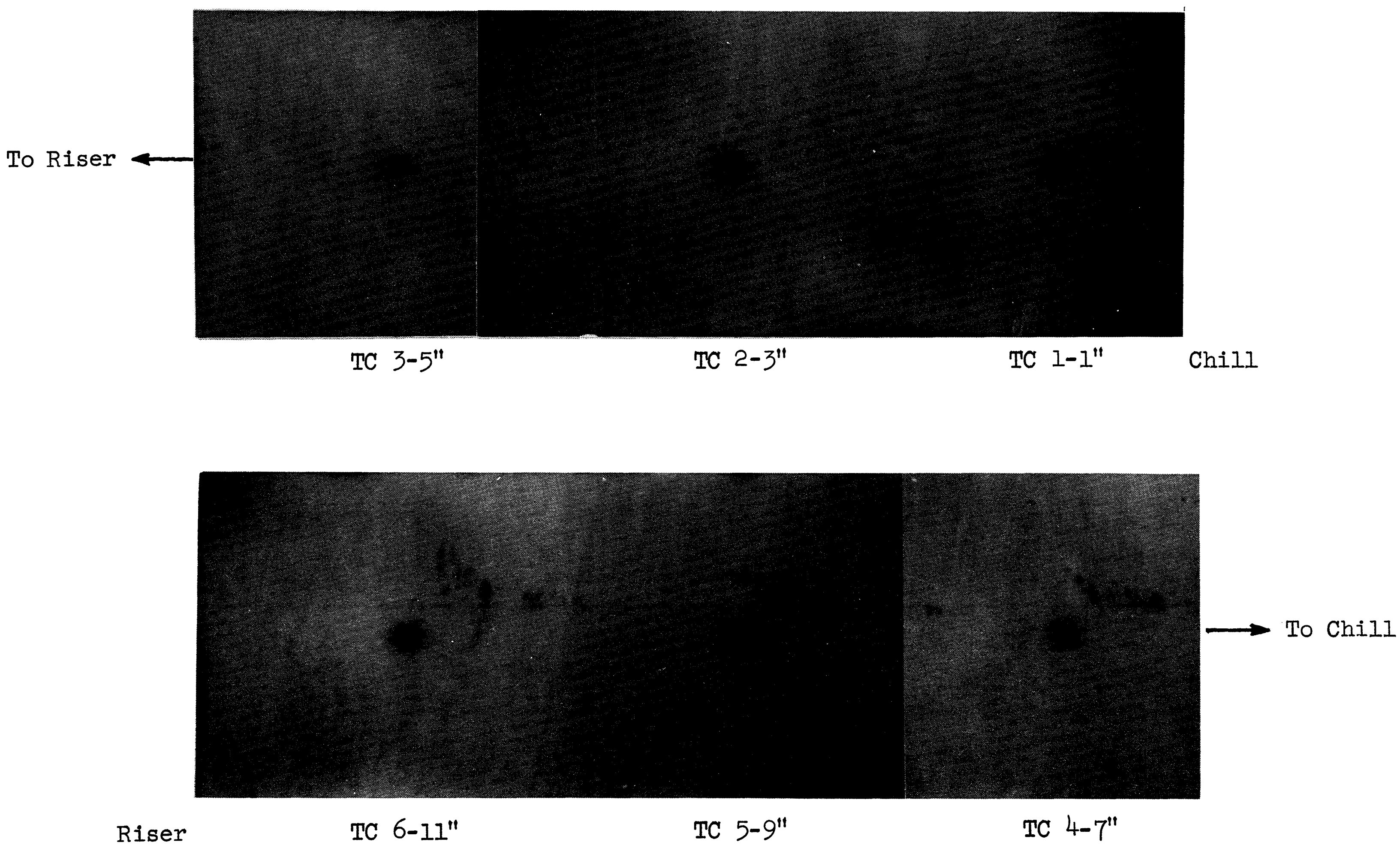

Figure 14. Radiograph of 1/2" vertical thick slice taken from the center of the bar. (X1) TCx refers to the thermocouple station number.

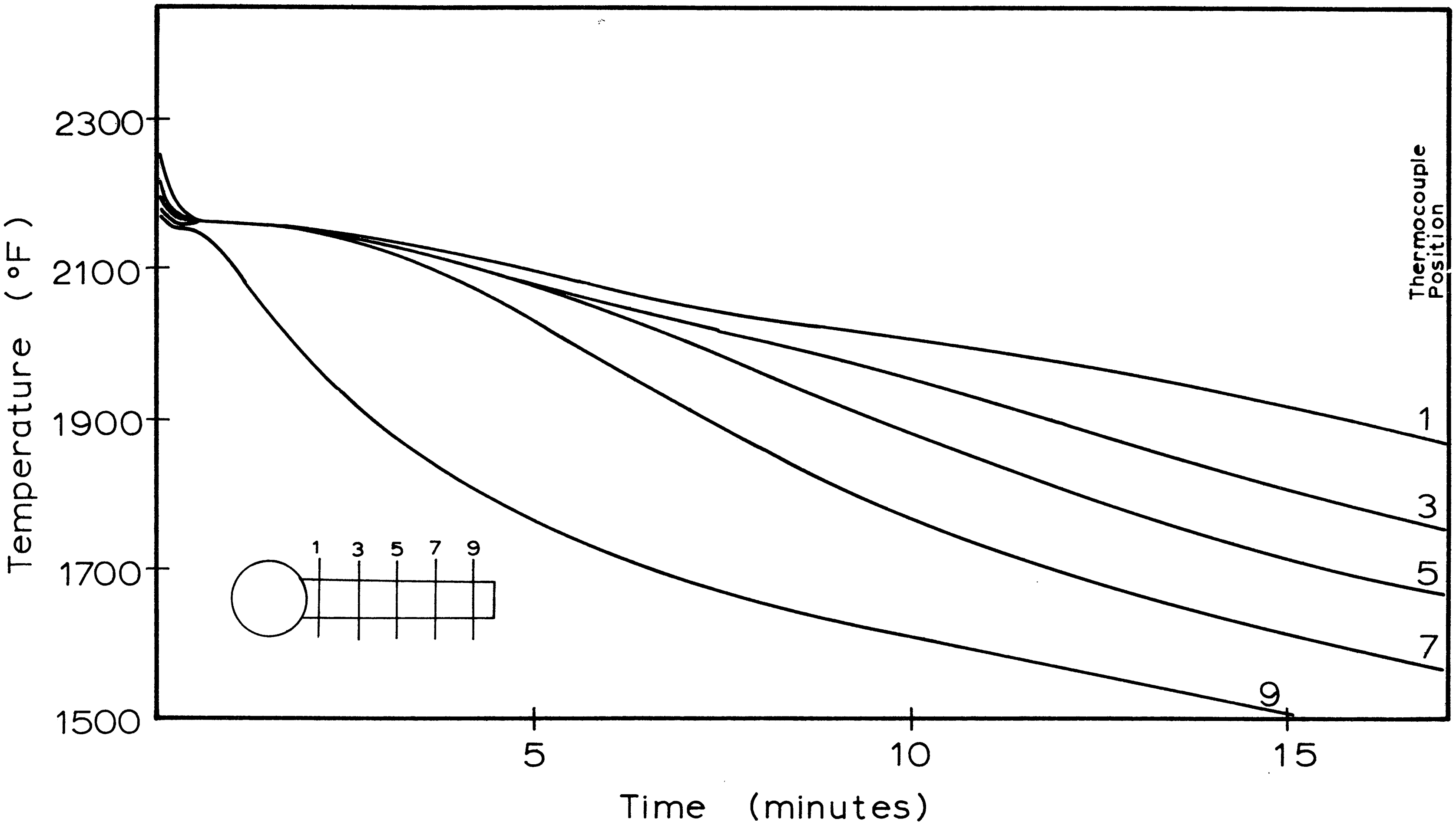

Figure 15. Cooling curves for a 2" x 2" x 10" end chilled bar cast from Cunisibe alloy. The more rapid cooling rates can be compared with a 2" x 2" x 12" bar as in Figure 6.

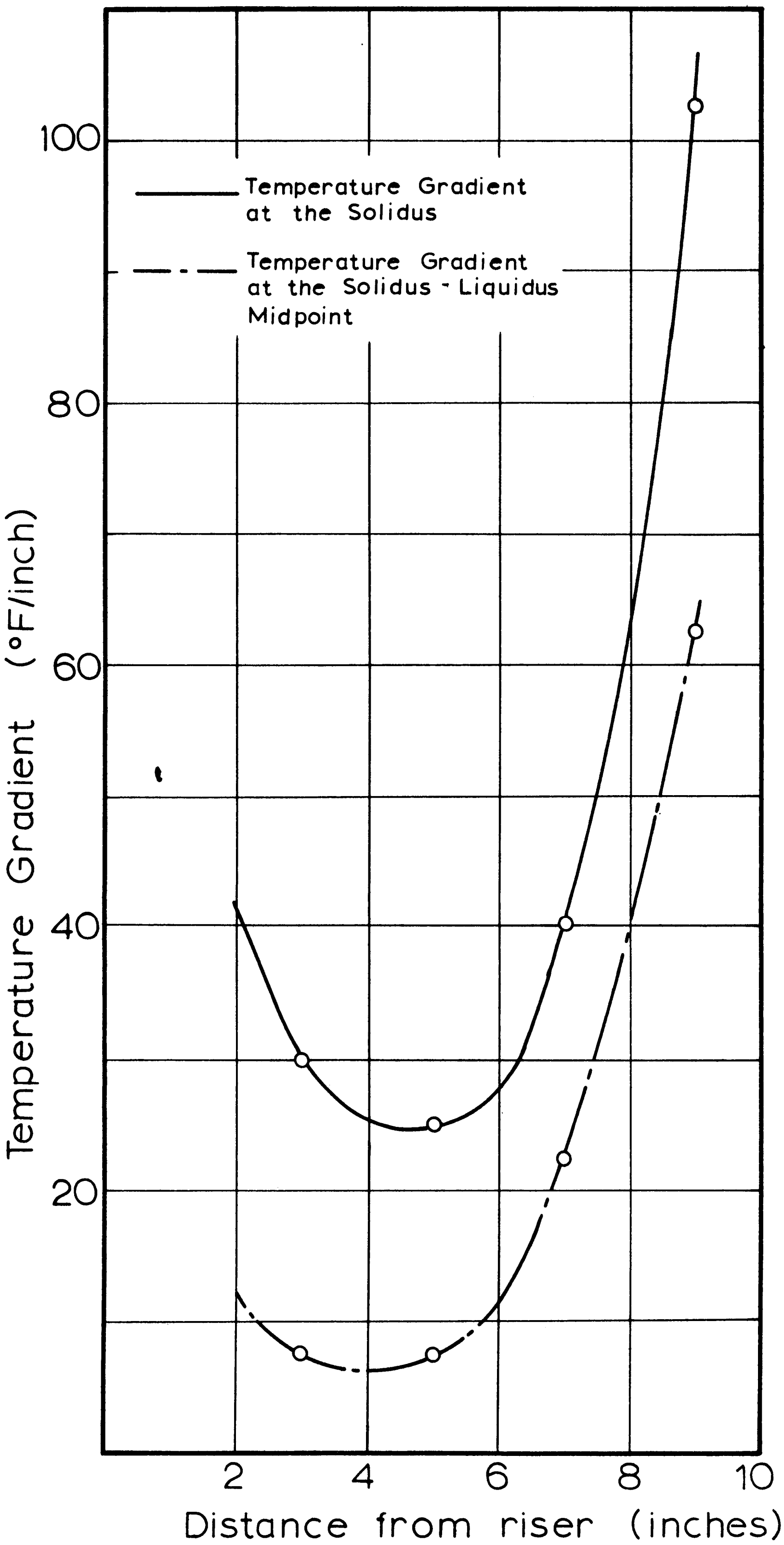

Figure 16. Thermal gradients for a 2" x 2" x 10" end chilled bar of Cunisibe. The data have been calculated by the secant method from the Cooling curves in Figure 15.

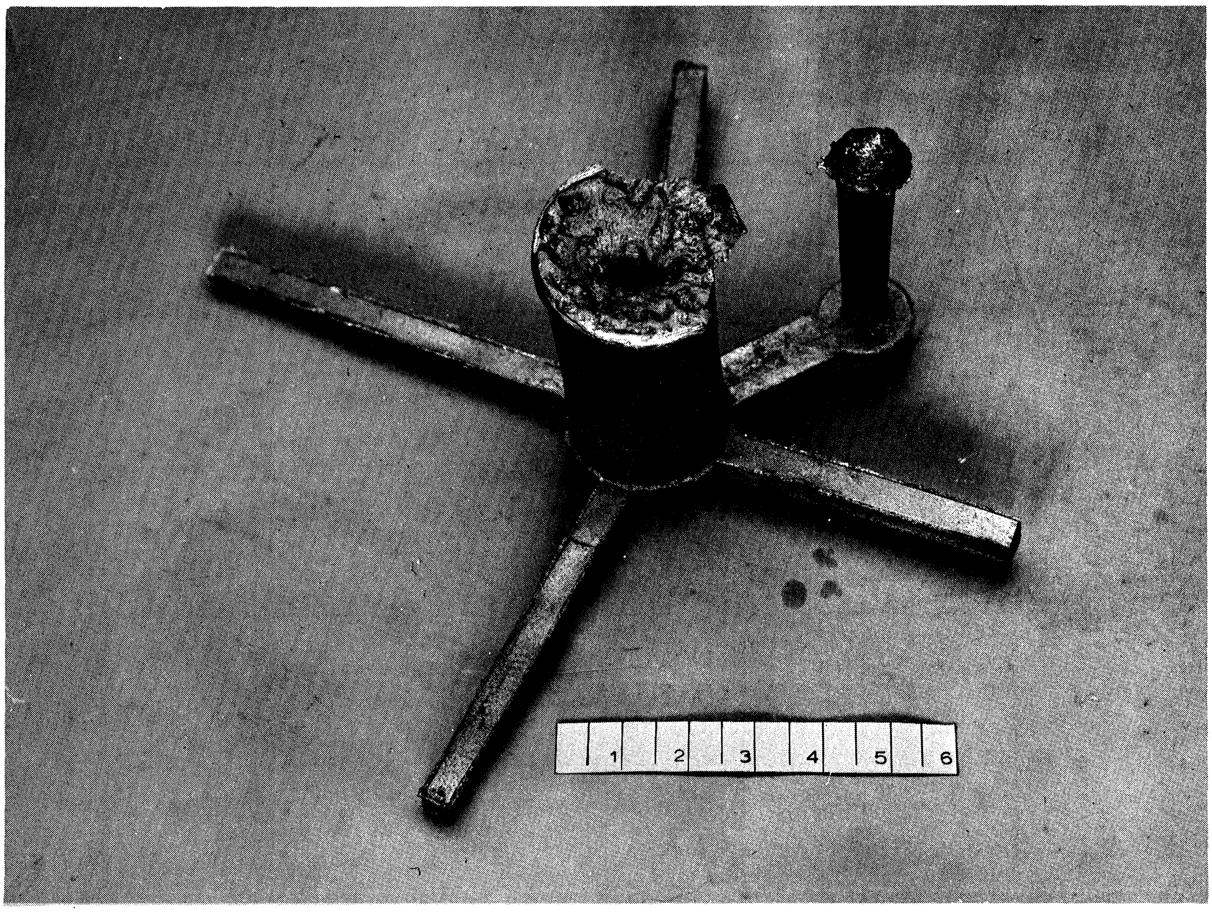

Figure 17. Feed distance castings poured when small bars were studied (less than 1/2" x 1/2" cross section).

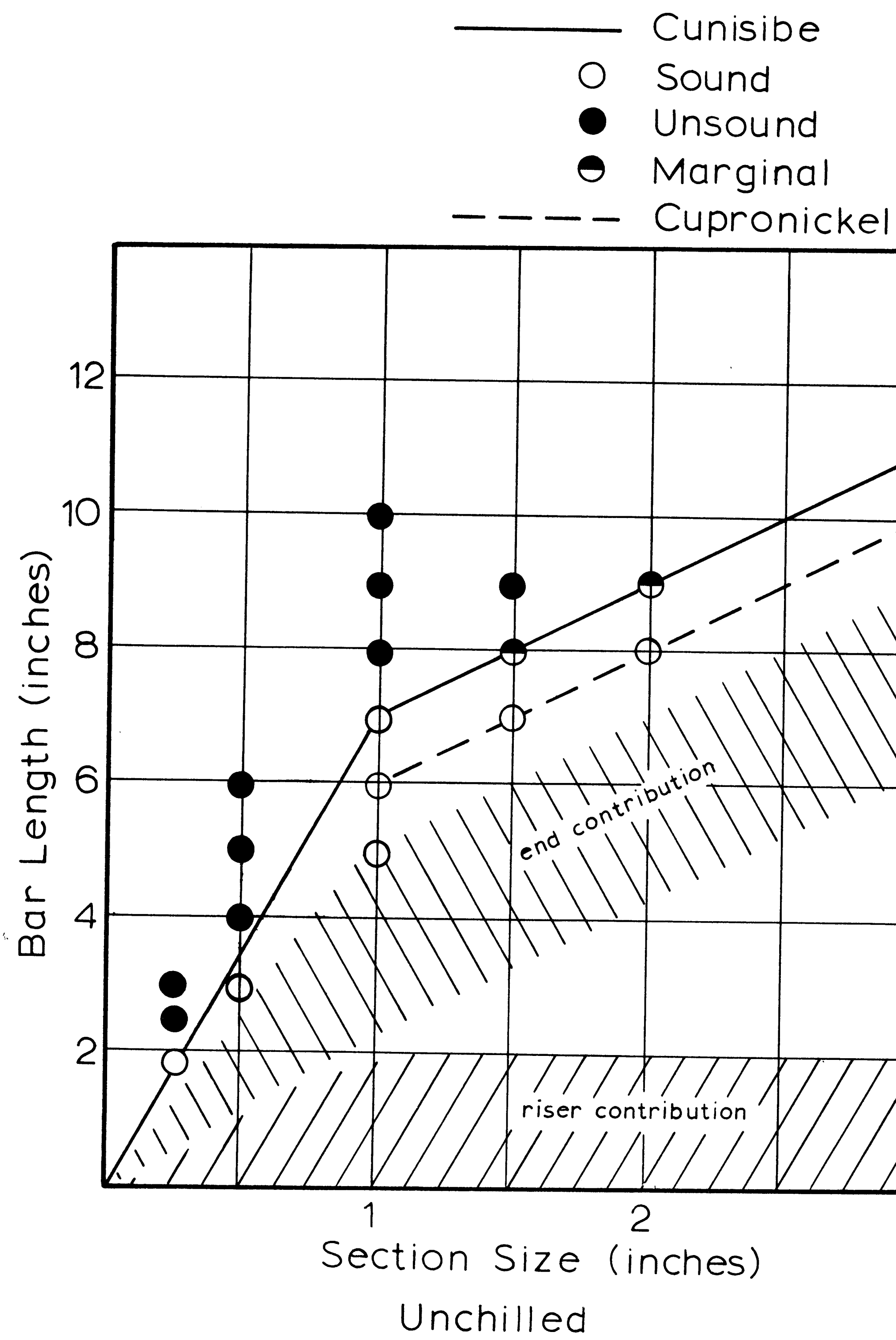

Figure 18a. Feeding distances in unchilled bars for Cunisibe alloy and 70-30 cupro-nickel.

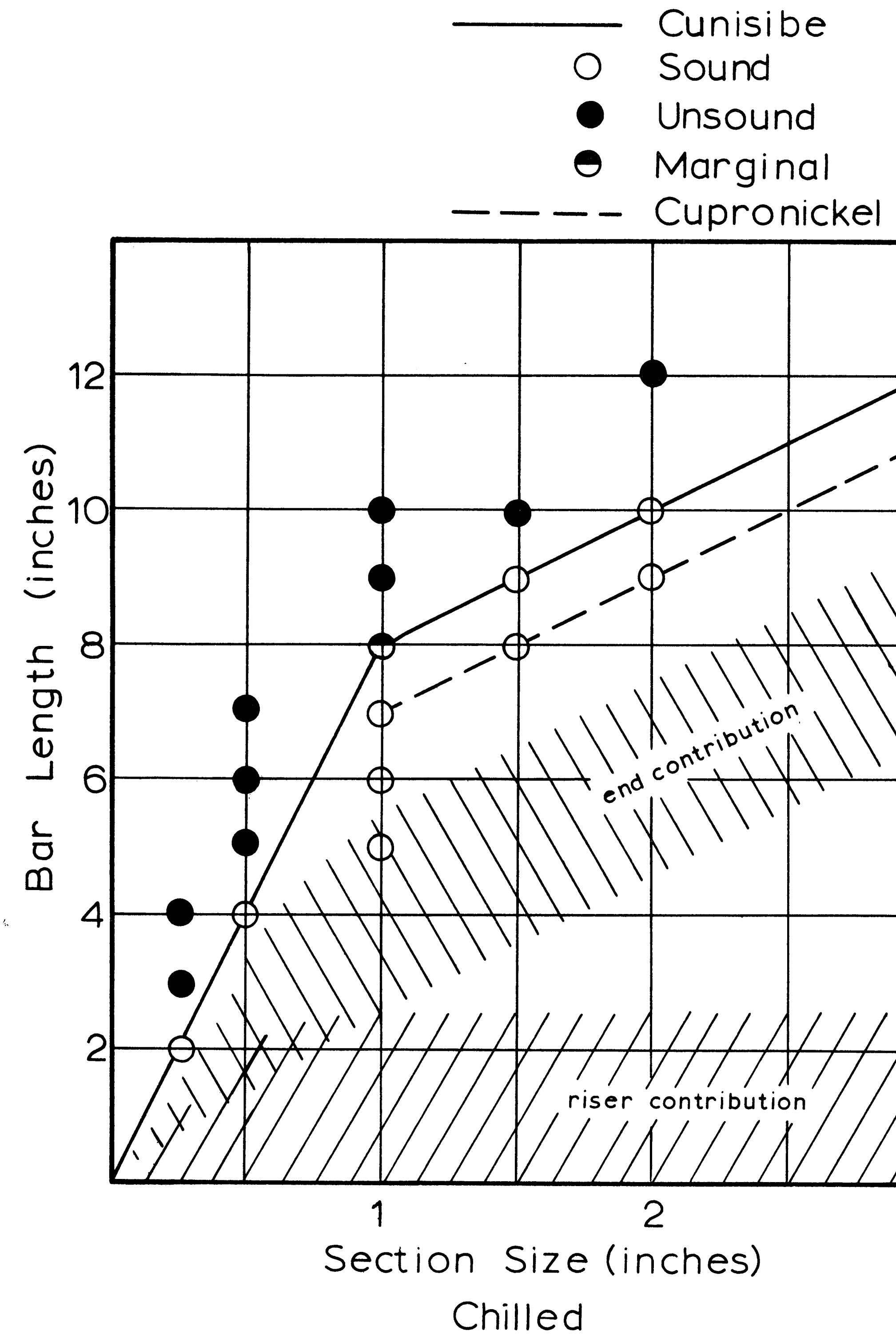

Fi_ure 18b. Feeding distances in end chilled bars for Cunisibe alloy and 70-30 cupro-nickel.

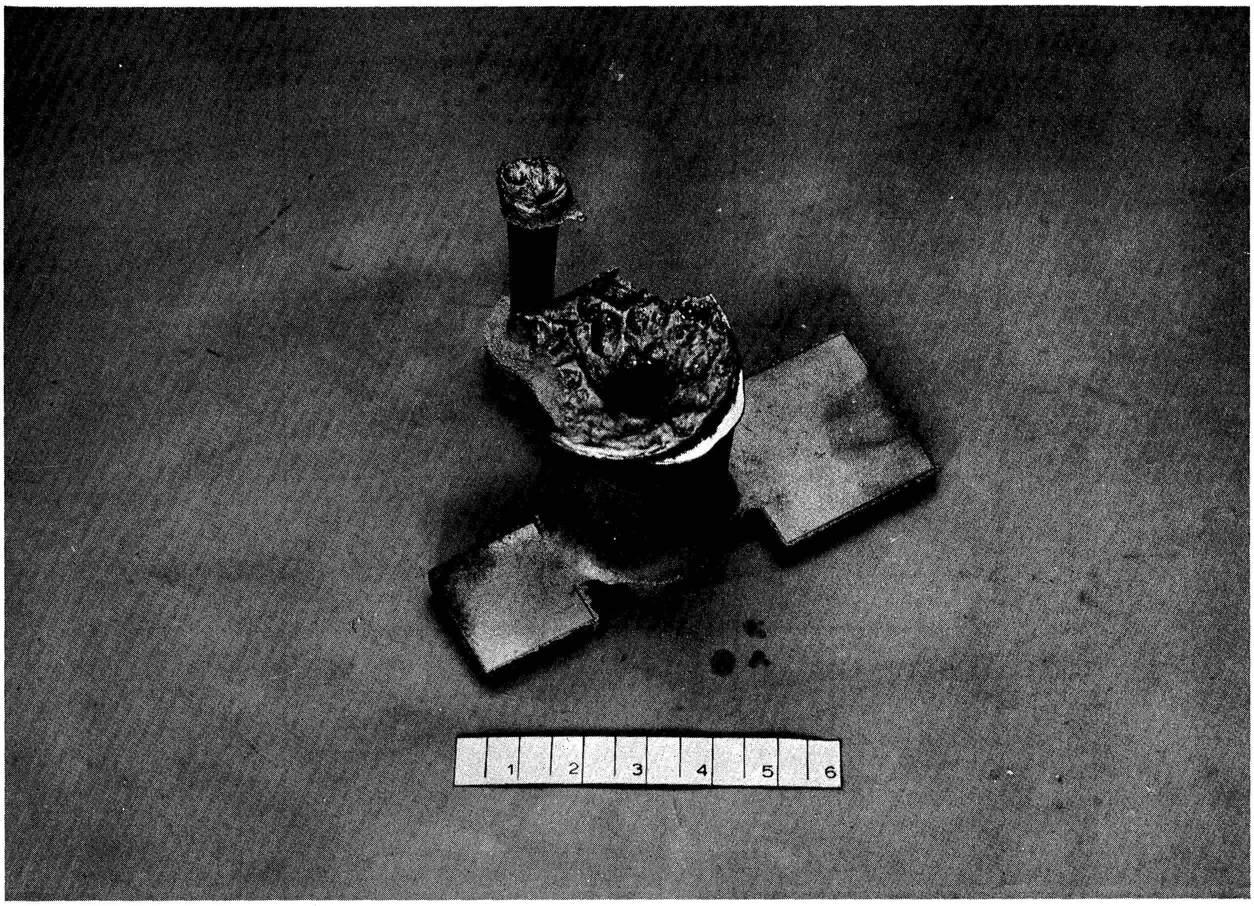

Figure 19. Feed distance castings poured when small plates were studied (for 1/2" thicknesses only).

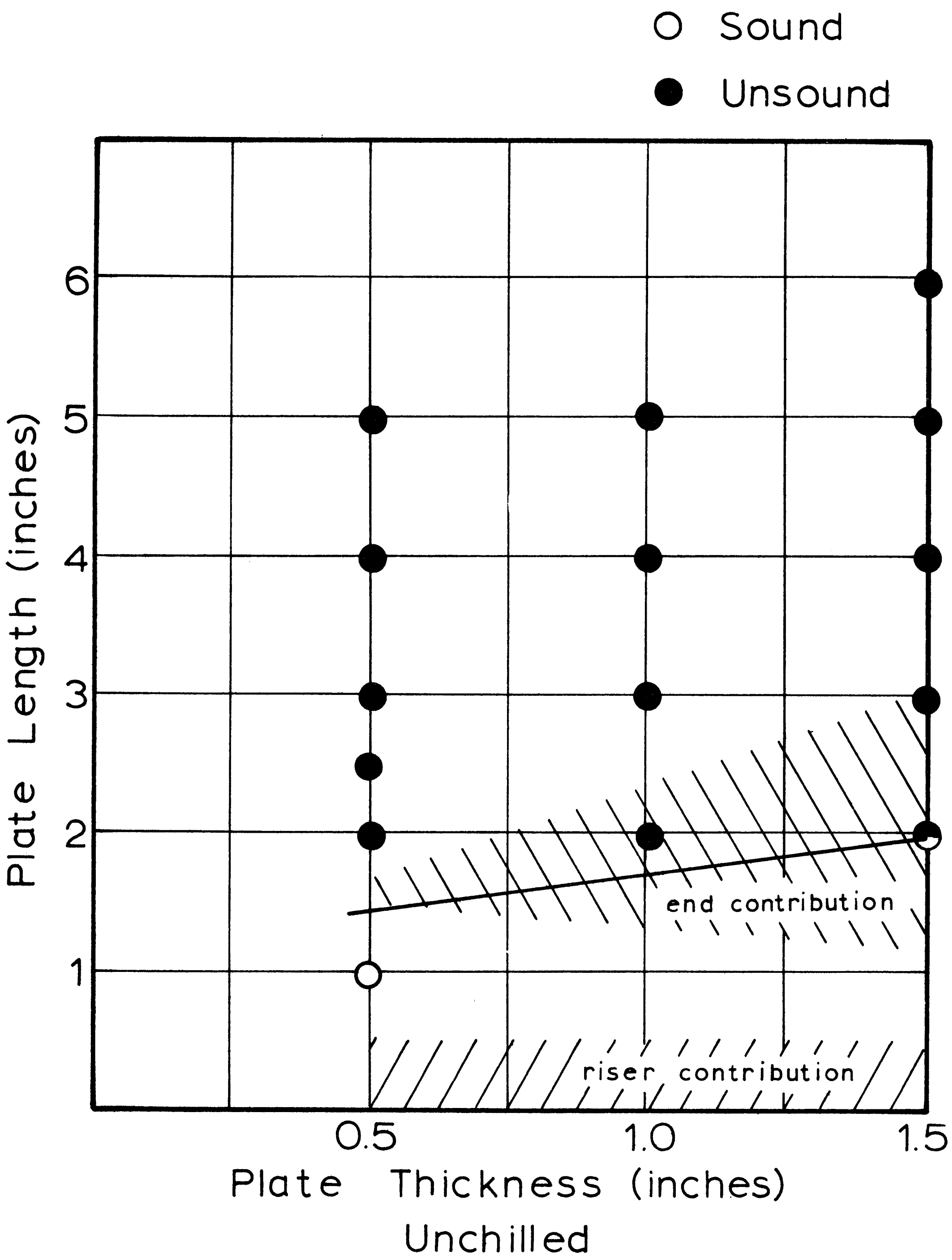

Figure 20a. Feeding distance in unchilled plates of Cunisibe alloy.

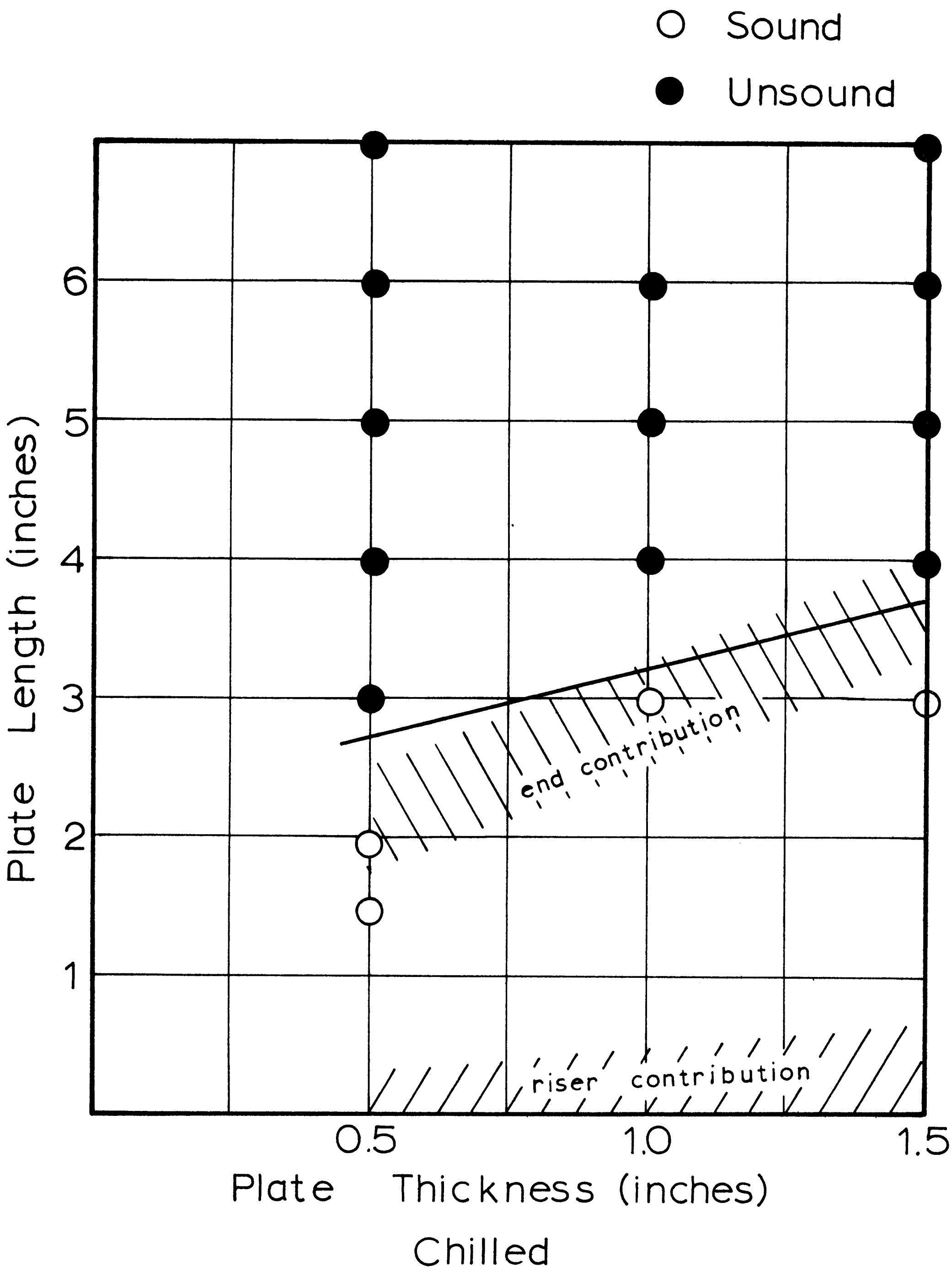

Figure 20b. Feeding distance in end chilled plates of Cunisibe alloy.

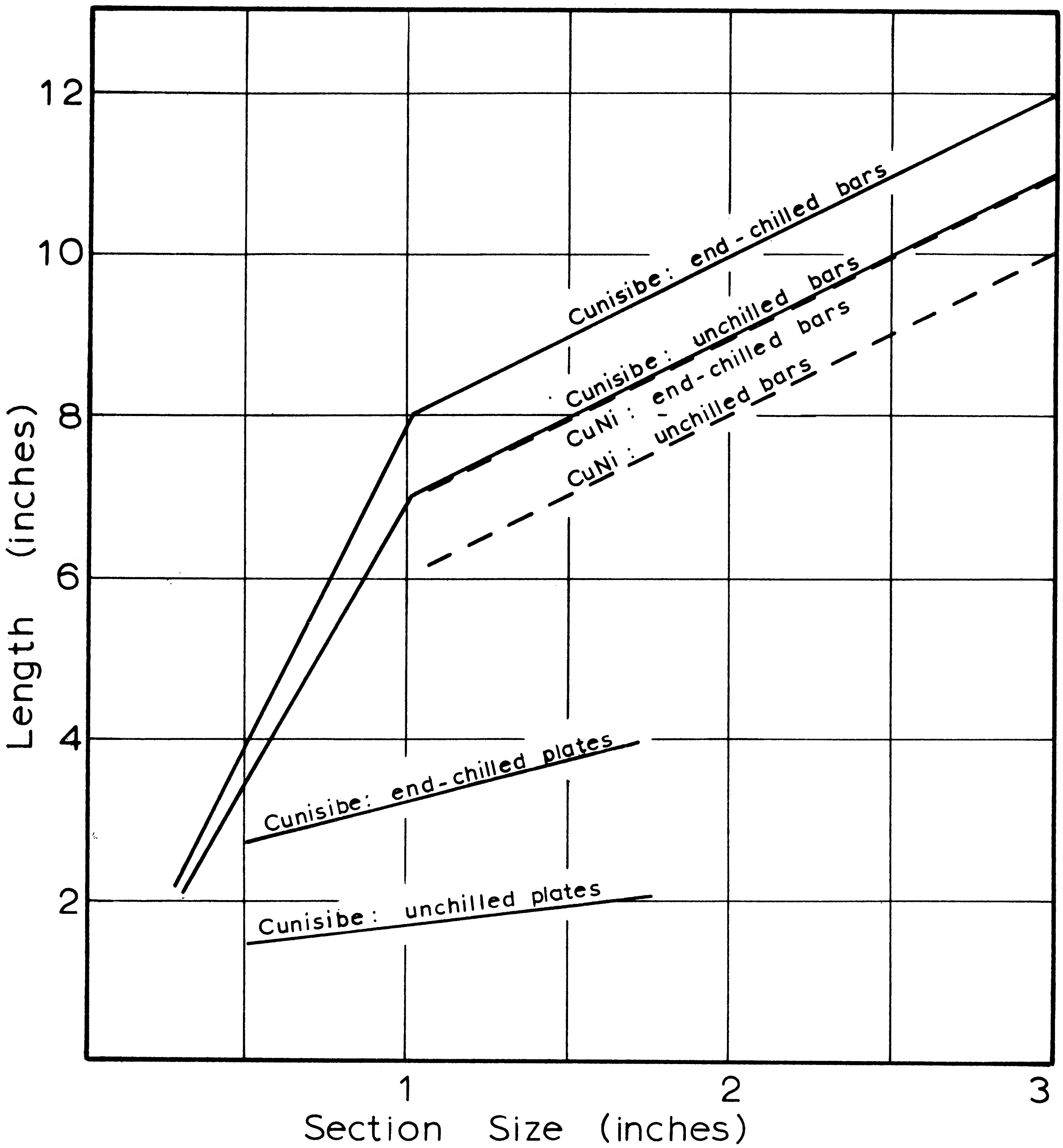

Figure 21. Summary of feeding distance in plates and bars in Cunisibel alloy. Bar data for 70-30 cupro-nickel have also been included from reference (7).

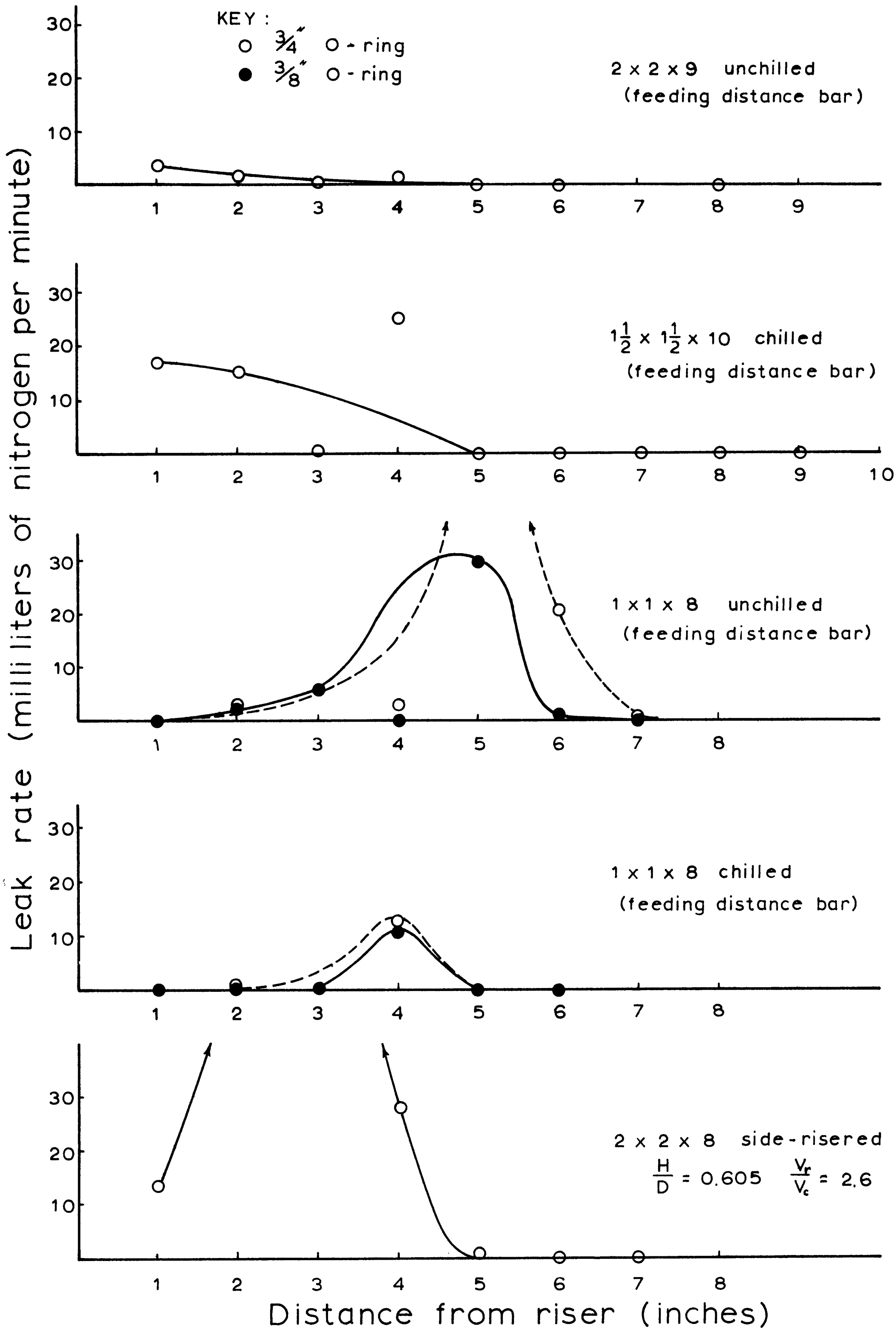

Figure 22. Pressure test of selected bars used in the feed distance study. The leak rate was determined at 100psig dry nitrogen pressure.

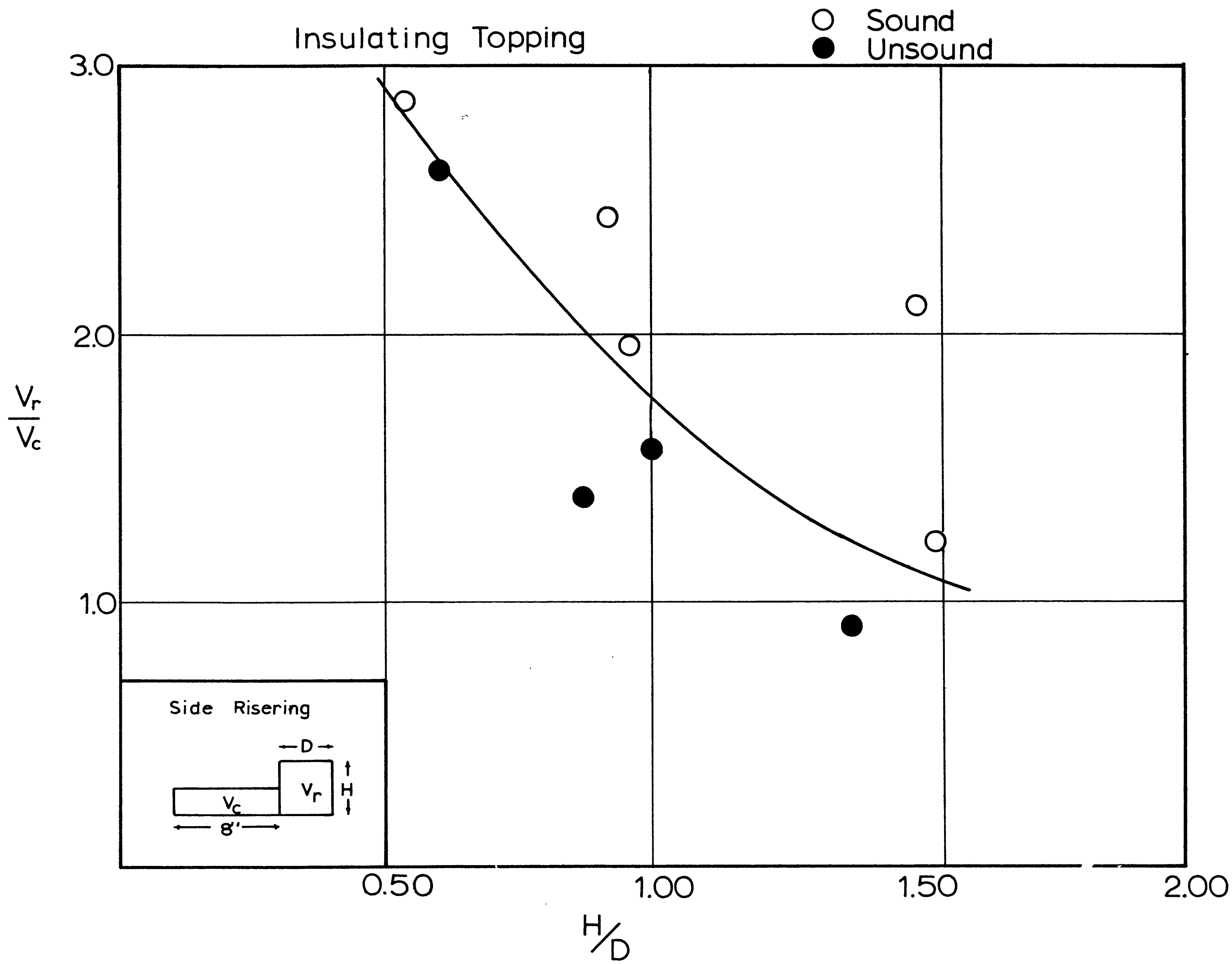

Figure 23. Volume ratio (V_r/V_c) vs the riser height to diameter ratio (H/D) for a 2" x 2" x 8" side risered bar.

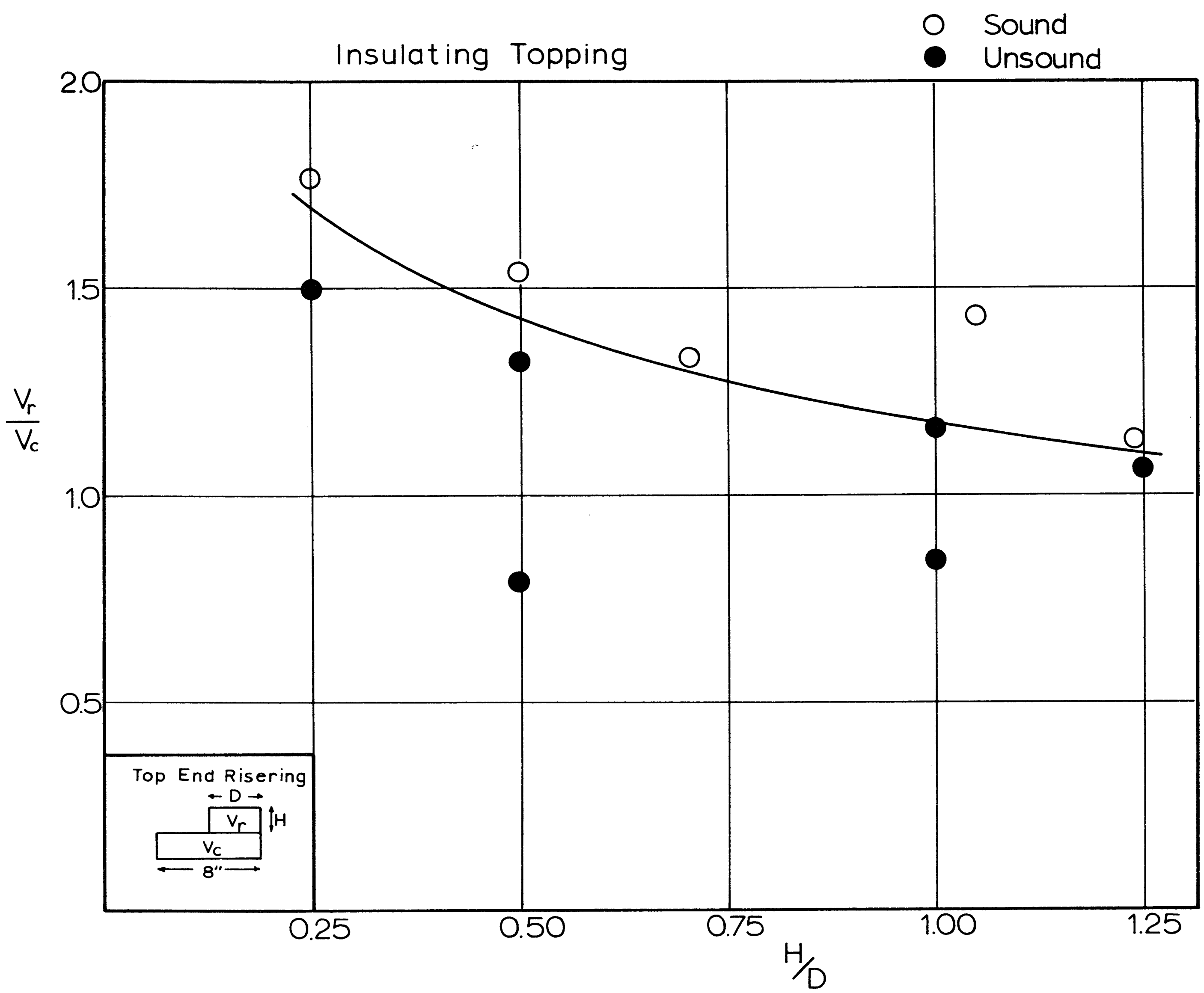

Figure 24. Volume ratio (V_r/V_c) vs the riser height to diameter ratio (H/D) for a 2" x 2" x 8" top risered bar.

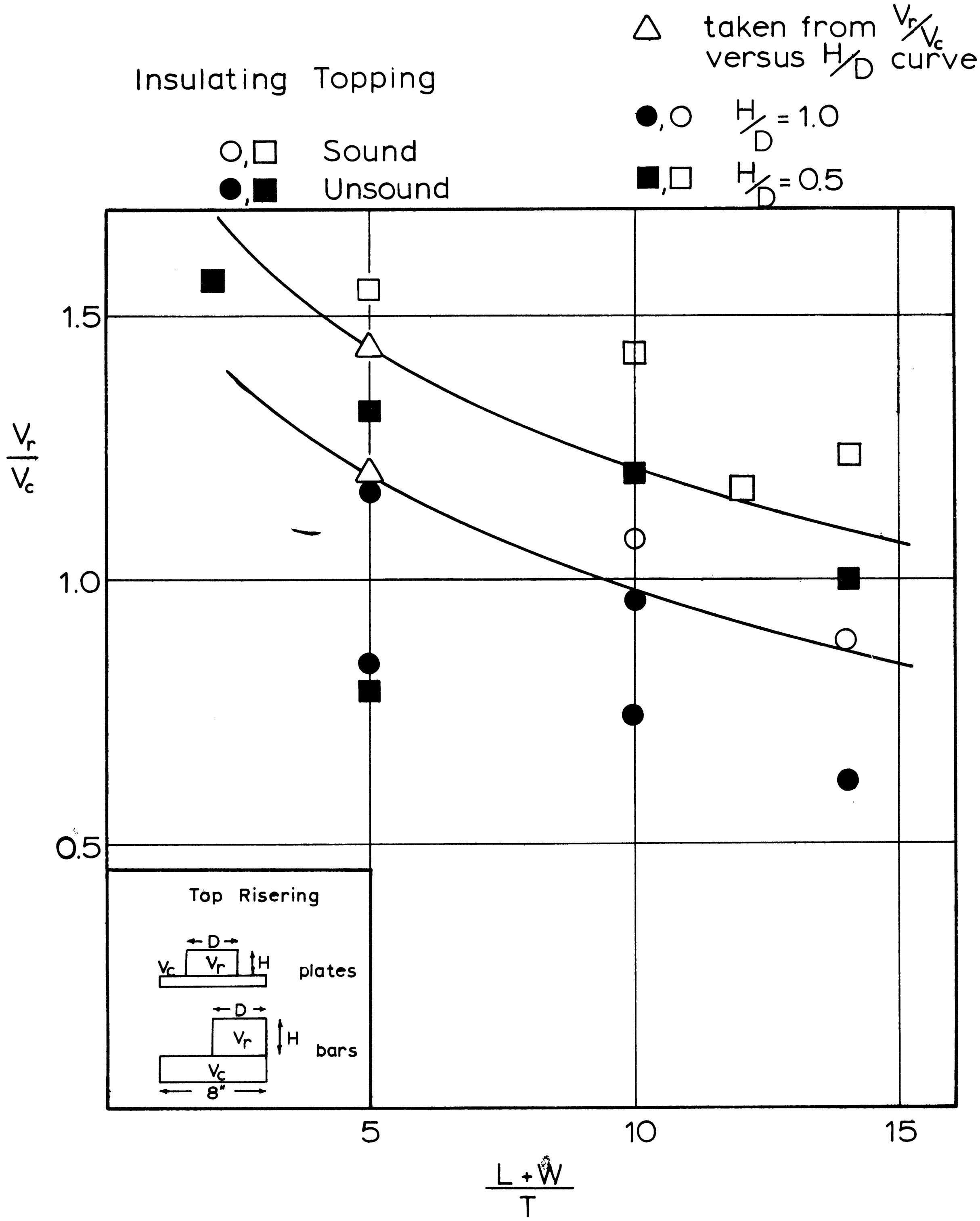

Figure 25. Risering curve for plates and bars of Cunisibe alloy cast with an insulating cover on open risers.

Figure 26. Top risered bar which shows the flow-off channel used to maintain a constant (H/D) ratio for the riser.

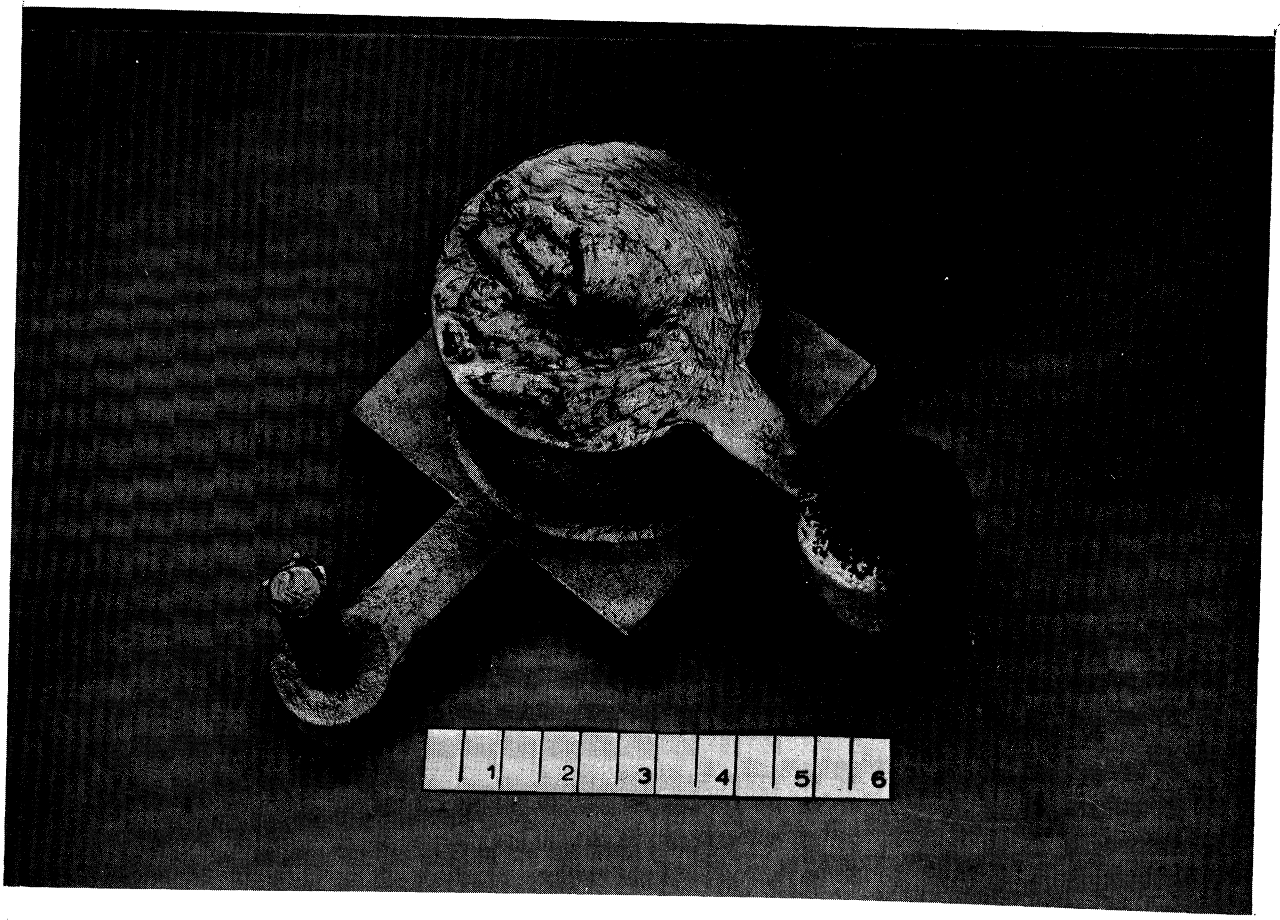

Figure 27. Top risered plate which shows gating and the use of the flow-off technique.

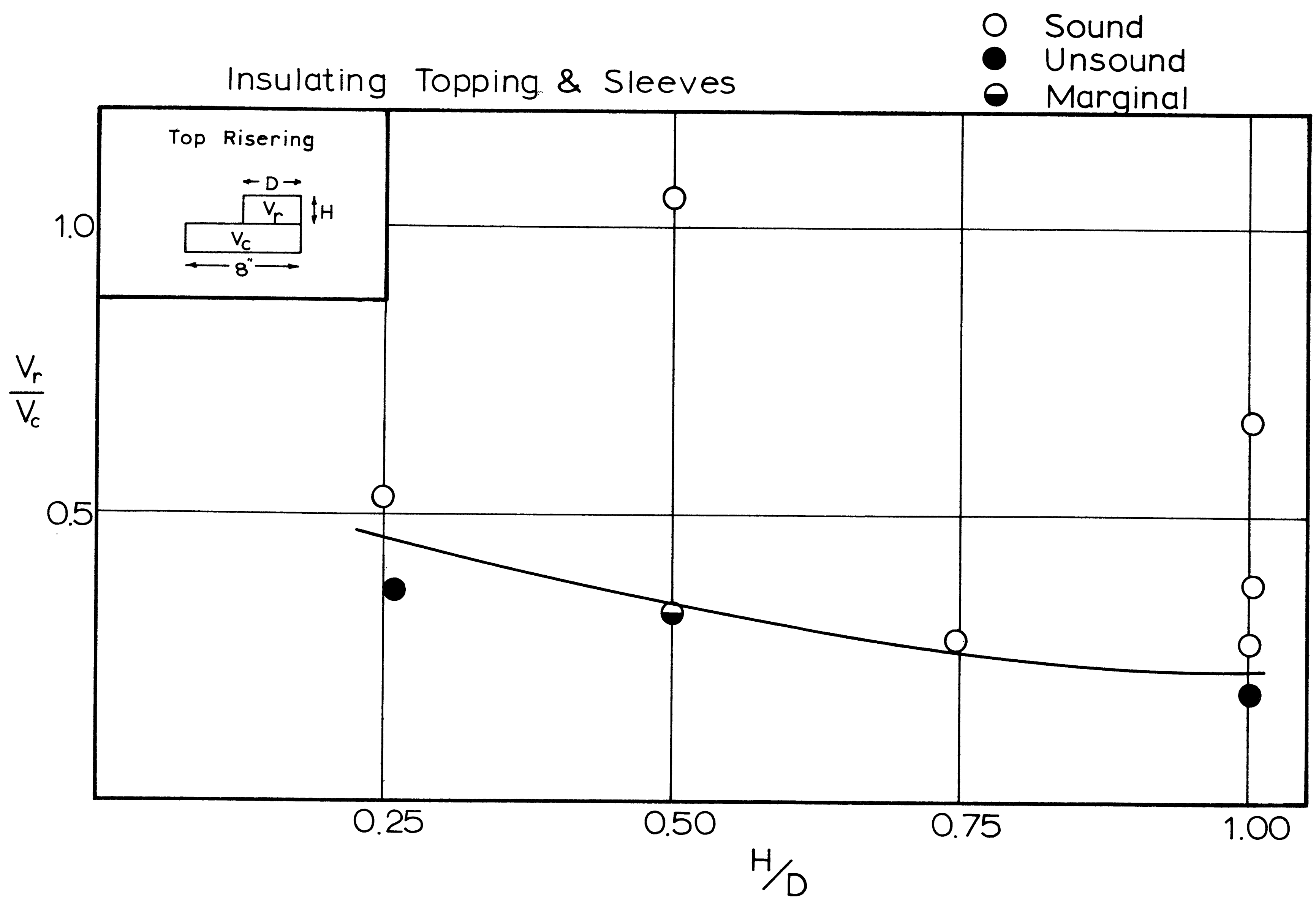

Figure 28. Volume ratio vs H/D of the top riser when insulating topping and insulating sleeves have been used.

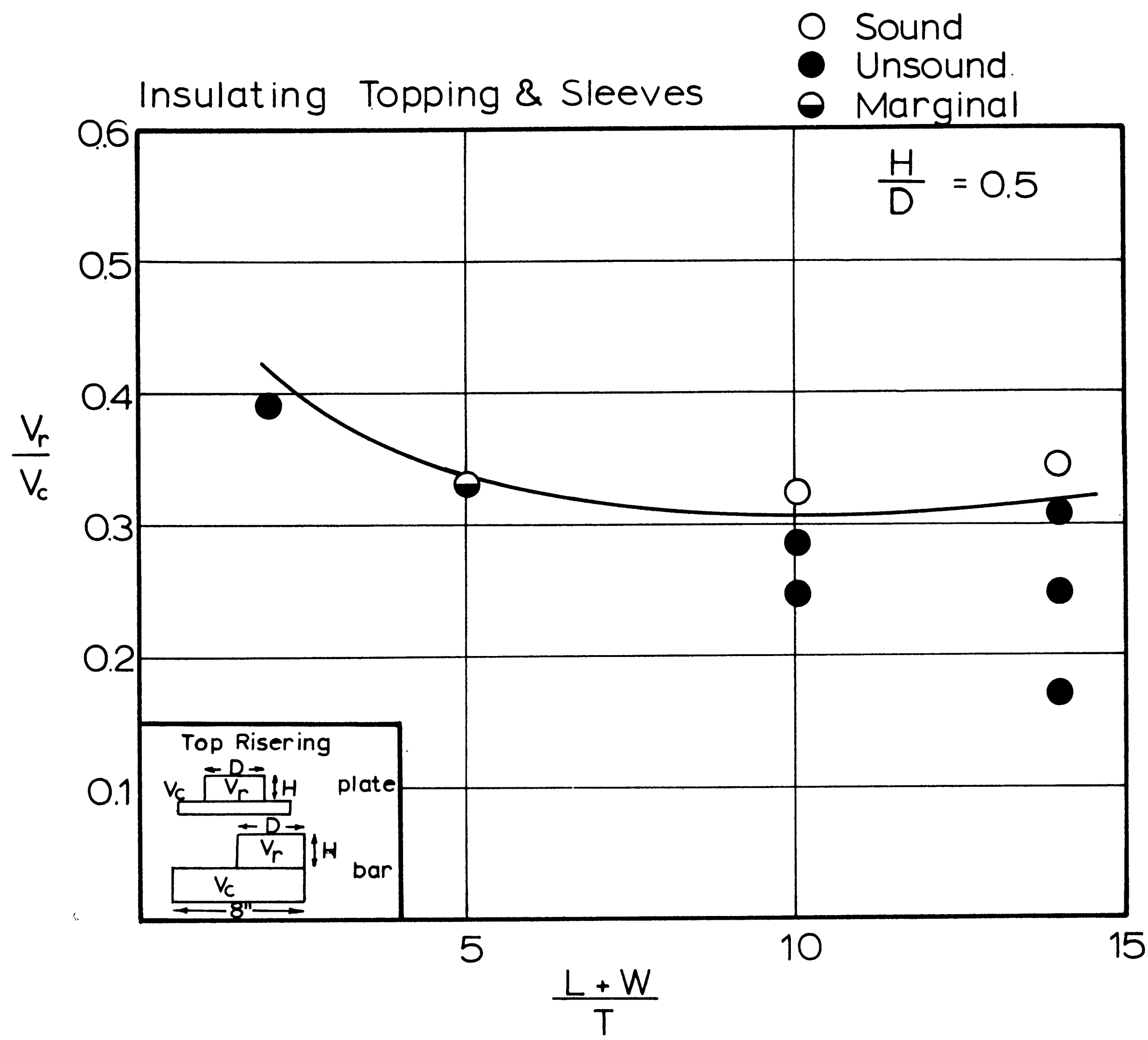

Figure 29. Risering curves for plates and bars when insulating topping and insulating sleeves are used. H/D values were 0.50.

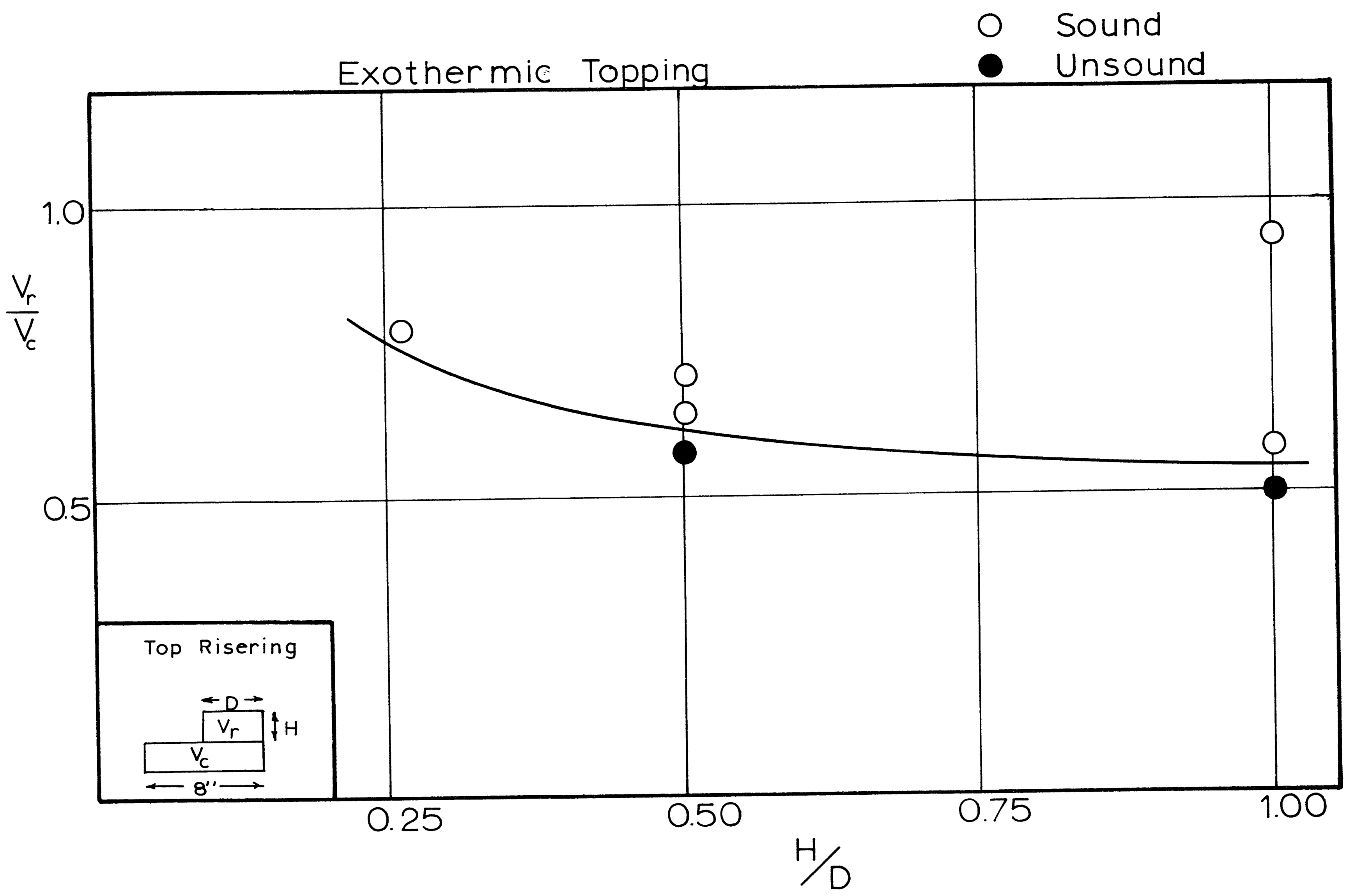

Figure 30. Volume ratio vs H/D ratio for castings top risered with exothermic topping only.

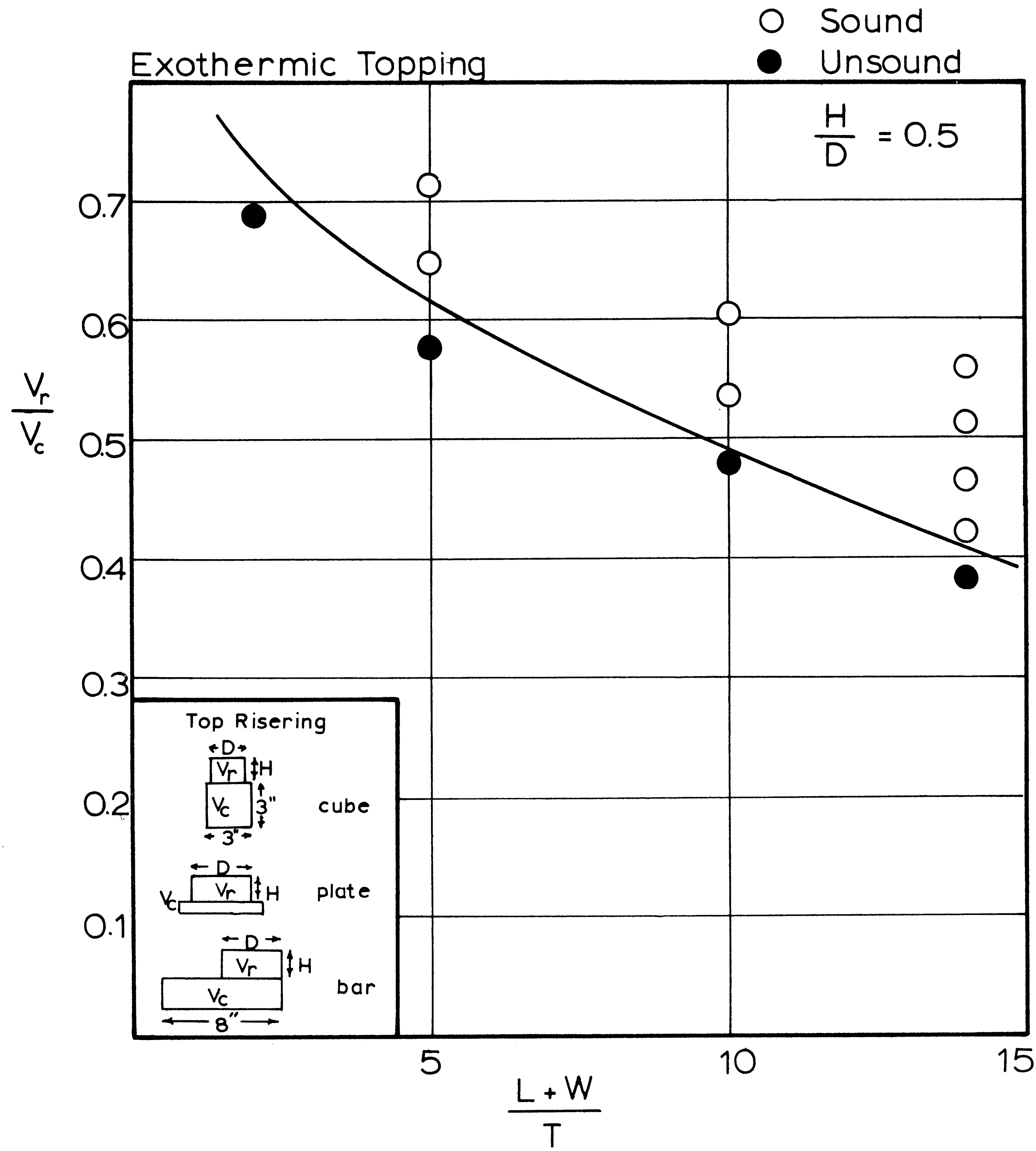

Figure 31. Risering curve for top risered casting made with exothermic topping. H/D = 0.50.

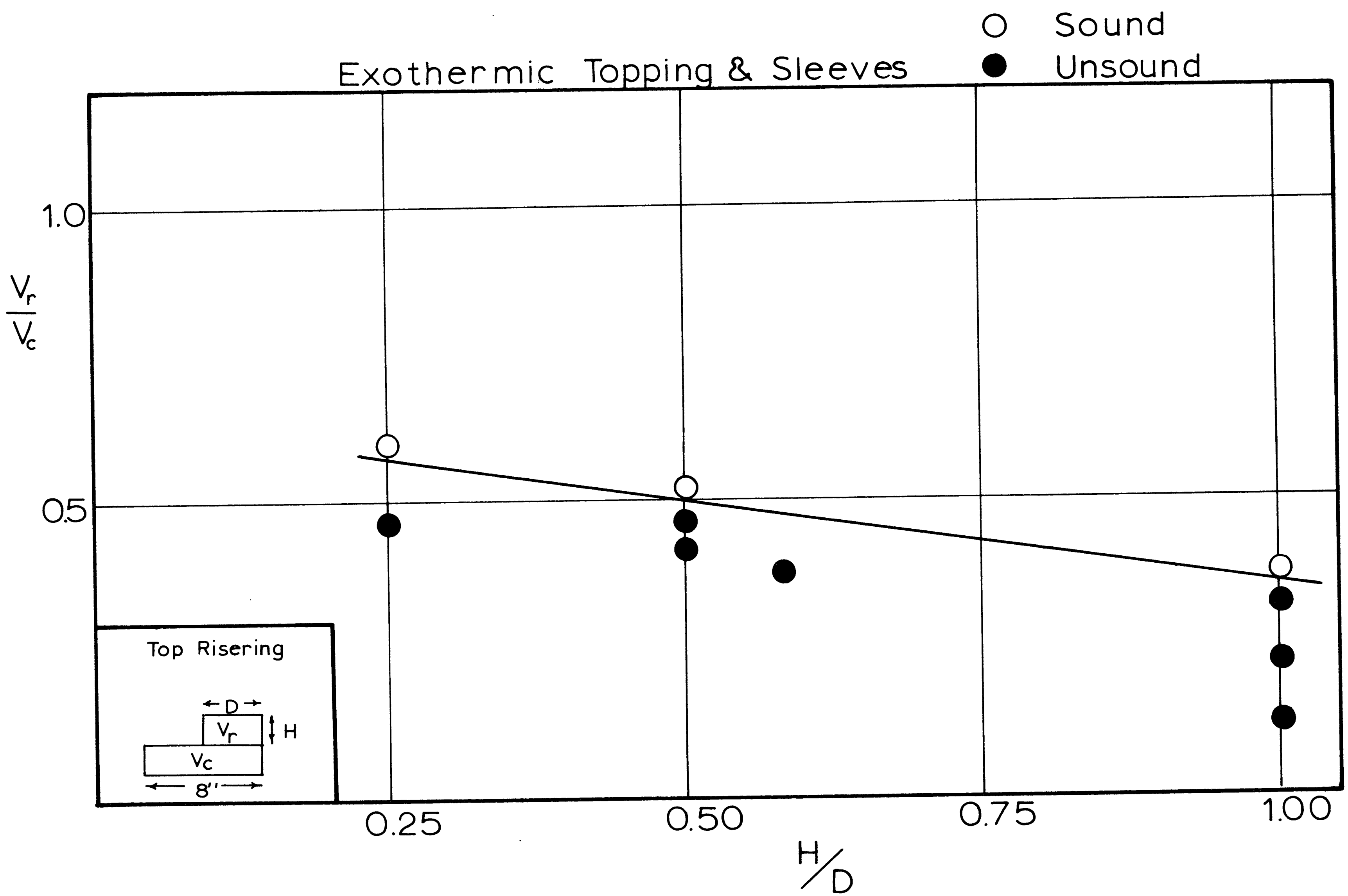

Figure 32. Volume ratio vs H/D ratio of the riser when both exothermic topping and exothermic sleeves are used.

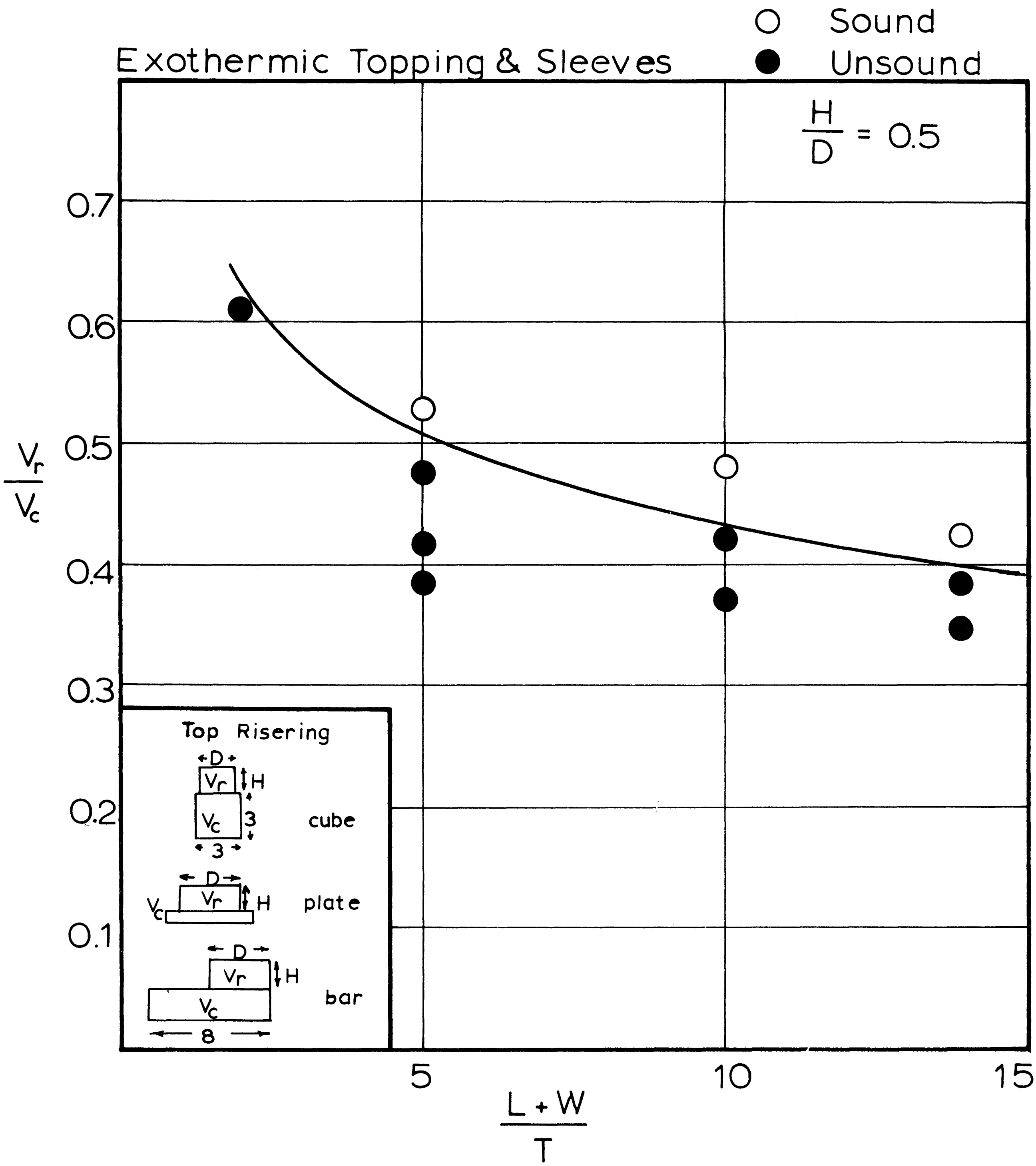

Figure 33. Risering curve for use when exothermic sleeves and exothermic topping are used. H/D = 0.50.

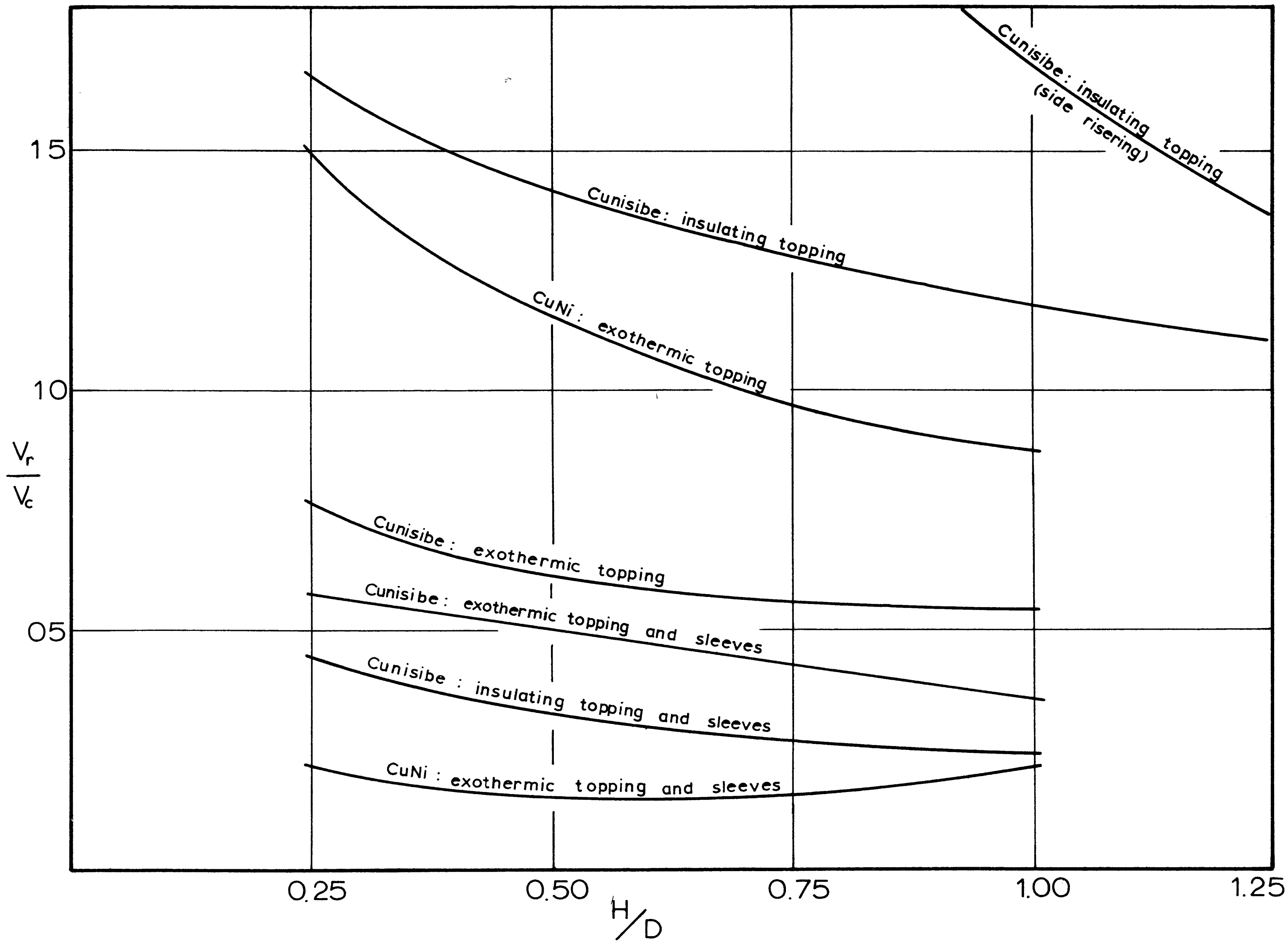

Figure 34. Summary of the volume ratio (V_r/V_c) vs height to diameter ratio of the riser (H/D) for several riser treatments.

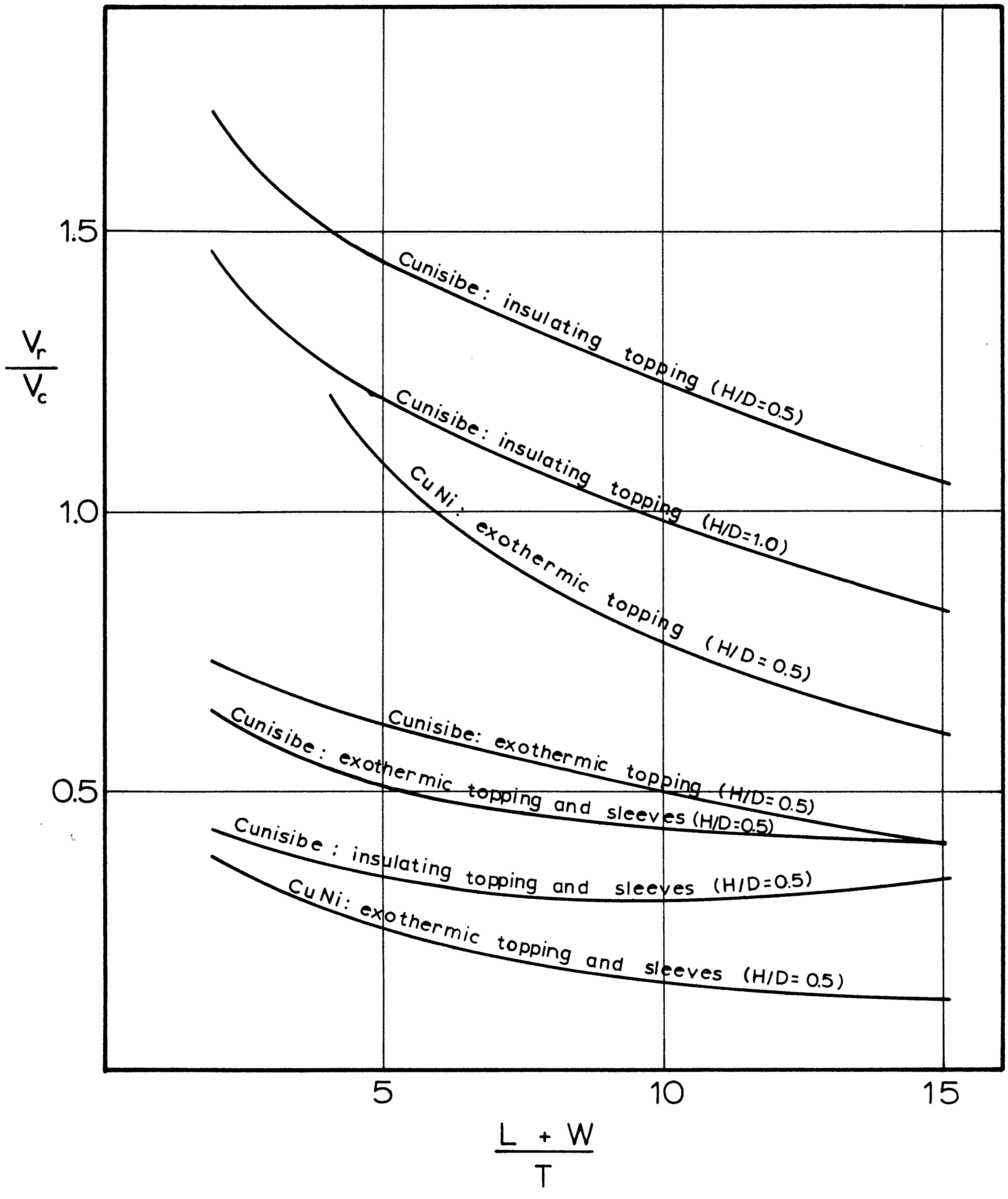

Figure 35. Summary of risering curves for both Cunisibe alloy and 70-30 cupro-nickel.

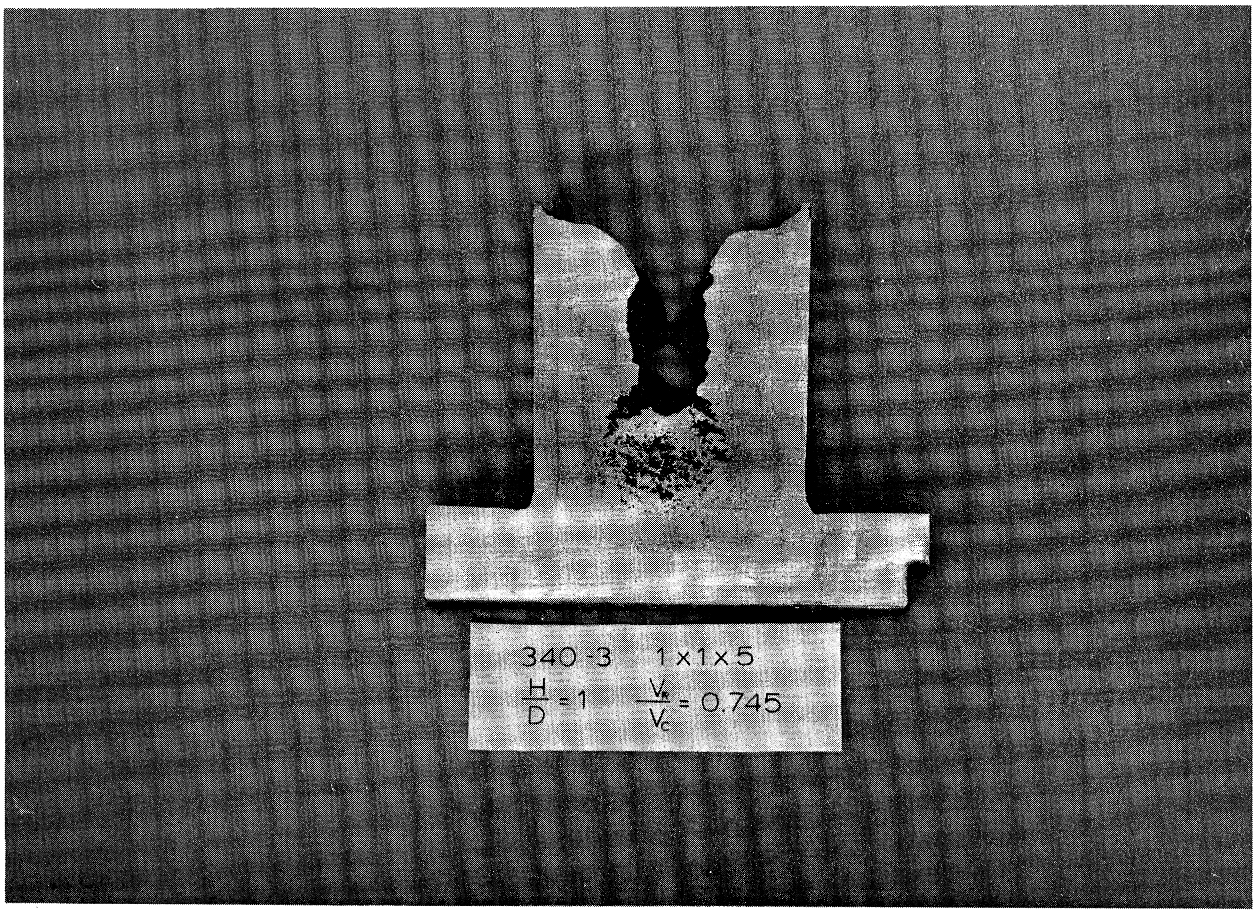

Figure 36. 1" x 5" x 5" plate cast with insulating riser topping. The casting was unsound as can be seen visually and verified radiographically.

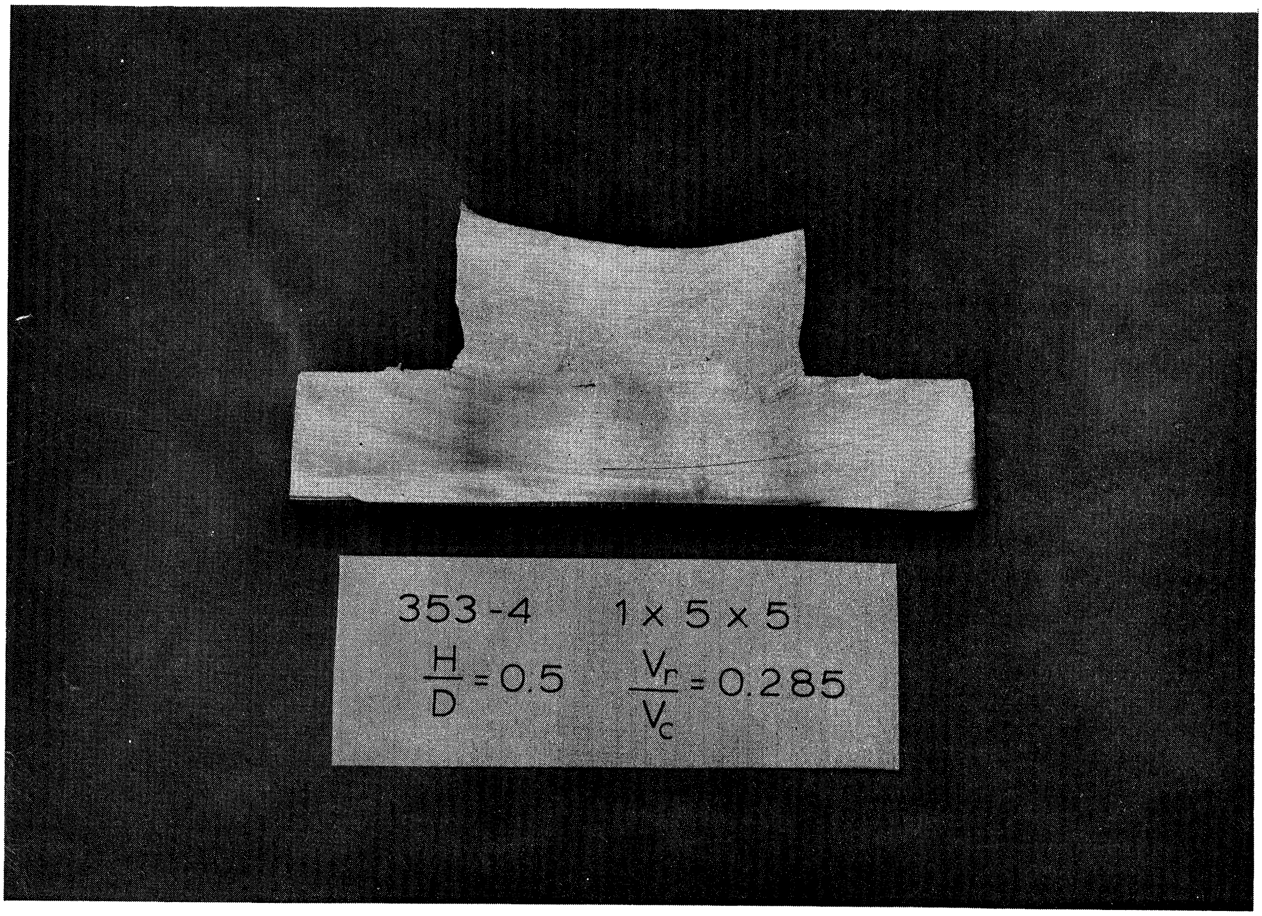

Figure 37. 1" x 5" x 5" plate cast with insulating topping plus insulating sleeves. A shrinkage pipe was not evident however the casting is radiographically unsound.

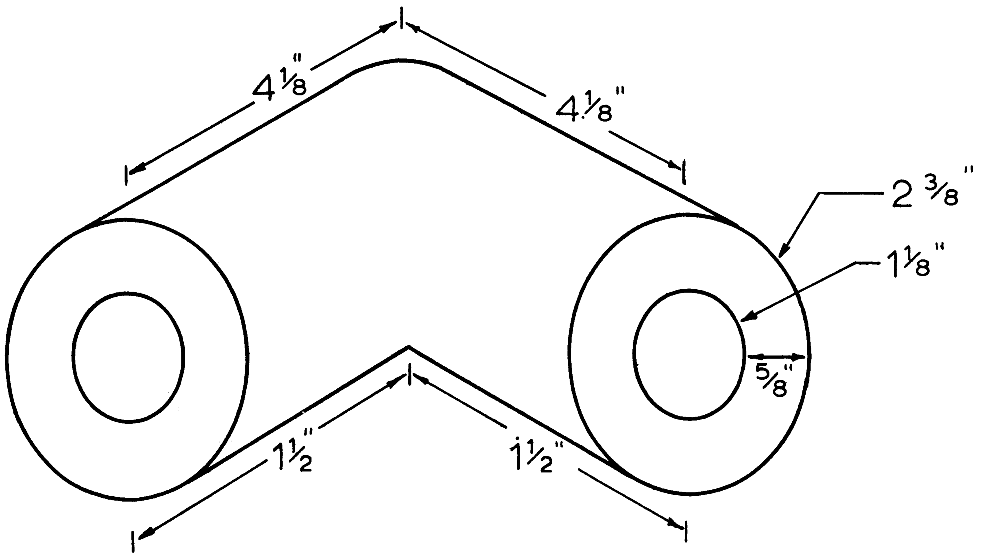

Equivalence

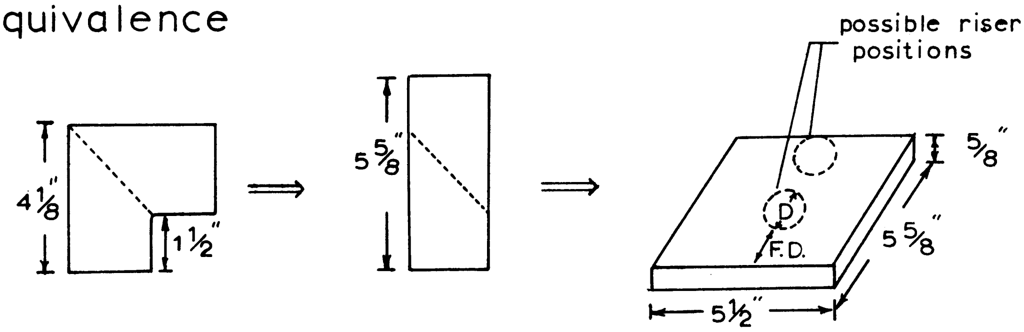

Circumference (outside) = 7.47 in.
Circumference (inside) = 3.54 in.
Circumference (median) = 5.50 in.

$$\text{Volume of casting} = \frac{\pi}{4}\left(5\tfrac{5}{8}\right)\left(\left(2\tfrac{3}{8}\right)^2 - \left(1\tfrac{1}{8}\right)^2\right)$$

$$= 19.4 \text{ in.}^3$$

$$\text{Shape factor} = \frac{L + W}{T} = \frac{5\tfrac{1}{2} + 5\tfrac{5}{8}}{\tfrac{5}{8}} = 17.8$$

Figure 38. 90° elbow and its equivalent section used as an illustration of the riser data.

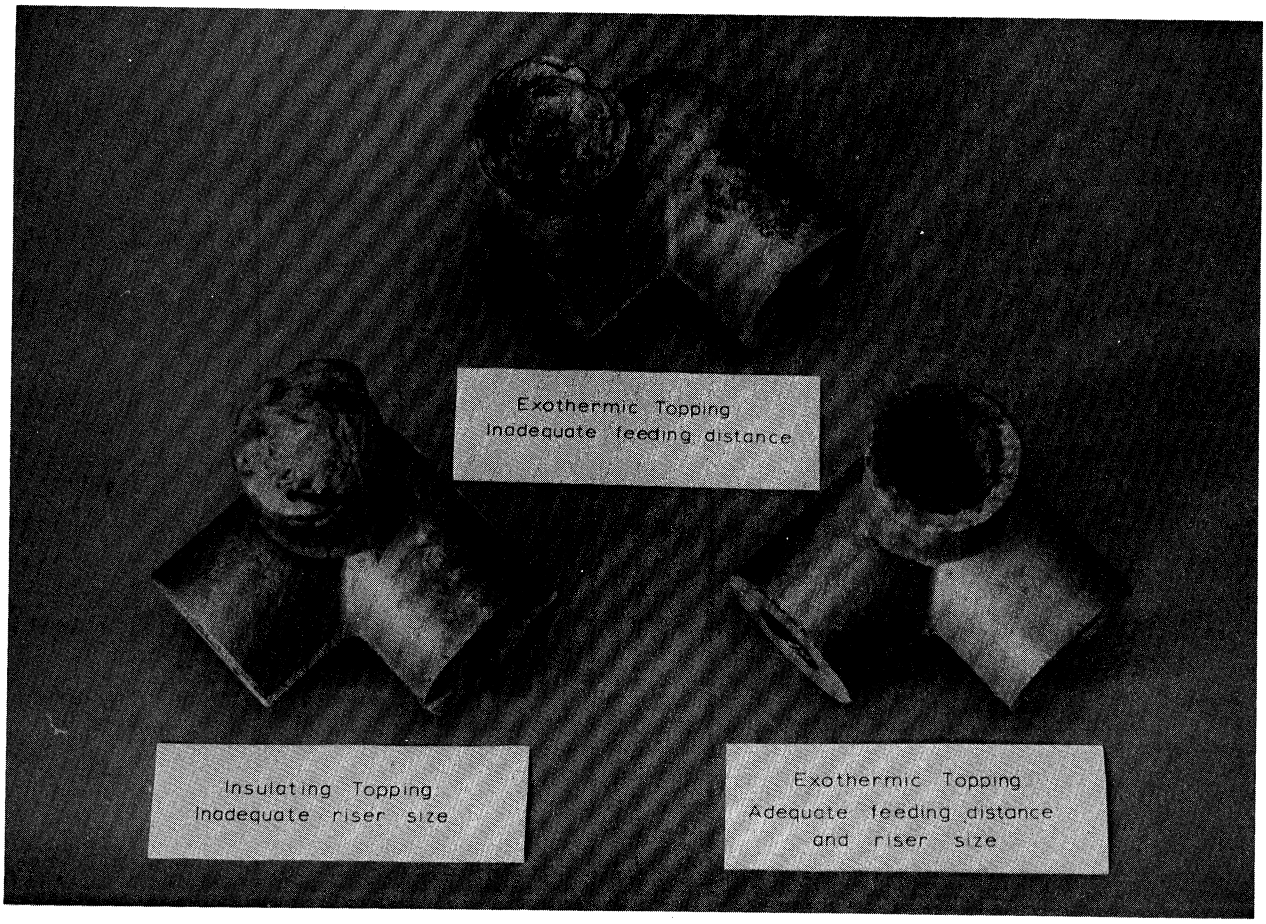

Figure 39. 1-1/4"-90° elbow cast in three different ways to illustrate use of the feeding distance and risering curves.

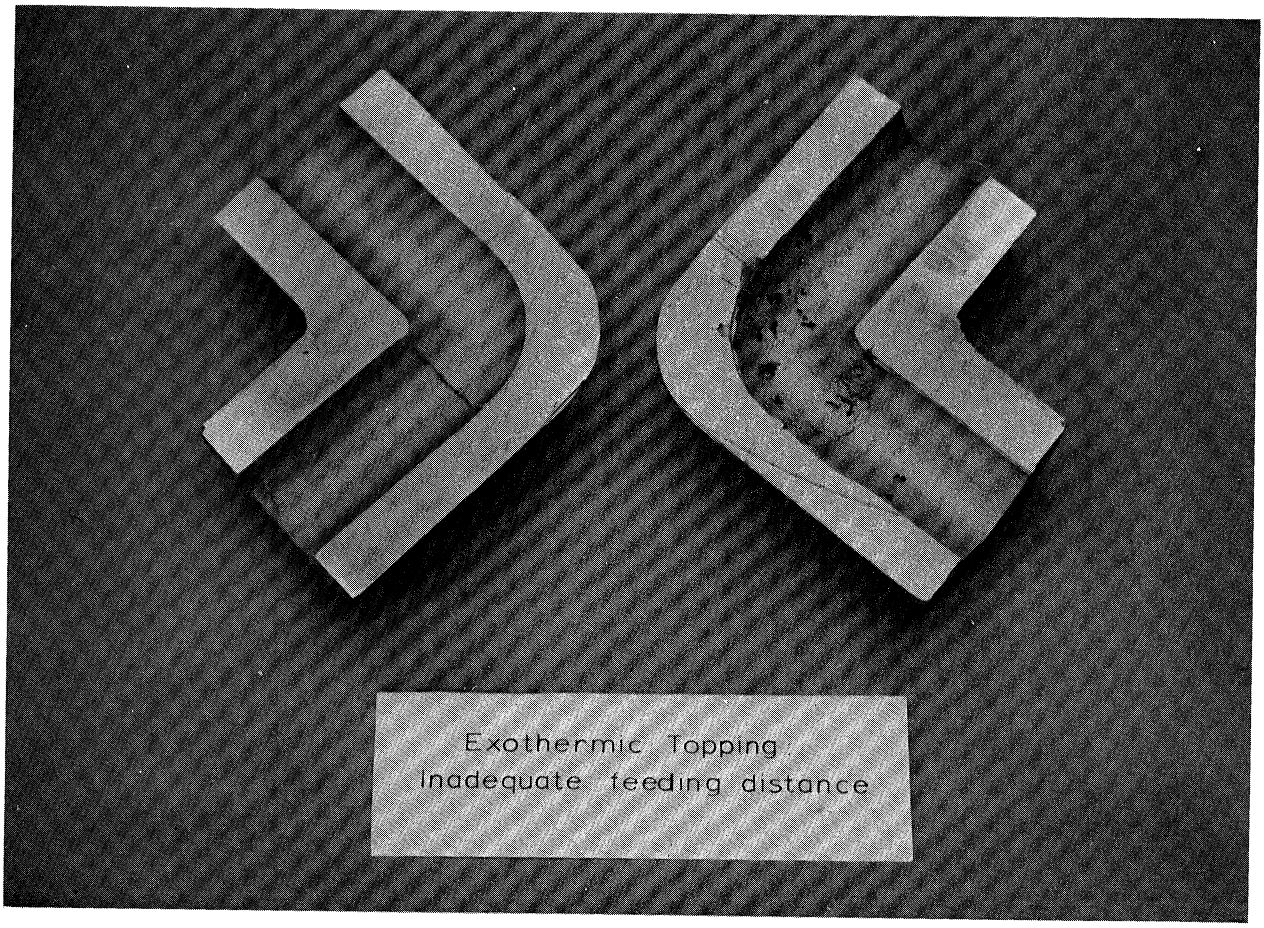

Figure 40. Sectioned 90° elbow which was risered at one end and chilled at the other. The surface shrinkage in the cope portion was due to inadequate feeding.

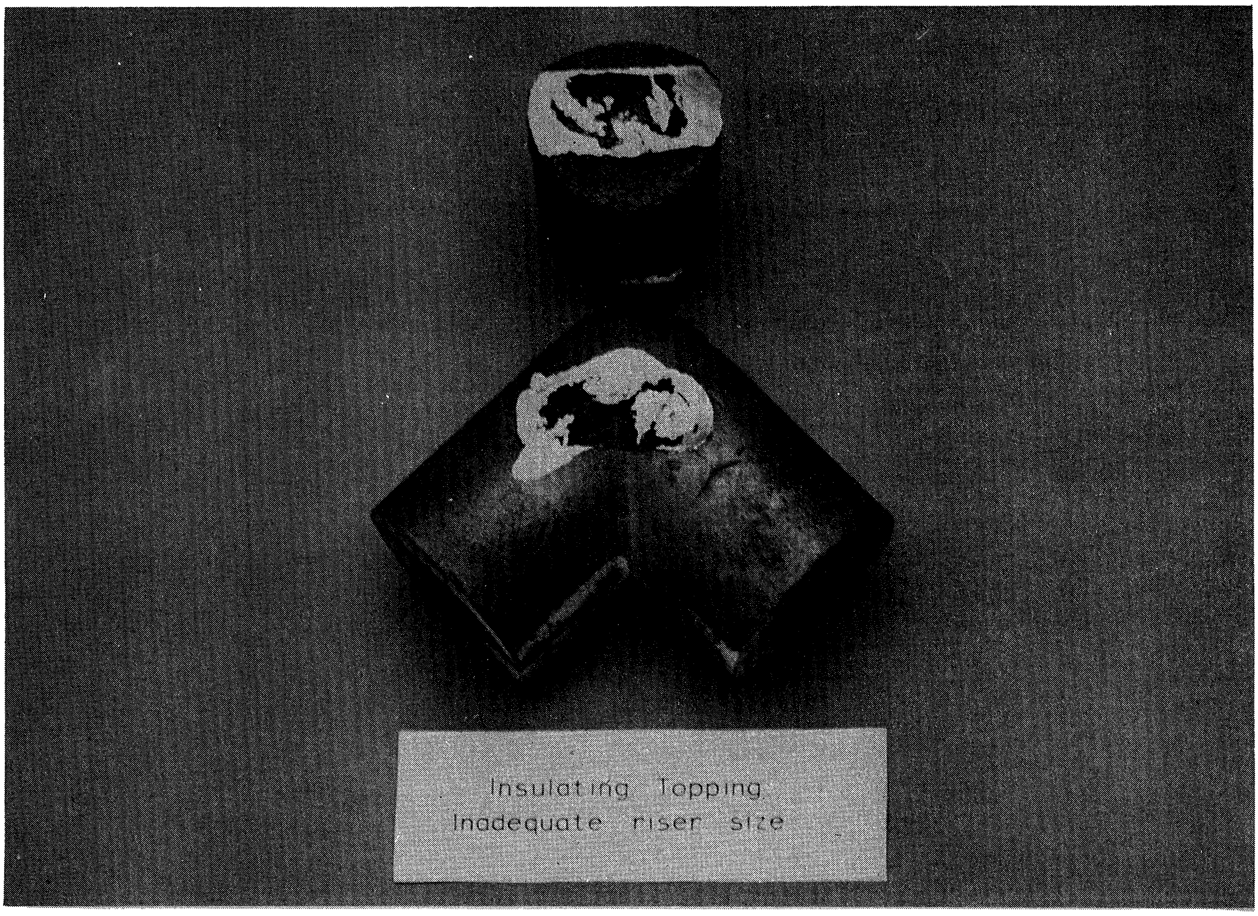

Figure 41. A riser adequate for exothermic topping is inadequate in height for insulating topping. The riser shrinkage has been pulled down into the casting.

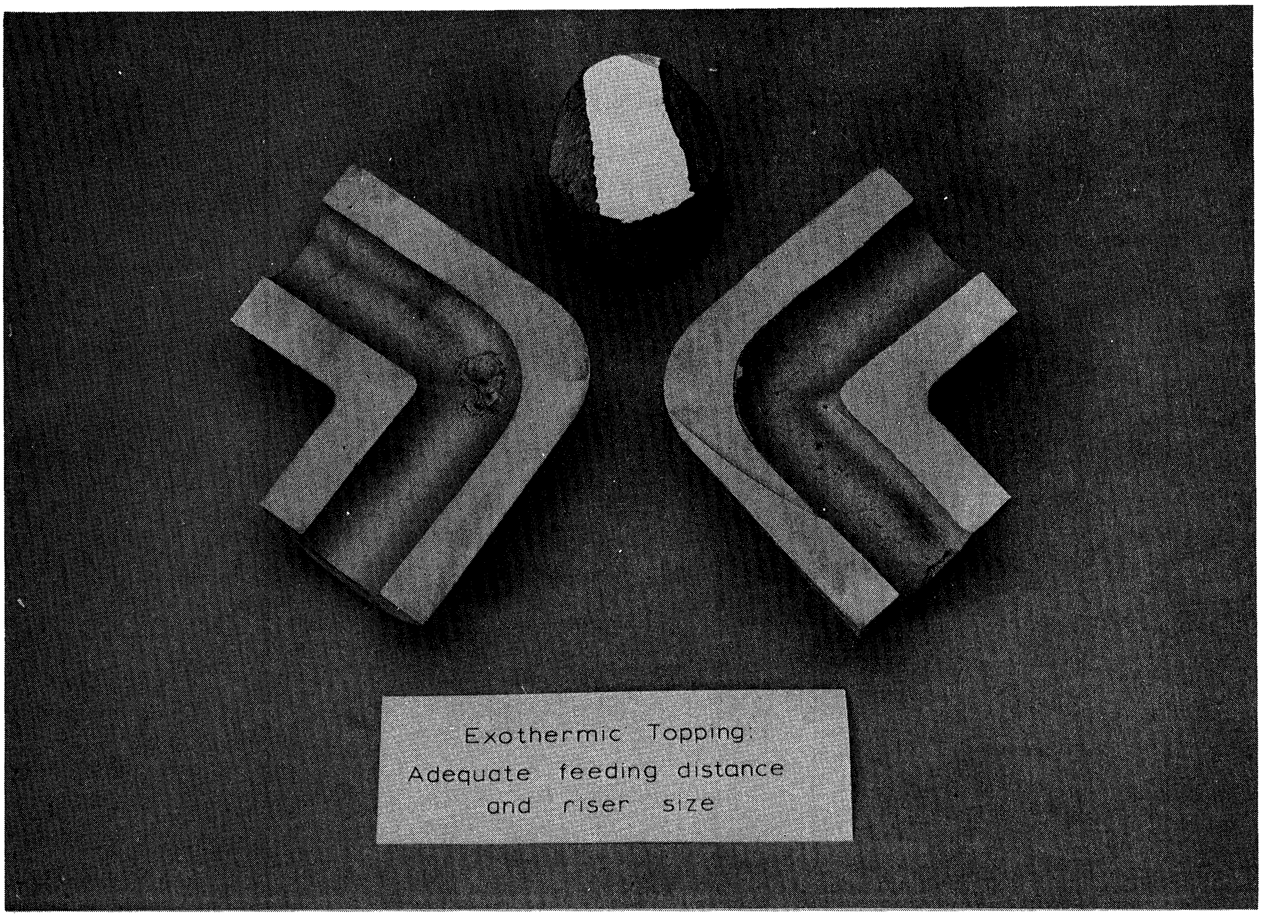

Figure 42. A correctly risered casting as also shown by radiography. The surface blemishes were due to some metal reaction with the uncoated CO_2 sand core.